Biomedicine & Pharmacotherapy 180 (2024) 117438

Contents lists available at ScienceDirect

Biomedicine & Pharmacotherapy

journal homepage: www.elsevier.com/locate/biopha

Review

The therapeutic potential of andrographolide in cancer treatment

Jiaxuan Hu [a,1], Yi Li [b,1], Xin Xie [c,1], Yunlei Song [a], Wenjing Yan [a], Yan Luo [a], Yumao Jiang [a,*]

[a] Key Laboratory of Prevention and Treatment of Cardiovascular and Cerebrovascular Diseases, Ministry of Education, Jiangxi Provincal Key Laboratory of Tissue Engineering, Scientific Research Center, Gannan Medical University, Ganzhou 341000, China

[b] Department of Anesthesiology, Ganzhou Key Laboratory of Anesthesiology, Ganzhou Key Laboratory of Osteoporosis Research, The First Affiliated Hospital of Gannan Medical University, Ganzhou 341000, China

[c] Key Laboratory of Prevention and Treatment of Cardiovascular and Cerebrovascular Diseases, Ministry of Education, Jiangxi Provincal Key Laboratory of Tissue Engineering, School of Pharmacy, Gannan Medical University, Ganzhou 341000, China

Abbreviations: 53BP1, P53-binding protein 1; 5-Fu, Fluorouracil; ABCB1, ATP binding cassette subfamily B member 1; AIM2, Absent In Melanoma 2; AKT, Protein kinase B; AMPK, AMP-activated protein kinase; Andro, Andrographolide; AP-1, Activator protein-1; As2O3, Arsenic trioxide; ATG, Autophagy-related protein; ATP, Adenosine 5′-triphosphate; Bad, BCL2-associcated agonist of cell death; Bak, BCL2-antagonist/killer; Bax, BCL2-Associated X; Bcl-2, B-cell lymphoma-2; Bcl-6, B-cell lymphoma 6 protein; Bcl-XL, B-cell lymphoma-extra-large; Bid, BH3 interacting domain death agonist; BIP, Immunoglobulin Heavy Chain-Binding Protein; BLM, Bleomycin; CAM, Chick Chorioallantoic Membrane; Caspase, Cysteinyl aspartate specific proteinase; CCL2, The C-C motif chemokine ligand 2; CDDP, Cisplatin; CDK, Cyclin-dependent protein kinase; CGAS, Cyclic GMP-AMP synthase; CHOP, C/EBP homologous protein 10; C-MET, C-Mesenchymal-epithelial transition factor; C-Myc, Avian myelocytomatosis virus oncogene cellular homolog; COX-2, Cyclooxygenase-2; CPP, Cell-penetrating peptide; CREB, Cyclic AMP-responsive element-binding protein; CXCL10, C-X-C motif chemokine 10; CXCR, CXC chemokine receptors; DDS, Drug Delivery Systems; DISC, Death-inducing signaling complex; DMBA, 7,12-Dimethylbenzanthracene; DNMT, DNA methyltransferases; Dox, Doxorubicin; DsDNA, Double-stranded DNA; EBV, The Epstein–Barr virus; ECM, Extracellular matrix; EGFR, Epidermal growth factor receptor; EMT, Epithelial-Mesenchymal Transition; ER, Endoplasmic Reticulum; ERK, Extracellular signal-regulated kinase; ESR1, Estrogen receptor 1; FADD, Fas-associating protein with a novel death domain; FBP1, Fructose-bisphosphatase 1; FOXM1, Forkhead box protein M1; FOXO3a, Forkhead box O3; GFR, Growth factor receptor; Gli1, GLI family zinc finger 1; GLUT1, Glucose transporters1; GPX4, Glutathione Peroxidase 4; GRP78, Glucose-regulated protein 78; GSDM, Gasdermin; GSDMD, Gasdermin D; GSH, Glutathione; GSK-3β, Glycogen synthase kinase-3β; HDAC, Histone deacetylase; HDAC4, EGFR-STAT1-Histone deacetylase; HIF-1α, Hypoxia inducible factor-1α; HK2, Hexokinase 2; HMGB1, High mobility group box 1; HO-1, Heme oxygenase 1; HRE, Hypoxia response elements; Hsp70, Heat shock protein; HuR, Human antigen R; HYP, Hydroxyproline; ICAM-1, Intercellular cell adhesion molecule-1; IFN-γ, Interferon-γ; IL, Interleukin; IRE1, Inositol-requiring enzyme 1; IκBα, Inhibitor kappa B alpha; JNK, Jun N-terminal kinase; Keap1;, vKelch-like ECH-associated protein 1; LC3B, Microtubule- associated protein 1 light chain 3; LDH, Lactate dehydrogenase; LDHA, Lactate dehydrogenase A; LEF, Lymphoid enhancer-binding factor; LKB1, Liver kinase B1; LncRNA, Long non-coding RNA; MAPK, Mitogen-activated protein kinase; MDA, Malondialdehyde; MDM-2, Murine double minute 2; MEF2D, Myocyte enhancer factor 2D; MEK, MAP kinase kinase; MLKL, Mixed lineage kinase domain-like protein; MMP, Matrix metalloproteinases; MPEG-PLA, Poly ethylene glycol-poly lactide; MTA1, Recombinant Metastasis Associated Protein 1; MTOR, Mammalian target of rapamycin; MyD88, Myeloid Differentiation Primary Response 88; NF-κB, Nuclear factor kappa-B; NICD1, Notch Intracellular Domain 1; NLRP3, Nucleotide- binding oligomerization domain, leucine- rich repeat and pyrin domain-containing 3; Notch1, Neurogenic locus notch homolog protein 1; Nrf2, Nuclear factor-erythroid 2 related factor 2; P38, P38 mitogen-activated protein kinase; P53, Tumor suppressor protein that protects from DNA damage; P70S6K, Ribosomal protein S6 kinase; PARP-1, PolyADP-ribosepolymerase; PCD, Programmed Cell Death; PCSK5, Proprotein convertase subtilisin/kexin type 5; PD-1, Programmed death 1; PDCD2, Programmed cell death 2; PDGFRβ, Platelet derived growth factor receptor beta; PDH, Pyruvate dehydrogenase complex; PDK1, Pyruvate dehydrogenase kinase 1; PD-L1, Programmed cell death-Ligand 1; PEPCK 1, Phosphoenolpyruvate carboxykinase 1; PFK, Phosphofructokinase; P-gp, P-glycoprotein; PI3K, Phosphatidylinositol-3-kinasePKM2, Pyruvate kinase M2; PLGA, Poly DL- lactide-Co-Glycolic acid; PTEN, Phosphatase and tensin homolog; RAD51, RAD51 recombinase; RASSF1A, Ras association domain family 1 isoform A; RIPK, Receptor-Interacting Protein Kinase; ROS, Reactive oxygen species; SLC7A11, Solute Carrier Family 7 Member 11; SLNs, Solid lipid nanoparticles; Smad, Drosophila mothers against decapentaplegic protein; SMO, Smoothened; SOD, Superoxide Dismutase; SOX9, SRY-Box Transcription Factor 9; SP1, Specificity Protein 1; SPC, Soybean-L- α- Phosphatidylcholine; STAT3, Signal transducer and activator of transcription 3; STING, Stimulator of interferon gene; TAMs, Tumor-Associated Macrophage; TBid, Truncated Bid; TCF-1, T cell factor 1; TF, Transferrin; TFRC, Transferrin Receptor; TGF-β1, Transforming growth factor-β; TIMP, Tissue inhibitor of matrix metalloproteinases; TLR4, Toll-like receptor 4; TME, Tumor microenvironment; TNF-α, Tumor necrosis factor-α; TOP2A, DNA topoisomerase II alpha; TRAIL, Tumor necrosis factor-Related Apoptosis Inducing Ligand; TSP-2, Thrombospondin 2; TXNRD1, Thioredoxin Reductase 1; ULK, Unc-51 like kinase; UPR, Unfolded Protein Response; VEGFR, Vascular endothelial growth factor receptor; XBP1, X-box binding protein 1; ΔΨm, Mitochondrial Membrane Potential.

* Corresponding author.
E-mail address: jiangyumao@gmu.edu.cn (Y. Jiang).

[1] Co-first authorship

https://doi.org/10.1016/j.biopha.2024.117438
Received 25 July 2024; Received in revised form 6 September 2024; Accepted 9 September 2024
Available online 19 September 2024

ARTICLE INFO

Keywords:
Andrographolide
Derivatives
Cancer therapy
Combined therapy
Molecular mechanism
Drug delivery system

ABSTRACT

Cancer poses a substantial global health challenge, necessitating the widespread use of chemotherapy and radiotherapy. Despite these efforts, issues like resistance development and severe side effects remain. As such, the search for more effective alternatives is critical. Andrographolide, a naturally occurring compound, has recently gained attention for its extensive biological activities. This review explores the role of andrographolide in cancer therapy, especially focusing on the molecular mechanisms that drive its anti-tumor properties. It also examines innovative methods to enhance andrographolide's bioavailability, thus boosting its effectiveness against cancer. Notably, andrographolide has potential for use in combination with various clinical drugs, and both preclinical and clinical studies provide strong evidence supporting its broader anticancer applications. Additionally, this paper proposes future research directions for andrographolide's anti-cancer effects and discusses the challenges in its clinical usage along with current research efforts to address these issues. In summary, this review underscores andrographolide's potential roles and contributes to the development of improved cancer treatment strategies.

1. Introduction

Cancer represents a major public health challenge globally, threatening human life. According to data from the International Agency for Research on Cancer, it is projected that there will be 28.4 million cancer patients worldwide by 2040, marking a 47 % increase from 2020 and becoming one of the leading causes of death [1,2]. Due to the complex nature of cancer and the significant variability in how different cancer types respond to treatment, combined with challenges such as tumor cell immune escape, drug resistance, and severe side effects of existing treatments, innovative strategies are urgently needed. These strategies include targeted autophagy regulation to improve cancer drug resistance [3,4], nanoparticle remodeling of the tumor microenvironment (TME) to enhance targeted delivery and boost immune responses [5], and the use of chitosan- and hyaluronic acid-based nanoarchitectures in phototherapy [6], among others. However, phytotherapy also represents a crucial approach to overcoming the limitations of current treatment regimens. Multi-targeted natural molecules offer valuable resources for developing new anti-tumor drugs. Research has demonstrated that active ingredients in natural plants, including alkaloids [7], polyphenols [8], flavonoids [9], and organic acids [10], possess anti-cancer properties. Notably, terpenoids such as β-elemene [11], perillyl alcohol [12], paclitaxel [13], and oridonin [14] have been used clinically in cancer treatment. Terpenoids hold significant promise as anti-tumor candidate drugs.

Andrographis paniculata (Burm. f.) Nees, commonly known as the "King of Bitterness," belongs to the Acanthaceae family. It has a long history of culinary and medicinal use in Southeast Asia, including China, Japan, and South Korea [15,16]. Studies have identified 187 chemical constituents in Andrographis paniculata, including andrographolide (Andro), deoxyandrographolide, neoandrographolide, andrographoside, and andrographosterin [17]. These chemical constituents underpin Andro's diverse biological activities and demonstrate significant pharmacological effects in treating various conditions, including anti-tumor [18], anti-viral [19], anti-inflammatory [20], anti-oxidant [21], Alzheimer's disease [22], heart protection [23], and liver protection [24]. The diterpene compound Andro was first extracted from the whole plant of Andrographis paniculata by Gorter in 1911, marking one of the earliest comprehensive studies on the chemical constituents of the plant [25]. Its molecular formula is $C_{20}H_{30}O_5$, and its structure primarily comprises a naphthalene ring, a γ-lactone ring, a double bond bridge connecting the naphthalene ring and the lactone ring, an outer ring double bond, and three hydroxyl groups (Fig. 1).

In recent years, substantial evidence has demonstrated that Andro generally inhibits the development of various cancers and regulates the cancer process through multiple targets, pathways, and mechanisms. Andro holds significant potential for clinical application as a cancer treatment. This review offers valuable insights into Andro's role in cancer treatment, particularly emphasizing the latest research on its molecular mechanisms of anti-tumor action. Additionally, it highlights the challenges associated with Andro's clinical application and explores ongoing efforts and future research directions aimed at overcoming these limitations. We also proposed a chronological study to investigate the inhibitory effect of Andro on a variety of cancers (Fig. 2).

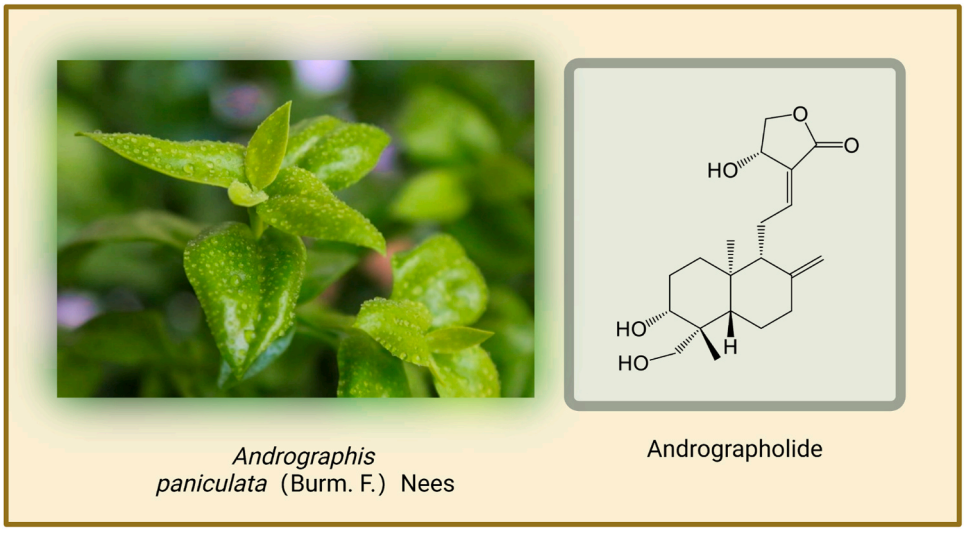

Fig. 1. Chemical formula of andrographolide and andrographolide.

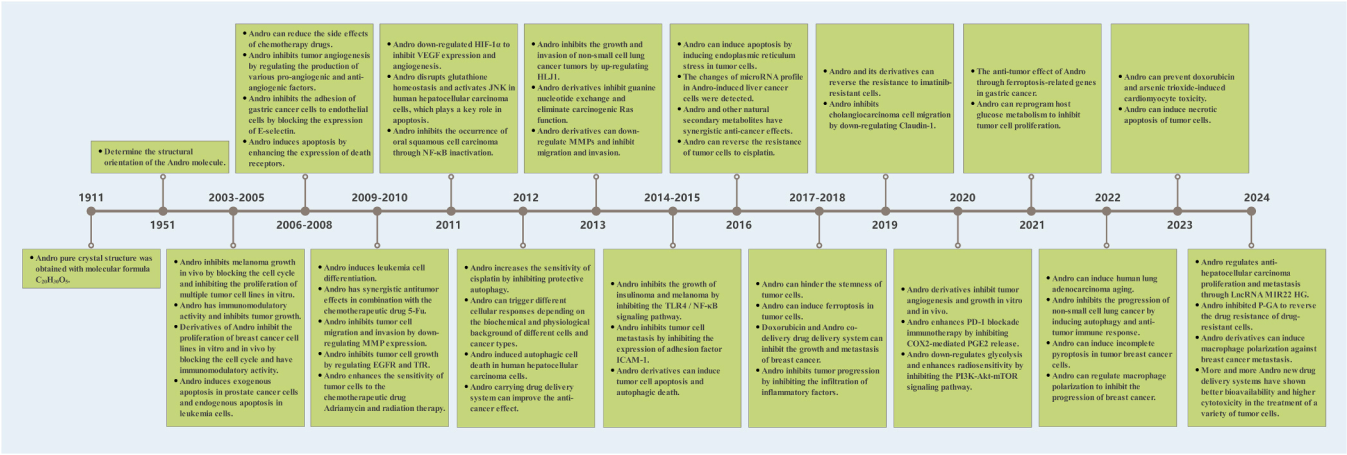

Fig. 2. Describe the timeline of the research activities of andrographolide in the treatment of tumors.

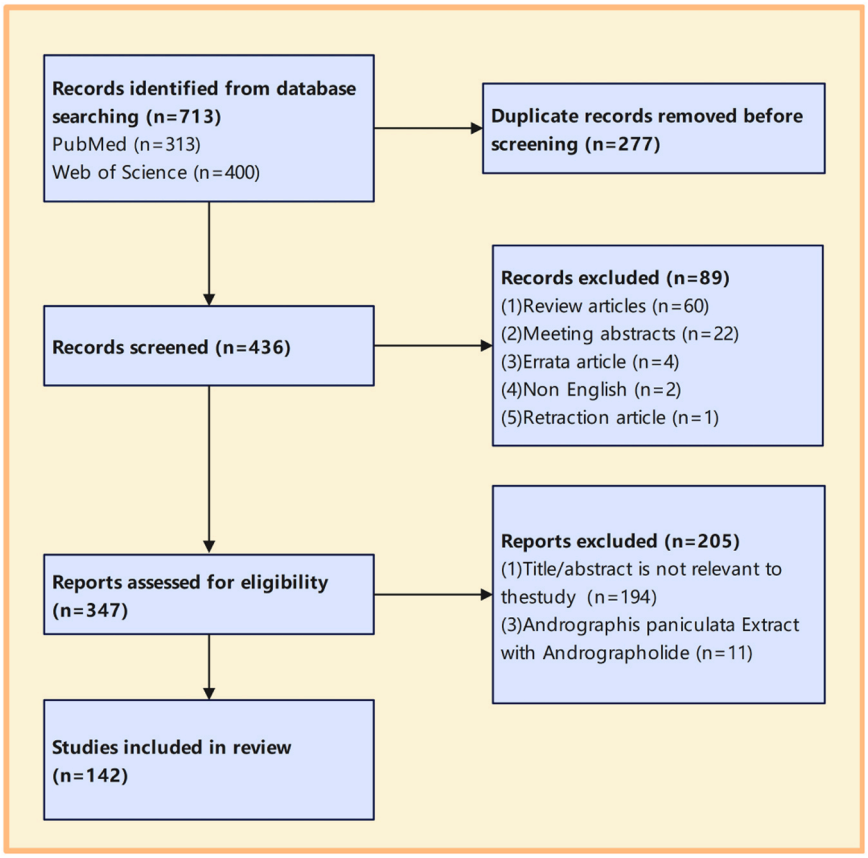

Fig. 3. Flow chart of literature retrieval process.

2. Method

We searched the PubMed and Web of Science databases for relevant articles published from January 1, 2014, to July 5, 2024, using the keywords "Andrographolide and Cancer". After excluding duplicate articles, reviews, conference abstracts, Chinese articles, and those deemed unrelated or underrepresented, 142 articles were included in the review. Details of this literature search are presented in Fig. 3.

3. The anti-tumor mechanism of Andro

As a novel anti-tumor agent, the mechanism of Andro involves multiple targets, pathways, and mechanisms (Fig. 4). This section reviews the molecular mechanisms underlying Andro's anti-tumor effects, with the aim of promoting its application in cancer treatment (Table 1).

3.1. Inhibition of proliferation

Uncontrolled cell proliferation is a hallmark of tumor cells. During the progression from normal to tumor cells, cells acquire the ability to generate growth signals, increase growth factor receptor (GFR) expression, evade growth inhibition signals, replicate indefinitely, and avoid terminal differentiation. This leads to uncontrolled cell cycle progression and unlimited proliferation. Andro can inhibit tumor cell

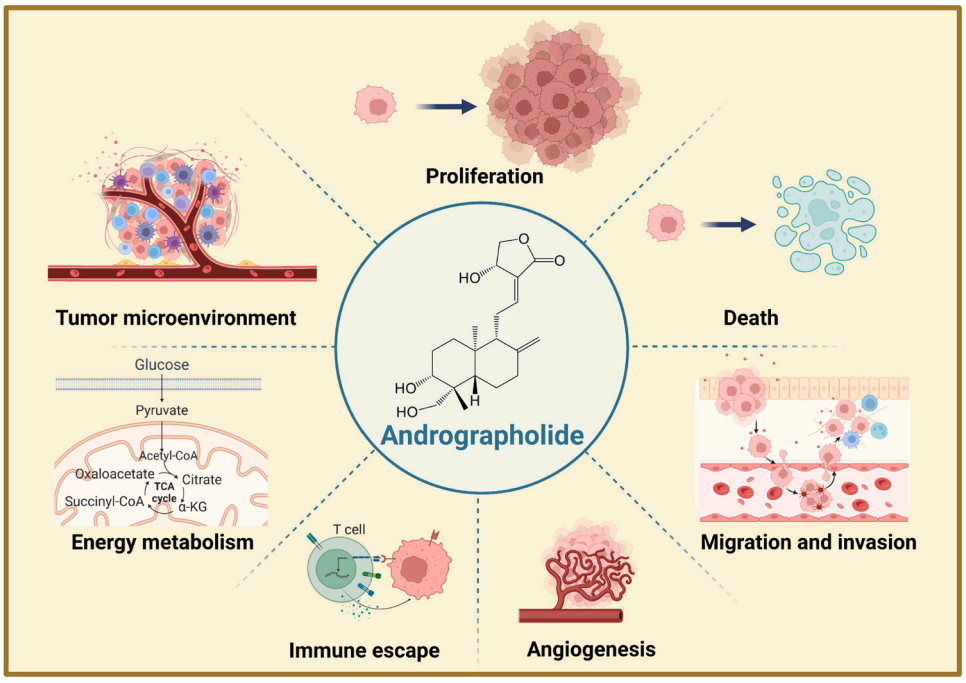

Fig. 4. Pharmacological activity of andrographolide.

proliferation by targeting these proliferation-related processes.

3.1.1. *Inhibition of growth signal transmission*

Compared with normal cells, tumor cells can escape dependence on growth factors by increasing the production of growth signals, upregulating GFRs, or altering the extracellular domain of GFRs to continuously send growth stimulation signals without ligand activation [26]. Studies have shown that Andro inhibits the proliferation of non-small cell lung cancer cells (H3255) by downregulating Transforming Growth Factor-β1 (TGF-β1) expression and Na^+-K^+-adenosine 5′-triphosphate (ATP) enzyme activity [27]. Additionally, in nasopharyngeal carcinoma cells (HK1 and CNE-1), Andro treatment reduces the expression of Epidermal Growth Factor Receptor (EGFR), Survivin, and Cyclin D1, thereby inhibiting tumor cell proliferation [28].

3.1.2. *Regulating cell cycle-related proteins*

The cell cycle is fundamental to cell life, and tumor cells maintain this process to support proliferation. In the normal cell cycle, Cyclin-dependent Protein Kinase (CDK) binds to Cyclin to drive the process forward [29]. Andro regulates cell cycle-related proteins through multiple pathways to block the cell cycle and inhibit tumor proliferation (Fig. 5). For instance, Andro C-3 and C-19 aryl acetal derivatives (Compounds 1 and 2, Fig. 6) interfere with colon and prostate cancer cells [30,31]. Additionally, in PANC-1 (with mutant tumor suppressor protein p53 R273H), HuCCT1 (with mutant p53 R175H), and HuCCT1 cell-transplanted mice, Andro inhibits Signal Transducer and Activator of Transcription 3 (STAT3) and induces the expression of Heat Shock Protein 70 (Hsp70), leading to the degradation of mutant p53 and upregulation of p21, which causes G0/G1 phase arrest [32]. Moreover, Andro C-17 and C-19 modified derivatives (Compound 3, Fig. 6) induce DNA damage and Poly (ADP-ribose) Polymerase-1 (PARP-1) cleavage by inhibiting DNA Topoisomerase II Alpha (TOP2A), upregulating p53, and inhibiting Cyclin D and CDK6, which results in G1 phase arrest [33].

Andro not only blocks the G0/G1 phase but also interrupts the tumor cell cycle in the G2/M phase through multiple pathways. Research has shown that Andro induces DNA damage by increasing reactive oxygen species (ROS) levels in HepG2, Huh7, and Hep3B hepatoma cells. It promotes p62 aggregation, degrades RAD51 recombinase (RAD51) and p53-binding protein 1 (53BP1), impairs DNA repair, increases p53 expression, inhibits Cyclin B1 and Cyclin-dependent Kinase 1 (CDC2), and induces cell cycle arrest in the G2/M phase [34]. Additionally, Andro downregulates SRY-Box Transcription Factor 9 (SOX9) by inhibiting T Cell Factor 1 (TCF-1) and bypassing β-catenin, which promotes the expression of p21 in chondrosarcoma cells and inhibits Cyclin D1, Cyclin E1, Cyclin E2, and Cyclin B1, leading to G2/M phase arrest [35]. Moreover, Andro increases the expression of Avian Myelocytomatosis Virus Oncogene Cellular Homolog (C-Myc) and upregulates p53 by activating Extracellular Signal-Regulated Kinase (ERK) 1/2, which activates BCL2-Associated X (Bax) and blocks DBTRG-05MG brain cancer cells in the G2/M phase [36]. Concurrently, Andro inhibits the phosphorylation of Glycogen Synthase Kinase-3β (GSK-3β), reduces β-catenin accumulation, decreases the expression of C-Myc and Cyclin D1, and blocks the cell cycle in the G2/M phase in osteosarcoma 143B, U2OS, MG-63, and SaoS-2 cells, as well as in 143B cell transplantation mouse models in vivo [37]. C-Myc is also involved in cell differentiation; its overexpression can compete with Mad to form the Max-Myc complex, inhibiting tumor cell differentiation and enhancing proliferation [38]. However, the effect of Andro on C-Myc's role in cell differentiation remains unstudied.

Researchers have made progress in understanding Andro 's impact on upstream targets of cell cycle-related proteins. Using computer-simulated molecular docking technology, it was discovered that Andro has a high affinity for Smoothened (Smo) in the Hedgehog pathway. It downregulates the expression of Smo and GLI Family Zinc Finger 1 (Gli1) in colon cancer HCT116 cells, thereby inhibiting CDC2 and Cyclin B1 expression and ultimately inducing G2/M phase arrest [18]. Additionally, a study using proteomic chips found that Andro binds to Programmed Cell Death 2 (PDCD2), affecting PDCD2's role in transporting cyclin RNA to cytoplasmic ribosomes. This interaction inhibits the nuclear export efficiency of CDC2, CDK2, CDK4, and CDK6 mRNA, reduces CDK protein expression, and blocks A549 lung cancer cells and HeLa cervical cancer cells in the G2/M phase [39]. However, these findings need further validation through surface plasmon resonance and biofilm light interference techniques.

Table 1
Information on the mechanism of andrographolide on various tumors.

Cancer type	Animal/cell model	Types	Routes	Dose	Effects and related mechanisms	Ref
Colon	HCT116 cell	In vitro	-	16–512 μM	↑ROS, Bax, Bad ↓Bcl−2, Cyclin B1, CDK1, Smo, Gli1	[18]
	HCT116 cell	In vitro	-	0.1–10 μM	↑p21 ↓CDK4	[30]
	HCT116 subcutaneous xenografts in Female Balb/C mice	In vivo	ip	100 mg/kg		
	HCT116 cell	In vitro	-	1–10 μM	↑tBid, Cleaved Caspase 8 ↓Caspase 8, Bid	[56]
	HCT116 cell	In vitro	-	10–20 μM	↓$p47^{phox}$, ROS, p-Src, p-Erk1/2, p-p38, p-c-Fos, p-c-Jun, p-p65, p-IκBα, IL−8	[95]
	HT−29 cell	In vitro	-	16–256 μM	↑ROS, Caspase 3activity	[46]
	HT−29 cell	In vitro	-	1–10 μM	↑p53, Cleaved PARP ↓TCF, β-catenin, C-Myc, Cyclin D1, Survivin, MMP−7	[72]
	HT−29 cell	In vitro	-	5 μM	↓p-VEGFR2, p-mTOR, p-AKT, p-MEK1/2, p-ERK1/2, p-p38	[85]
	HT−29 subcutaneous xenograft male C57BL/6 mice	In vivo	ip	2 mg/kg		
	DMBA induced colon cancer female Sprague Dawley rals	In vivo	po	10, 30, 100 mg/kg	↑p53 ↓Caspase 3	[40]
	SW−480 cell	In vitro	-	16–512 μM	↑ROS, Bax, Bad ↓Bcl−2, Notch 1, Jagged 1	[96]
	DLD1 cell	In vitro	-	80~ 320 μM	↑ROS, Caspase 3 activity	[97]
	Colo205, T84 cell	In vitro	-	45 μM	↑ROS, IRE1, XBP1, CHOP, Caspase 3 ↓Cyclin B1, p-AKT	[58]
	T84, HCT116, Colo205 cell	In vitro	-	45 μM	↑IRE1, XBP1, CHOP, Caspase 3 ↓Bcl−2	[59]
	Colo205, T84 cell	In vitro	-	45 μM	↑RASSF1A, TSP−2 ↓VEGFR1, VEGFR2, p-AKT, FOXM1	[82]
	HT−29, HCT116 cell	In vitro	-	4 μM	↑ROS, p-JNK1/2, Cleaved Caspase 9, Cleaved Caspase 3, Cleaved PARP	[98]
	HT−29 Subcutaneous xenografts in male nude mice	In vivo	ip	2 mg/kg		
Liver cancer	HUVECs cell	In vitro	-	Andro：2.5 μM	↓p-ERK1/2, p-p38, p-JNK/SAPK, p- VEGFR2	[84]
	Hep3B subcutaneous xenografts in C57BL/6 mice	In vivo	ip	3, 10, 30 mg/kg		
	HepG2，Huh7，Hep3B cell	In vitro	-	30 μM	↑ROS, p62, p53, Cleaved PARP, Bax, Cleaved Caspase 3, BRCA1 ↓Cyclin B1, CDK1, RAD51, 53BP1	[34]
	p62 knockout HepG2/ HepG2 subcutaneous xenografts in Balb/c nude mice	In vivo	ig	15/30 mg/kg		
	SK-Hep−1，HepG2 cell	In vitro	-	0–100 μM	↑MIR22HG, Cleaved Caspase 9, Cleaved Caspase 7, Cleaved Caspase 3 ↓Bcl−2, Caspase 9, Caspase 7, Caspase 3, HMGB1, MMP−9	[57]
	SK-Hep−1 subcutaneous xenografts and lung metastases tail vein injected in Balb/c nude mice	In vivo	ig	20, 40 mg/kg		
	Hep3B，HepG2 cell	In vitro	-	25, 50 μM	↓c-Jun, VEGFD	[78]
	Hep3B subcutaneous xenografts in specific pathogen-free nude male mice	In vivo	ip	5, 10 mg/kg		
	Hep3B，HepG2 cell	In vitro	-	0–50 μM	↓MTA1, HDAC1, HIF−1α, VEGFA	[80]
	Hep3B subcutaneous xenografts in specific pathogen-free nude male mice	In vivo	ip	10 mg/kg		
	Hep3B，SMCC7721 cell	In vitro	-	50 μM	↑miR−222–3p, miR−106 b−5p, miR−30 b−5p, miR−23 a−5p	[99]
	Hep3B subcutaneous xenografts in specific pathogen-free nude male mice	In vivo	ip	10 mg/kg		
Lung cancer	A549 cell	In vitro	-	1–5 μM	↑ROS	[47]
	H3255 cell	In vitro	-	1–5 μM	↓VEGF, TGF-β1, PKC	[27]
	H1975 cell	In vitro	-	0–20 μM	↑Bax, Bak, PEPCK1, FBP1, PFK, Cyt C, Cleaved Caspase 8, Cleaved Caspase 9, Cleaved Caspase 3 ↓Bcl−2, PKM2, LDHA, GLUT1	[91]
	H460，H1650 cell	In vitro	-	0–30 μM	↑ROS ↓GPX4, SLC7A11	[63]
	Lewis subcutaneous homografts of C57BL/6 mice	In vivo	ip	5, 10 mg/kg		
	H1975，H1299 cell	In vitro	-	0–50 μM	↑ROS, p62, LC3B ↓p-STAT3, PD-L1	[87]
	H1975 subcutaneous xenografts in female nude mice, Lewis homograft female C57bl/6 J mice	In vivo	ip	Andro：2.5, 5, 10 mg/kg anti-PD−1：10 mg/kg		

(*continued on next page*)

Table 1 (*continued*)

Cancer type	Animal/cell model	Types	Routes	Dose	Effects and related mechanisms	Ref
	A549，H292 cell	In vitro	-	0–75 μM	↑ROS, Cleaved Caspase 9, Cleaved Caspase 3, Cleaved PARP ↓PDK1, PDK2, PDK3, p-PDH1	[89]
	A549，H1299 cell	In vitro	-	0–50 μM, 0–20 μM	↑ATF4, Noxa, Cleaved PARP, Cleaved Caspase 3 ↓Puma, Bid, Bim, Bik, Bax, Bak, C-Myc, Caspase 3	[100]
	A549, H1975 cell	In vitro	-	0–20 μM	↑p53, p21, γ-H2AX, p27 ↓Skp2	[101]
	A549 Subcutaneous xenograft BALB/c nude female mice	In vivo	ip	50, 100, 150 mg/kg		
Lymphoma	MCF−7 cell	In vitro	-	Andro：16 μM TRAIL：8 ng/ml	↑ROS, DR4, p53, Bid, Bax, Cleaved Caspase 9, Cleaved Caspase 8, Cleaved Caspase 3, Cleaved PARP, Cleaved GSDME	[65]
	MCF−7 cell	In vitro	-	70 μM	↑PDCD4 ↓p65, p-p65, miR−21–5p	[102]
	MMTV-PyMT mice	In vivo	ip	5 μg/g		
	MDA-MB−231 cell	In vitro	-	0–10 μg/ml	↑E-cadherin ↓N-cadherin, Vimentin, EGFR, p-EGFR, p-STAT1, HDAC4	[67]
	MDA-MB−231 cell	In vitro	-	0–30 μM	↓p-IκBα, MMP−9	[70]
	MDA-MB−231 heterozygous anterior tibial tuberosity injected BALB/c mice	In vivo	ip	50 mg/kg		
	MDA-MB−231 cell	In vitro	-	5–20 μM，20 μM	↑TIMP3 ↓miR−21–5p, MMP−9	[86]
	4T1 cell	In vitro	-	50–200 nM	↓MMP−2, MMP−9	[75]
	4T1 homozygous tail vein injection of female BALB/c mice	In vivo	ip	1, 5 mg/kg		
	HUVECs cell	In vitro	-	20 μM,	↓p-VEGFR2, p-ERK, p-AKT	[83]
	4TI in situ homograft BALB/c nude mice	In vivo	po	5, 10, 20 mg/kg		
	MDA-MB−231，MCF−7 cell	In vitro	-	0–20 μM	↑Bax, Cleaved Caspase 9, Cleaved Caspase 3	[81]
	MDA-MB−231 subcutaneous xenografts in BALB/c female athymic nude mice	In vivo	-	5, 10 mg/kg	↓Bcl−2, COX−2, p300 HAT, p65/p50, c-Fox, CREB2, CD31	
	MDA-MB−231，HCC1937，HCC1806 cell	In vitro	-	25 μM	↓Wnt−5a, β-catenin, MMP−9, MMP−2, PDGF-AA, CCL2	[93]
	MDA-MB−231 was injected subcutaneously into the mammary fat pad in BALB/c mice, HCC1806, 4T1 was injected subcutaneously into the mammary fat pad in Female NOD/SCID mice	In vivo	ip	200 mg/kg		
	T47D，MDA-MB−231 cell	In vitro	-	0.1–1 μM	↑p−4EBP1, p-P70S6K ↓HIF−1α, p-AKT, p-mTOR	[103]
	MDA-MB−231 intraperitoneal injection in BALB/c females nude mice	In vivo	po	25, 50, 100 mg/kg		
Prostate cancer	PC−3 cell	In vitro	-	Andro：20 μM；TRAIL：20 ng/ml	↑ROS, DR4, p53, p-p53, Cleaved Caspase 8, Cleaved Caspase 3, Cleaved PARP ↓FLIP, Caspase 8, Caspase 3	[42]
	PC−3 subcutaneous xenografts in BALB/c mice	In vivo	ip	Andro：10 mg/kg TRAIL：100 μg		
	PC−3，DU145，LNCaP cell	In vitro	-	0.1–100 μM	↑Cleaved caspase 8, Cleaved caspase 9, tBid, Bax ↓Cyclin D1, CDK4, CDK1, Caspase 8, Caspase 9, Bid, Bcl−2	[31]
	PC−3，DU145，C4–2b cell	In vitro	-	7.5–20 μM	↓CXCR3, CXCR7	[76]
	PC−3，22RV1 cell	In vitro	-	10–25 μM	↑ATM、BRCA2、BRIP1、CLSPN, NBN, γH2AX	[104]
	22RV1 in situ xenograftmale ICR-SCID mice	In vivo	ip	10 mg/kg	↓MMP−11, pH3, Ki−67	
Melanoma	B16 cell	In vitro	-	10 μM	↓TLR4, MyD88, p-IκBα, p-p65, p-p50, CXCR4, IL−6	[77]
	B16 subcutaneous homografts of C57BL/6 J mice	In vivo	ip	5 μg/g		
	$CD133^+$ tumour stem cell	In vitro	-	50–150 μM	↓Notch1, NICD1, CD133, p- MEK3/6, p-p38, c-Jun, c-Fos, MMP−2, MMP−9, VEGF	[79]
	$CD133^+$ tumour stem cell + B16F10 subcutaneous homograft in NOD/SCID or C57BL/6 J mice	In vivo	ip	50, 150 mg/kg		
Glioma	DBTRG−05 MG cell	In vitro	-	13.95, 27.9 μM	↑ERK1/2, C-Myc, p53	[36]
	C6 cell	In vitro	-	5–20 μM	↑Cleaved caspase 7, Cleaved PARP, p-p53, p53, p-ERK1/2, p-p38 MAPK	[49]
	C6 Subcutaneous homografts in ICR male mice	In vivo	is	30 μL（20 μM）		

(*continued on next page*)

Table 1 (*continued*)

Cancer type	Animal/cell model	Types	Routes	Dose	Effects and related mechanisms	Ref
	U251 , U87 cell U87 (shPCSK5/ shNC) subcutaneous xenograft Female athymic BALB/c nude mice	In vitro In vivo	- iv	0–100 μM 10 mg/kg	↑E-cadherin ↓N-cadherin, Vimentin, PCSK5, p-STAT3, MMP−2, MMP−9	[73]
	GBM8401 , U251 cell	In vitro	-	0–40 μM	↑p-c-Raf, p-MEK, p-ERK1/2, p-JNK1/2 ↓CREB, MMP−2	[74]
Gastric cancer	SGC7901 cell	In vitro	-	5–40 μM	↑Bax, Bak, TIMP−1, TIMP−2, Cyclin B1, p-CDC2 ↓Bcl−2, Survivin, MMP−2, MMP−9, CD147	[69]
	SGC7901 , AGS cell	In vitro	-	20 μM	↑p53 ↓MDM−2, Bcl−2, Caspase 9, Caspase 3, PARP	[48]
	MKN74 , NUGC4 cell	In vitro	-	40 μg/ml	↑HMOX1, GCLC, GCLM	[105]
	AGS , SNU601 , SUN638 cell	In vitro	-	Andro:10, 15 μM TRAIL:5, 10 ng/ml	↑ROS, p53, p21, DR4, DR5, Bak, Bax ↓Bcl−2	[41]
Osteosarcoma	SW1353 , Hs819.T cell	In vitro	-	5–50 μM	↑p21, Bad, Cleaved Caspase 3, β-Tubulin ↓p27, Cyclin D1, Cyclin E2, Bcl−2, TCF−1, SOX9, Lamin-A	[35]
	MG−63 , U2OS cell	In vitro	-	3–60 μM	↑LC3B, Beclin, ATG5, PI3K classIII, E-cardherin ↓PI3K classI, p-AKT, p-mTOR, p-JNK, p-ERK, p-p38 Vimentin, N-cardherin, Snail	[61]
	143B , U2OS , MG−63 , SaoS−2 cell 143B injected into the proximal tibia periosteum of female nude mice	In vitro In vivo	- ig	5–20 μM ; 5, 10, 15 mg/kg	↑Bad, Cleaved Caspase 3, Cleaved PARP, E-cardherin ↓PCNA, Cyclin B1, Bcl−2, Snail, Vimentin, N-cardherin, MMP−2, MMP−7, MMP−9, β-catenin, C-Myc, Cyclin D1, p-GSK3-β, p-AKT, p65	[37]
	HOS , U2OS , SAOS−2 , MG−63 cell HOS-Luc subcutaneous xenografts in Female Balb/c- nude mice	In vitro In vivo	- ip	0–80 μM ; 15, 30 mg/kg	↑ROS, Cleaved Caspase 9, Cleaved Caspase 8, Cleaved Caspase 3, Cleaved PARP, p-JNK ↓PARP	[106]
Leukaemia	U937 cell	In vitro	-	5.4 μM	↑Bax, Bad, Cyto-Cyt c, Cleaved PARP, Beclin 1, ATG3, ATG7, ATG5 ↓Bcl-XL, Bcl−2, Mito-Cyt c, PARP, p-PI3K, p-AKT, p-PDK1, p-GSK3β, p-mTOR, LC3BI/II	[62]
	Jurkat cell Jurkat subcutaneous xenografts in Nude mice	In vitro In vivo	- ip	5–20 μg/ml 50, 100, 200 mg/kg	↑Cleaved Caspase 3, p-p38, p-p53 ↓Caspase 3, p-AKT	[107]
Bladder cancer	T24 cell	In vitro	-	Andro : 8 μM TRAIL : 2 ng/ml	↑Cleaved PARP1, Cleaved Caspase 3, Cleaved Caspase 9, DR4, DR5, p53 ↓CD147, MMP−9, PARP1, Caspase 3, Caspase 9, Caspase 8, RelA, clAP2	[43]
	T24 , 5637 cell 5637 Subcutaneous xenografts in BALB/c nude mice	In vitro In vivo	- ip	0–40 μM, 0–80 μM 10 mg/kg	↑Cleaved Caspase 3, Cleaved Caspase 9, Bax ↓MMP−9, Bcl−2, p65, Survivn, p- PI3K, p- AKT, p-mTOR	[52]
Multiple myeloma	OPM1 cell	In vitro	-	1–10 μM	↓TLR4, NF-κB	[51]
	RPMI−8226 , U266 cell	In vitro	-	20, 40 μM	↑p21, p-p38 ↓CDK2, CDK4, Cyclin D1, Nrf2, HO−1, GPX4, SLC7A11	[64]
Nasopharyngeal Carcinoma	C666–1 cell	In vitro	-	25–100 μM	↑Bax, Cleaved Caspase 3, p-LKB1, p-AMPK ↓ Bcl−2, Caspase 3, p-P70S6K, p-S6	[53]
	HK1 , CNE−1 cell	In vitro	-	5–25 μM	↓EGFR, Survivin, Cyclin D1, MMP−9, VEGF, ICAM−1	[28]
Kidney cancer	786–0 , OS-RC−2 , ACHN cell	In vitro	-	Andro : 5 μM TRAIL : 50 ng/ml	↑γ-H2AX, Bax, Cleaced PARPP, Cleaced Caspase 8, Cleaced Caspase 9, DR4 ↓PARP, Caspase 8	[44]
	HEK−293 cell	In vitro	-	0–20 μM	↑p53, Bax, Cleaved PARP ↓Bcl-XL, NF-κB	[50]
Bile duct cancer	KKU-M213 cell	In vitro	-	8.0 μM	↑Cleaved PARP1, p53, Bax ↓TOP2A, CDK6, Cyclin D1	[33]
	KKU-M213 cell	In vitro	-	0–50 μM	↑p-p38, Snail, p-JNK ↓claudin−1	[108]
Cervix	Hela, Siha cell HeLa subcutaneous xenograft in Female C57 BL/6 mice	In vitro In vivo	- ip	0–10 μM 15, 30 mg/kg	↑PTEN , Bax ↓NF-κB, COX−2, PI3K, p-AKT, Bcl−2	[54]
Burkitt's lymphoma	Burkitt's lymphoma patient-derived xenografts in NOD-SCID or BALB/c nude mice	In vivo	ip	25 mg/kg	↑c-Jun, Caspase 3	[55]
Thyroid cancer	8505 C , CAL62 cell	In vitro	-	60 μM	↑Cleaved PARP, Cleaved Caspase 3 ↓PARP, Caspase 3, Bcl−2, Bcl-XL, HK2, PKM 2, PFKM, LDHA	[90]
Abdominal aortic aneurysm	Mouse aortic smooth muscle cell Elastase perfusion induces abdominal aortic aneurysms in Male C57BL/6 J mice	In vitro In vivo	- ip	15 μM 5 mg/kg	↓p-NF-κB, α4 integrin, CCL2, CXCL10, TNFα, IFNγ	[94]

(*continued on next page*)

Table 1 (*continued*)

Cancer type	Animal/cell model	Types	Routes	Dose	Effects and related mechanisms	Ref
Pancreatic Bile duct cancer	PANC−1 , HuCCT1 cell HuCCT1 subcutaneous xenografts in female BALB/c mice	**In vitro** **In vivo**	- ip	12.5–100 μM 10 mg/kg	↑wtp53, p21, Cleaved Caspase 3, Hsp70, Hsp90 ↓mtp53, Caspase 3, MDM2, STAT3	[32]
Lung cancer Cervical cancer	A549 , HeLa cell A549 Subcutaneous xenografts in nude mice	**In vitro** **In vivo**	- ip	12.5, 25 μM ; 30 mg/kg	↓PD2, CDK1, CDK2, CDK4, CDK6	[39]
Leukaemia Multiple myeloma	THP−1 , H929 cell	**In vitro**	-	50 μM	↑ROS ↓Caspase 7, Caspase 3	[45]
Nasopharyngeal Cancer Oral Cancer	HONE1-EBV , SCC25-EBV , HSC1-EBV cell	**In vitro**	-	35–36.3 μM	↑DNMT1, DNMT3B, HDAC5, RIPK1, RIPK3, MLKL ↓MEF2D, SP1, SP3	[60]
Oral cancer	C33A , SiHa , CaSki cell	**In vitro**	-	0–160 μM	↑E6, p53 ↓HERC4, SMURF2	[109]
Breast Cancer Ovarian cancer	MDA-MB−231 , SKOV−3 cell	**In vitro**	-	0–50 μM ;	↑TIMP1 ↓p-p65, MMP−7	[110]

↓indicates inhibition/reduction, while ↑indicates increase/promotion; ip, Intraperitoneal; Ig, intragastric; po, Oral administration; iv, Intravenous; is, In situ injection

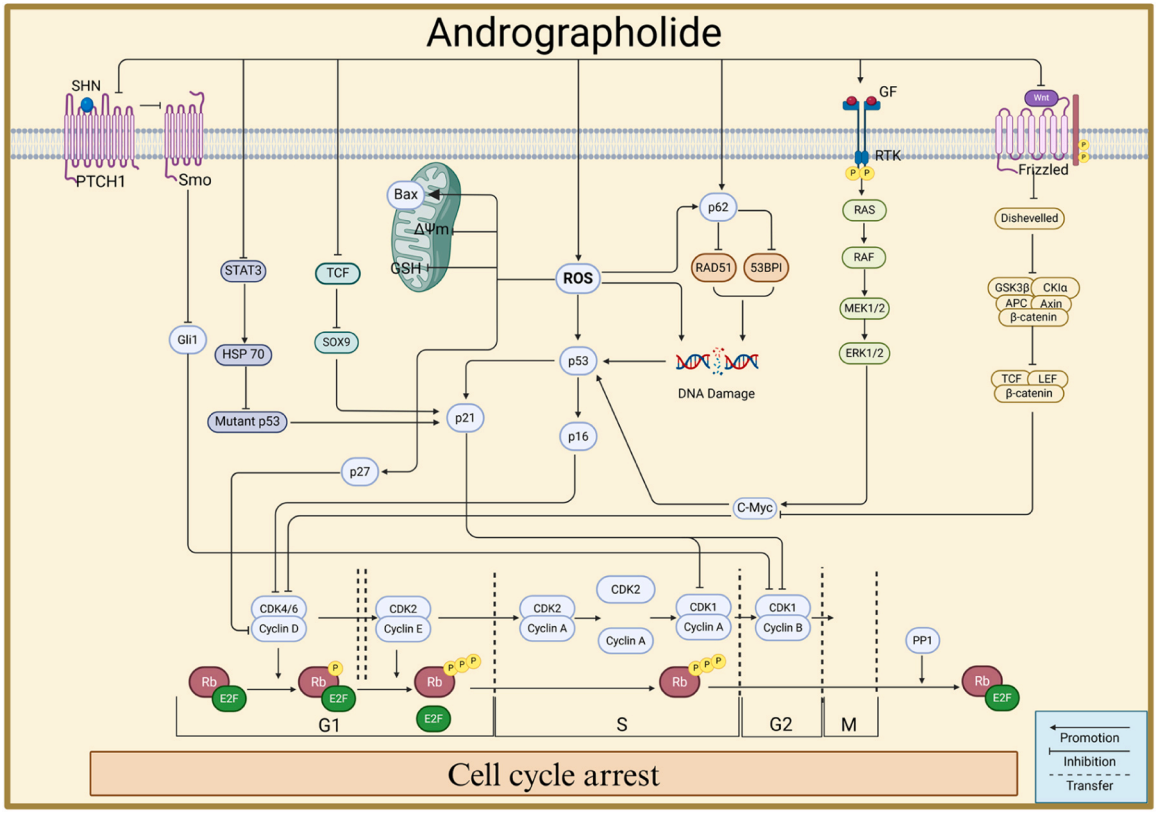

Fig. 5. Anti-proliferation mechanism of andrographolide. Andrographolide regulates the CDK-cyclin complex by downregulating STAT3/HSP70, TCF-1/SOX9, ERK1/2, GSK-3β/β-catenin, and the Hedgehog pathway, inhibiting TOP2A expression, inducing DNA damage, and increasing ROS content to prevent cell cycle progression.

3.1.3. Inhibition of abnormal telomerase activation

Telomeres are DNA repeat sequences at the ends of eukaryotic chromosomes that maintain chromosome stability and ensure proper cell division in conjunction with telomere-binding proteins. As cells divide, telomeres gradually shorten but are stabilized through telomerase activity. Tumor cells maintain telomere length by activating telomerase, which promotes division and stabilizes chromosomes. Regulating telomerase activity can help inhibit tumor cell proliferation. Studies have shown that Andro inhibits telomerase activity and disrupts chromosome stability in a rat colon and lung cancer model induced by 7,12-Dimethylbenz[*a*]anthracene (DMBA), thereby impeding tumor cell progression through the cell cycle [40]. However, the specific mechanism by which Andro affects tumor telomerase requires further investigation, which may offer new avenues for innovative treatment strategies.

3.2. Inducing programmed cell death

Programmed cell death (PCD) represents a controlled form of cell death regulated by various biological macromolecules, distinguishing it from accidental cell death. PCD is crucial in numerous biological processes, including development, cell differentiation, maintenance of

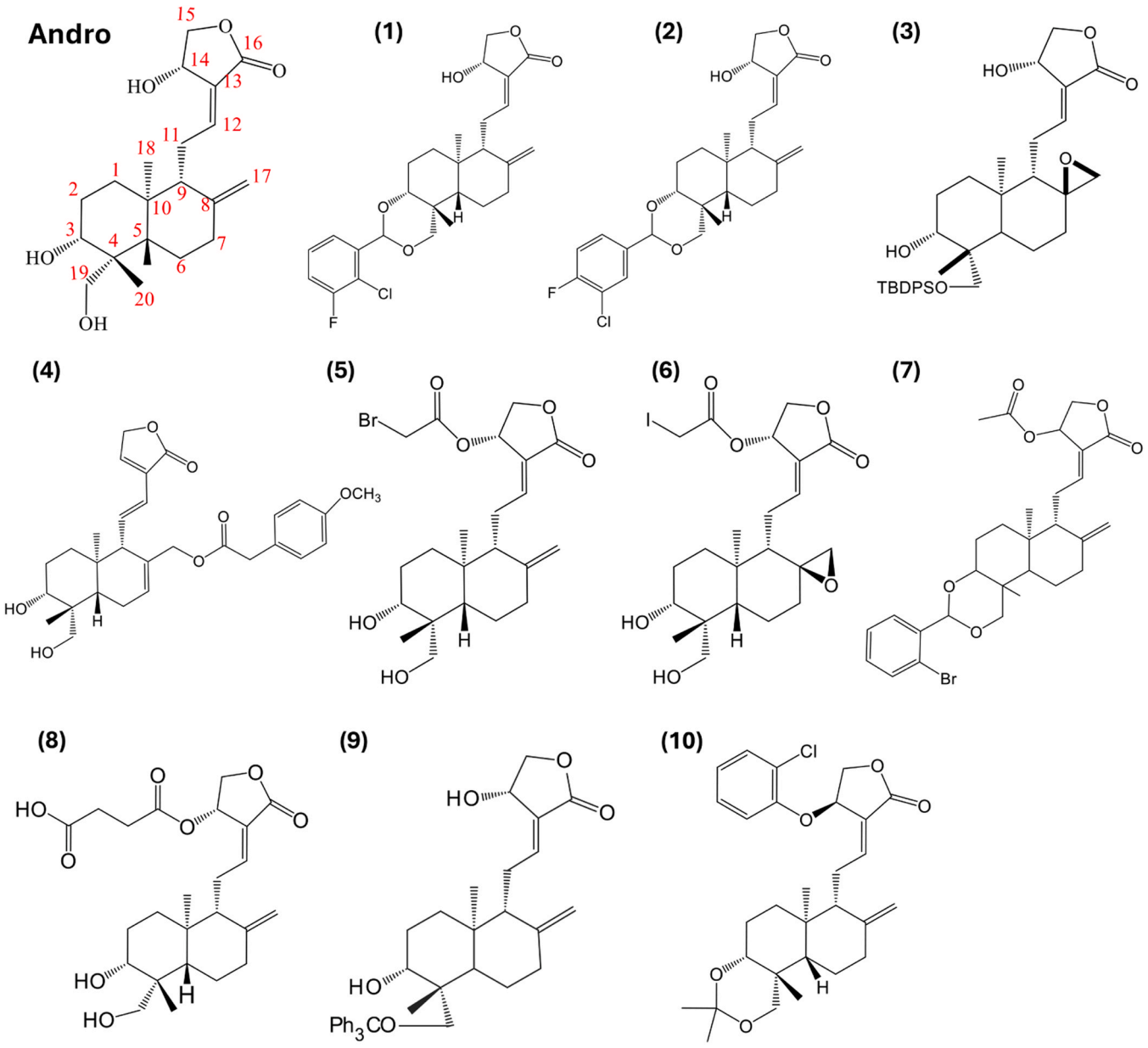

Fig. 6. Andrographolide anti-tumor derivatives.

cellular balance, and removal of defective or malignant cells, making it a key target for cancer chemotherapy. Extensive studies have demonstrated that Andro can regulate various PCD mechanisms, including apoptosis, autophagy, ferroptosis, and pyroptosis (Figs. 7 and 8). This section summarizes the mechanisms by which Andro regulates PCD and offers new insights into its potential significance in tumor therapy.

3.2.1. Apoptosis

3.2.1.1. Exogenous apoptosis. Exogenous apoptosis involves the formation of the death-inducing signaling complex (DISC) through the activation of cell surface receptors. The cytoplasmic tail of these receptors binds to Fas-Associating Protein with a Novel Death Domain (FADD), which then activates Cysteinyl Aspartate-Specific Proteinase (Caspase) 8 to induce programmed cell death. Impaired death receptor signaling pathways are a key mechanism by which tumors evade exogenous apoptosis. Andro can interfere with this pathway, triggering exogenous apoptosis in gastric cancer [41], prostate cancer [42], bladder cancer [43], and kidney cancer [44] cells.

3.2.1.2. Endogenous apoptosis. Endogenous apoptosis, or mitochondrial apoptosis, refers to cell death induced by the disruption of mitochondrial membrane channels following intracellular homeostasis imbalance. Andro can induce mitochondrial apoptosis in tumor cells through multiple pathways.

One trigger of the mitochondrial apoptosis pathway is the disruption of the redox system balance. Studies have shown that Andro increases intracellular ROS levels and depletes Glutathione (GSH), disrupting redox balance and inducing mitochondrial stress apoptosis in leukemia and multiple myeloma [45], colon cancer [46], and other cells. Similar effects were observed with Andro C-17 derivatives (Compound 4, Fig. 6) in non-small cell lung cancer A549 cells [47].

The p53 signaling molecule is crucial in the mitochondrial apoptosis pathway. Research indicates that Andro downregulates the p53 negative regulator Murine Double Minute 2 (MDM-2), leading to upregulation of p53 in gastric cancer SGC7901 and AGS cells. This upregulation inhibits B-cell lymphoma-2 (Bcl-2), disrupts Mitochondrial Membrane Potential ($\Delta\Psi m$), activates Caspase 9 and Caspase 3, increases Cleaved PARP levels, and ultimately induces mitochondrial apoptosis [48]. In glioma

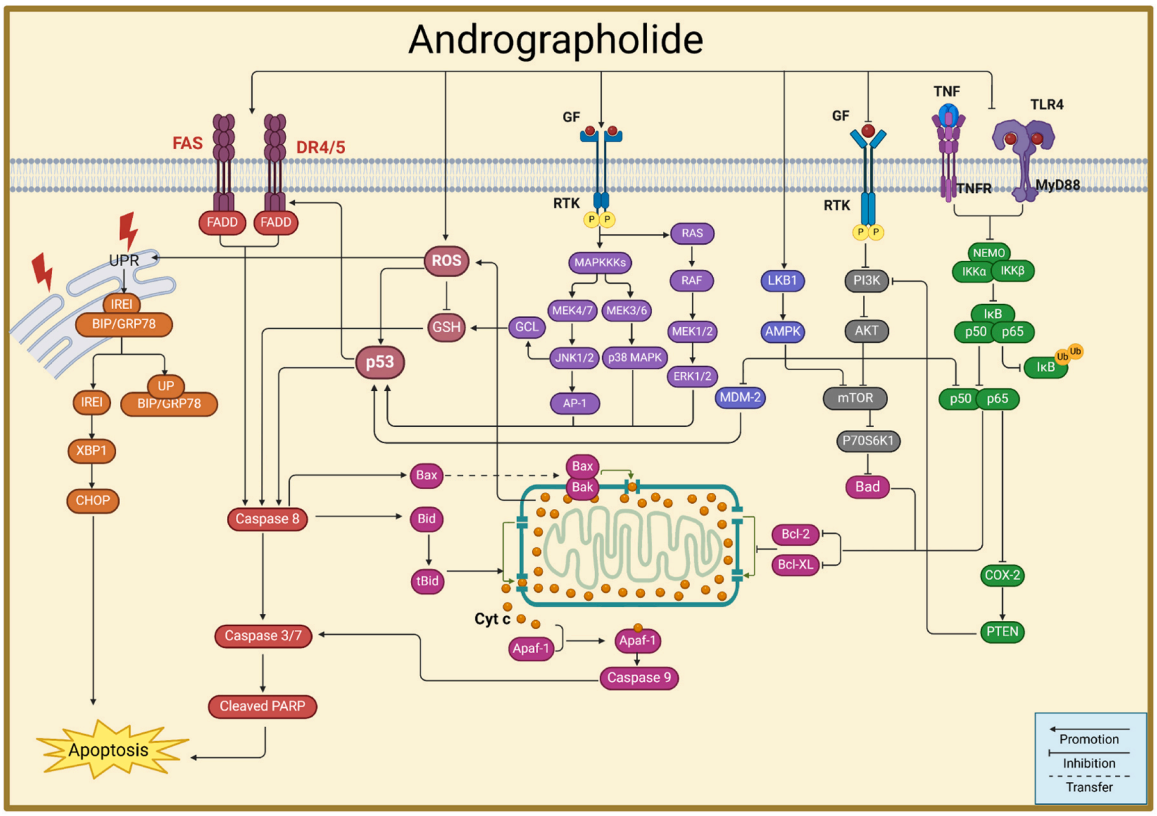

Fig. 7. Mechanism of andrographolide-induced endogenous, exogenous and endoplasmic reticulum stress-mediated apoptosis. Andrographolide regulates apoptosis in tumor cells induced by intracellular, exogenous, and endoplasmic reticulum stress by modulating MAPK, PI3K/AKT, NF-κB, LKB1/AMPK, and LncRNA, while disrupting redox homeostasis.

C6 cells, Andro increases p53 levels by upregulating ERK expression, activates Caspase 7, and upregulates Cleaved PARP to induce endogenous apoptosis [49]. Additionally, C-14 ester derivatives (Compounds 5 and 6, Fig. 6) induce apoptosis in renal cancer HEK-293 cells by upregulating p53, increasing the Bax/B-cell lymphoma-extra-large (Bcl-XL) ratio, activating Caspase 3, and inhibiting Nuclear Factor Kappa-B (NF-κB) [50]. In summary, Andro regulates p53 through various mechanisms to trigger endogenous apoptosis in tumor cells.

In addition to the aforementioned pathways, NF-κB, Phosphatidylinositol-3-Kinase (PI3K)/Protein Kinase B (AKT), and AMP-Activated Protein Kinase (AMPK) signaling pathways are crucial in disrupting mitochondrial integrity and inducing endogenous apoptosis in tumor cells. Studies have shown that Andro intervenes in multiple myeloma OPM1 cells by downregulating Toll-Like Receptor 4 (TLR4), inhibiting NF-κB expression, increasing Caspase 9/3 activation, and inducing apoptosis [51]. Moreover, Andro inhibits the PI3K/AKT pathway, thereby inducing mitochondrial-dependent apoptosis in bladder cancer T24 and 5637 cells [52]. Additionally, Andro activates Liver Kinase B1 (LKB1) and AMPK, inhibits Mammalian Target of Rapamycin (mTOR) activity, relieves the inhibition of Ribosomal Protein S6 Kinase (p70S6K) on BCL2-Associated Agonist of Cell Death (Bad), and activates mitochondria-mediated apoptosis in nasopharyngeal carcinoma C666–1 cells [53]. Furthermore, Andro reduces the binding of p65 to the promoter region of Cyclooxygenase-2 (COX-2) by downregulating p65, inhibits COX-2 expression, and diminishes COX-2's inhibition of Phosphatase and Tensin Homolog (PTEN). This results in the downregulation of PI3K and p-AKT, increases the Bax/Bcl-2 ratio, and triggers apoptosis in cervical cancer cells [54]. Molecular docking predictions suggest that Andro can directly bind to c-Jun and Caspase 3, upregulate their expression, and inhibit Burkitt lymphoma cell proliferation [55].

It is important to note that endogenous and exogenous apoptosis often occur simultaneously and interact with each other. Studies have shown that Andro derivatives (Compound 7, Fig. 6) trigger apoptosis in HCT116 cells by activating Caspase 8, which upregulates Truncated BH3 Interacting Domain Death Agonist (tBid) [56]. This indicates that pro-apoptotic Bcl-2 family members, such as Bid and Bax, act as key mediators, transmitting the Andro-initiated cell death signal from Caspase 8 to the mitochondria, and subsequently to downstream effector Caspases, ultimately triggering apoptosis.

Additionally, the role of Long Non-Coding RNA (LncRNA) in tumor cell proliferation has garnered significant attention. Our study found that Andro competes with Bcl-2 mRNA for binding to Human Antigen R (HuR) by upregulating LncRNA MIR22 HG. This interaction destabilizes Bcl-2 mRNA, reduces Bcl-2 protein expression, induces mitochondrial stress and Cytochrome C (Cyt C) release, activates the Caspase cascade, and ultimately triggers endogenous apoptosis in liver cancer cells [57]. However, research on Andro Andro 's impact on tumorigenesis and development through non-coding RNA regulation is still limited, highlighting the need for further investigation in this area.

3.2.1.3. Endoplasmic reticulum stress-mediated apoptosis. The endoplasmic reticulum (ER) is responsible for the proper folding of proteins. When ER stress occurs due to endogenous or exogenous factors, proteins cannot be correctly folded. Cells respond to the accumulation of misfolded or unfolded proteins in the ER through the unfolded protein response (UPR), which can trigger apoptosis. Thus, inducing ER stress may serve as an effective strategy for promoting tumor cell apoptosis. Consistent with this hypothesis, Andro triggers ER stress by increasing ROS levels, leading to an accumulation of improperly folded proteins. It competes with Inositol-Requiring Enzyme 1 (IRE1) for binding to Immunoglobulin Heavy Chain-Binding Protein (BIP)/Glucose-Regulated Protein 78 (GRP78). IRE1 enhances the expression of C/EBP Homologous Protein 10 (CHOP) by promoting the maturation of X-Box Binding Protein 1 (XBP1) mRNA. CHOP subsequently upregulates the Bax/Bcl-2

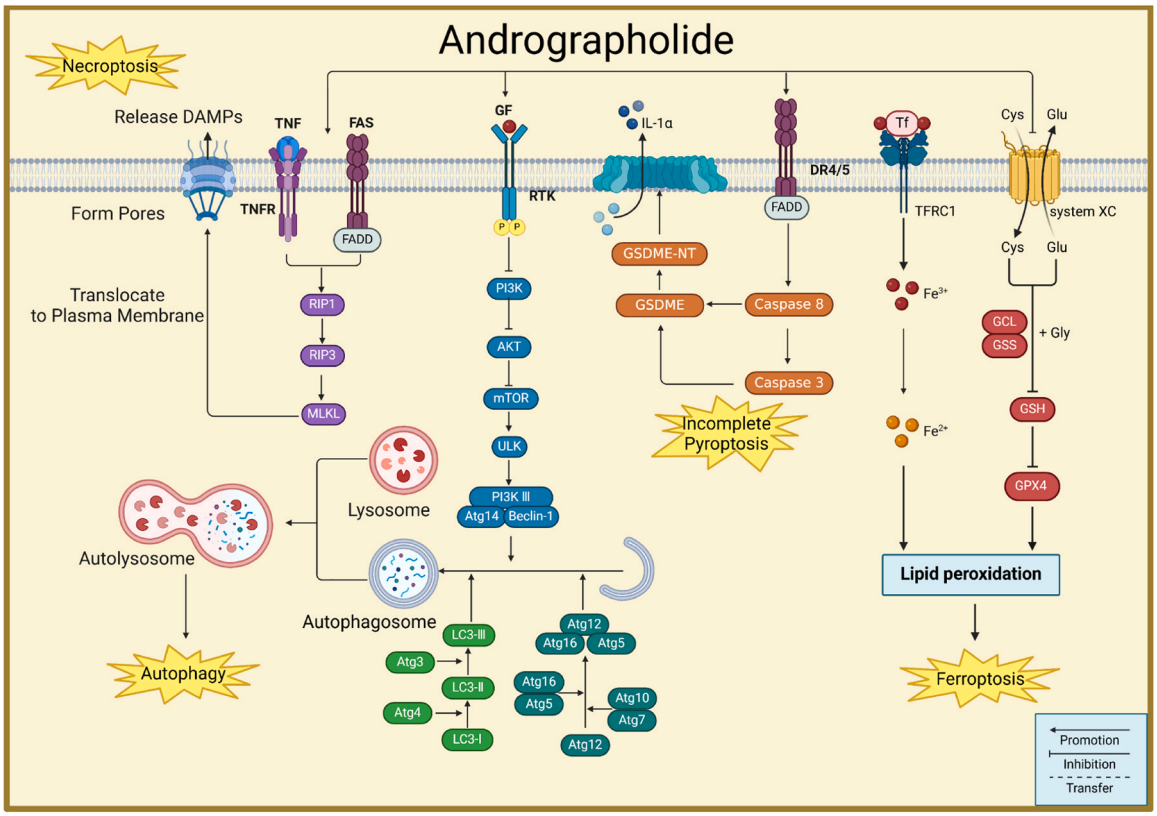

Fig. 8. Mechanism of andrographolide-induced necroptosis, autophagic death, ferroptosis and pyroptosis. Andrographolide regulates necroptosis by upregulating necroptosis-related proteins while exerting antiviral effects. It also regulates autophagic cell death by modulating the PI3K/AKT/mTOR pathway, ferroptosis by affecting intracellular redox homeostasis and the Nrf2/HO-1 pathway, and pyroptosis by inducing GSDME cleavage.

ratio, activating the mitochondrial apoptosis pathway in colon cancer Colo 205 and T84 cells [58,59]. This indicates an intersection between ER stress-mediated apoptosis and mitochondrial-mediated endogenous apoptosis at the molecular level. However, reports on Andro-induced ER stress-mediated apoptosis in tumor cells are still limited, suggesting a need for further research, which could facilitate the development of targeted therapies.

3.2.1.4. Necroptosis. Necroptosis is a form of programmed cell death that resembles necrosis, characterized by cell membrane destruction and swelling of both the cell and organelles. It serves as a defense mechanism against viral infections. The Epstein-Barr virus (EBV) infection cycle includes both lytic and latent phases, with the lytic phase closely associated with the development of head and neck cancers. Studies have demonstrated that Andro inhibits the transcription factors Myocyte Enhancer Factor 2D (MEF2D), Specificity Protein 1 (SP1), and SP3 by upregulating the expression of DNA Methyltransferases (DNMT) 1, DNMT3B, and Histone Deacetylase (HDAC) 5. This inhibition reduces EBV lysis and reactivation. Concurrently, Andro promotes the expression of key necroptosis molecules, including Receptor-Interacting Protein Kinase (RIPK) 1, RIPK3, and Mixed Lineage Kinase Domain-Like Protein (MLKL), thereby inducing necroptosis in EBV-positive human nasopharyngeal carcinoma HONE1-EBV cells and oral squamous cell carcinoma SCC25-EBV and HSC1-EBV cells [60]. These findings suggest that Andro, with its antiviral properties, holds potential for treating viral infection-related tumors.

3.2.2. Autophagic death

Autophagy is a self-degradation process that occurs in normal cellular function. Under conditions of nutrient deficiency, autophagy promotes cell survival; however, excessive autophagy can lead to autophagic cell death, which has become a target for cancer treatment. Studies have demonstrated that Andro can activate the Unc-51 like kinase (ULK) complex by inhibiting the expression of PI3K class I, AKT, and mTOR in osteosarcoma MG-63 and U-2OS cells, subsequently activating the PI3K class III complex. The PI3K class III complex includes Beclin-1, which recruits various proteins involved in the maturation and extension of autophagosomes. Additionally, Andro treatment led to an increased expression level of Autophagy-related protein 5 (ATG5) and a decreased ratio of Microtubule-associated protein 1 light chain 3 (LC3B) I/II, which induced autophagic cell death. Moreover, Andro simultaneously activated Jun N-terminal kinase (JNK); JNK-specific inhibitors reduced ATG5 expression and the decline in the LC3B I/II ratio [61]. Andro can induce autophagic cell death of tumor cells through mitochondrial stress, oxidative stress, inhibition of the PI3K/AKT/mTOR signaling pathway, and activation of the JNK signaling pathway. Furthermore, studies on its derivatives revealed that the C-14 modified derivative AG-4 of Andro (Compound 8, Fig. 6) can disrupt mitochondrial membrane permeability and induce mitochondrial-mediated apoptosis by increasing ROS levels. This derivative can also induce autophagic death and apoptosis in leukemia U937 cells by inhibiting the PI3K/AKT/mTOR pathway, with both processes influencing each other during compound 8-mediated cell death [62]. This suggests that autophagic death and apoptosis can occur simultaneously and interact. However, as autophagy is a "double-edged sword," it is essential to be cautious when interpreting experimental results. Given that autophagic cell death is significant for treating apoptosis-resistant tumors, Andro shows considerable potential as a therapeutic agent for controlling the progression of such tumors.

3.2.3. Ferroptosis

Ferroptosis is an iron-dependent form of regulated cell death

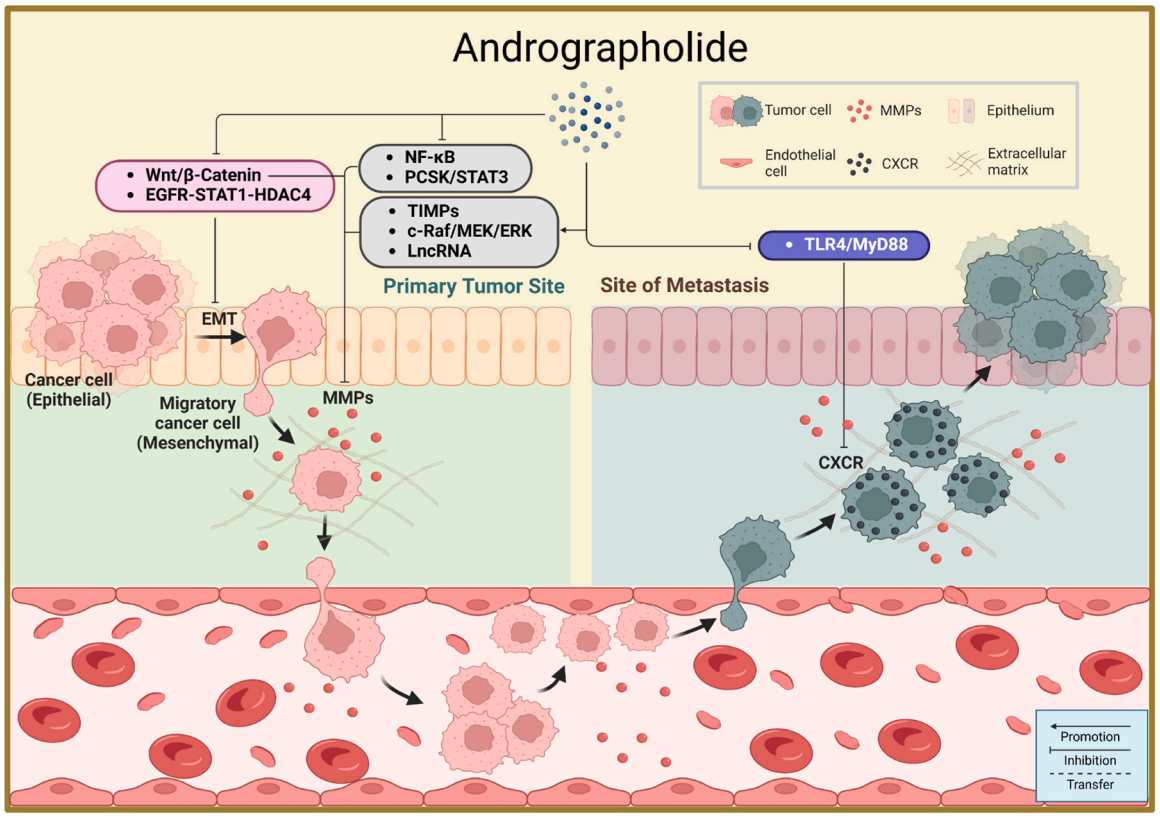

Fig. 9. Mechanism of andrographolide against invasion and migration. Andrographolide reverses EMT by regulating Wnt/β-catenin, EGFR/STAT1/HDAC4 to reduce migratory ability. It also decreases extracellular matrix damage by inhibiting MMPs through the regulation of NF-κB, PCSK/STAT3, TIMPs, MAPK, and LncRNA. Additionally, the migration ability of tumor cells is inhibited by modulating TLR4/MyD88.

characterized by excessive oxidation of polyunsaturated fatty acids and rupture of the plasma membrane. Transferrin (TF) binds to Fe^{3+} and facilitates its entry into cells through Transferrin Receptor 1 (TFRC1), where Fe^{3+} is reduced to Fe^{2+}. Fe^{2+} then generates hydroxyl radicals through the Fenton reaction, triggering lipid peroxidation. To counteract lipid peroxidation, Glutathione Peroxidase 4 (GPX4) converts lipid hydroperoxides into lipid alcohols using GSH, which is reduced from extracellular cystine by the system XC composed of Solute Carrier Family 7 Member 11 (SLC7A11) and SLC3A2. Studies have shown that Andro inhibits the expression of SLC7A11 and GPX4, leading to mitochondrial dysfunction, increased ROS, membrane potential damage, and GSH depletion in tumor cells, thus accelerating ferroptosis in H460 and H1650 cells [63]. Nuclear factor erythroid 2 related factor 2 (Nrf2) is a key regulator of the antioxidant response, promoting the transcription of Heme oxygenase 1 (HO-1) and mitigating lipid peroxidation. Andro inhibited the expression of Nrf2 and HO-1 by activating P38 mitogen-activated protein kinase (p38), which increased lipid peroxidation, downregulated GPX4 and SLC7A11, and ultimately induced ferroptosis in RPMI-8226 and U266 cells [64]. Although research on Andro-induced ferroptosis remains limited, tumor cells that are resistant to apoptosis may still be susceptible to other forms of programmed cell death, particularly in the context of chemotherapy resistance linked to apoptosis inhibition. Therefore, using natural products such as Andro to induce ferroptosis offers a promising and innovative strategy for overcoming drug resistance in tumors. By targeting specific cellular pathways and mechanisms, ferroptosis presents a unique approach to circumvent resistance and enhance treatment outcomes, making it an attractive area for future cancer therapeutic research and development. Exploring the targets of Andro in triggering ferroptosis is of significant importance.

3.2.4. *Pyroptosis*

Pyroptosis is a recently discovered form of programmed cell death, also known as Gasdermin (GSDM)-mediated programmed necrosis, resulting from extracellular or intracellular homeostasis disorders related to innate immunity. Inflammatory caspases (Caspase 1/4/5/11) are activated during pyroptosis. These activated caspases cleave Gasdermin D (GSDMD) at a specific site between the N-terminus and the C-terminus, releasing the N-terminal fragment from the inhibitory C-terminal domain. The N-terminal fragment of GSDMD (GSDMD-NT) binds to phosphatidylinositol on the inner side of the plasma membrane, forming pores that induce cell lysis and release pro-inflammatory cytokines such as Interleukin-1 (IL-1) and IL-18. Pyroptosis not only regulates physiological processes such as cell proliferation, stress response, and homeostasis but also acts as a tumor suppressor mechanism. Reports have shown that morphological characteristics of pyroptosis, Lactate dehydrogenase (LDH) release, and GSDME cleavage were observed in breast cancer MCF-7 cells treated with Andro combined with Tumor Necrosis Factor-Related Apoptosis-Inducing Ligand (TRAIL). This suggests that Andro can induce pyroptosis through GSDME cleavage and enhance TRAIL-induced tumor inhibition [65]. Additionally, recent studies have indicated that a small number of tumor cells undergoing pyroptosis can effectively regulate the tumor immune microenvironment, thereby activating T cell-mediated anti-tumor immune responses [66]. Considering that Gasdermin family proteins may serve as potential biomarkers for tumor immunotherapy, developing agonists for these proteins could provide new strategies for cancer treatment.

3.3. *Inhibition of tumor cell invasion and migration*

Tumor cell migration and invasion are crucial aspects of tumor development and are major contributors to tumor proliferation and metastasis. Thus, inhibiting the invasion and systemic spread of tumors

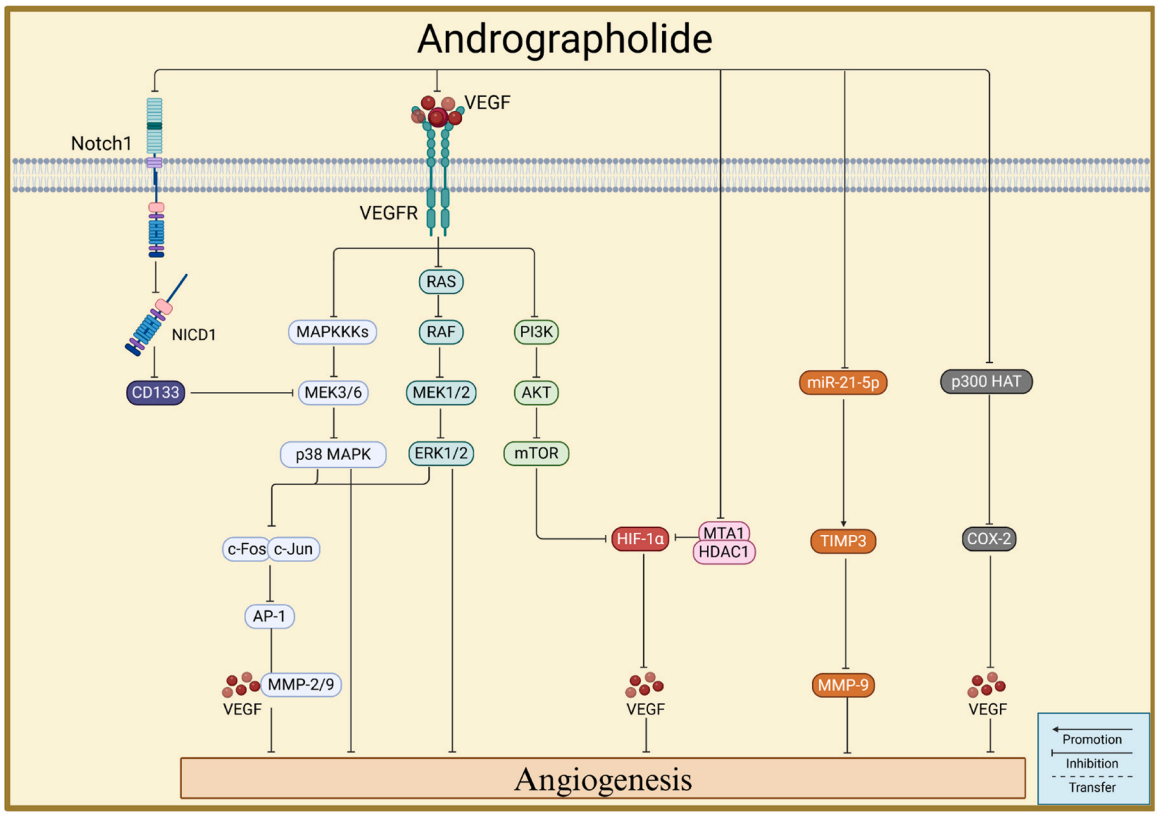

Fig. 10. Mechanism of andrographolide against angiogenesis. Andrographolide inhibits angiogenesis by regulating MAPK, Notch1, PI3K/AKT/mTOR, p300 HAT, and miR-21–5p to downregulate the expression and interaction of VEGF and VEGFR.

to adjacent normal tissues is essential for improving patient prognosis. The process of tumor invasion and metastasis involves several key stages: detachment of tumor cells from the extracellular matrix (ECM), invasion of surrounding tissue and the basal membrane, infiltration into the bloodstream, metastasis and survival in the circulation, migration, stagnation, and extravasation at distant sites, and ultimately the formation of metastases. These stages require angiogenesis, matrix degradation, disruption of cell-to-cell and cell-to-matrix adhesion, and increased cell motility (Fig. 9).

3.3.1. *Inhibit of Epithelial-Mesenchymal Transition*

Compared to normal cells, tumor cells undergo a loss of epithelial cell characteristics (such as decreased expression of E-cadherin and cytoskeletal keratin) and acquire mesenchymal phenotypes (such as increased expression of N-cadherin and Vimentin). This process, known as Epithelial-Mesenchymal Transition (EMT), is crucial for tumor invasion. Andro can inhibit the EMT process by blocking the Wnt/β-catenin signaling pathway, thereby reducing the invasion capability of osteosarcoma. Studies have shown that Andro inhibits β-catenin dissociation by targeting GSK-3β, decreases β-catenin accumulation in tumor cells, prevents its translocation to the nucleus, and its binding to TCF/Lymphoid Enhancer-Binding Factor (LEF). This action downregulates Vimentin and the E-cadherin repressor Snail, leading to increased expression of E-cadherin, thus inhibiting EMT and reducing the invasion and migration of osteosarcoma 143B and MG-63 cells, as well as decreasing lung metastasis in the 143B orthotopic tumor model [37]. Additionally, Andro reverses the EMT process by inhibiting the EGFR--STAT1-HDAC4 pathway, restoring E-cadherin expression, and decreasing levels of N-cadherin and Vimentin proteins, which ultimately inhibits the invasion and migration of MDA-MB-231 cells [67].

3.3.2. *Inhibit of matrix metalloproteinases*

Tumor cells can secrete Matrix Metalloproteinases (MMPs) to degrade the ECM, facilitating invasion and dissemination throughout the body via the circulatory system [68]. Tissue Inhibitor of Matrix Metalloproteinases (TIMP) inhibits MMP activity through non-covalent binding. Andro can upregulate TIMP-1 and TIMP-2, inhibit MMP-9 and MMP-2 activity, and thereby suppress the invasion of gastric cancer SGC7901 cells [69]. Additionally, Andro inhibits tumor metastasis by preventing the degradation of Inhibitor kappa B alpha (IκBα), reducing the nuclear translocation of NF-κB p65, and downregulating MMP-9 expression in breast cancer [70,71]. The Andro analogue 19-O-triphenylmethyl Andro (Compound 9, Fig. 6) inhibits β-catenin nuclear translocation by preventing β-catenin phosphorylation and its binding to TCF/LEF, thereby reducing MMP-7 expression and inhibiting colon cancer cell metastasis [72]. Furthermore, knockdown of proprotein convertase subtilisin/kexin type 5 (PCSK5) reduces the expression of p-STAT3 and MMPs, and inhibits the invasion of glioblastoma cells induced by IL-6, with a more pronounced inhibitory effect when combined with Andro intervention [73]. In glioma research, Andro activates ERK through the c-Raf/MAP kinase kinase (MEK)/ERK pathway, inhibiting the DNA-binding activity of Cyclic AMP-responsive Element-Binding Protein (CREB) in the MMP-2 promoter region and reducing MMP-2 expression [74]. Although non-coding RNAs, such as LncRNAs, have been extensively studied for their role in regulating tumor metastasis, research on Andro's effects through non-coding RNAs is limited. However, it has been found that Andro upregulates MIR22 HG and its derivative miR-22–3p, inhibits the expression of its target molecule High Mobility Group Box 1 (HMGB1), and decreases downstream factor MMP-9, thereby inhibiting liver cancer metastasis both in vitro and in vivo [57].

Tumor cells can recruit fibroblasts, macrophages, and other cells, which secrete MMPs in an inflammatory environment to degrade the ECM and facilitate metastasis. Studies have shown that Andro derivatives (Compound 10, Fig. 6) can prevent IL-4 and IL-13-induced macrophages from transforming into M2-like phenotypes, inhibit the

mRNA expression of MMP-2 and MMP-9 in these M2-like macrophages, and reduce the migration and invasion of 4T1 breast cancer cells under the influence of the conditioned medium from M2-like macrophages [75]. In summary, Andro inhibits MMPs through multiple mechanisms, thereby preventing tumor metastasis.

3.3.3. Inhibition of chemokine receptors

Chemokine receptors on cancer cells influence the site of metastasis. Specific chemokines produced by metastatic sites can attract circulating cancer cells to migrate to the "pre-metastatic niche," creating favorable conditions for tumor cell colonization. Andro can downregulate the expression of chemokine receptors to inhibit tumor metastasis. Reports indicate that Andro reduced the migration ability of prostate cancer PC3 and DU145 cells by inhibiting CXC chemokine receptors (CXCR) 3 and CXCR7 [76]. Additionally, Andro inhibited the expression of Myeloid Differentiation Primary Response 88 (MyD88) by targeting TLR4 in melanoma B16 cells, thereby preventing IκBα phosphorylation, reducing the nuclear translocation of p65 and p50, and blocking NF-κB binding to the CXCR4 promoter, which ultimately inhibited tumor migration. Furthermore, B-cell lymphoma 6 protein (Bcl-6) promotes CXCR4 expression, and Andro's inhibition of Bcl-6 further downregulates CXCR4 [77].

3.4. Inhibit angiogenesis

As tumor tissue grows, existing blood vessels can no longer supply sufficient oxygen and nutrients, necessitating the formation of new blood vessels for continued exponential growth; otherwise, the tumor will cease growing or even die. Therefore, inhibiting tumor angiogenesis is a crucial anti-tumor strategy. Andro can inhibit tumor angiogenesis by targeting and suppressing Vascular Endothelial Growth Factor (VEGF) and Vascular Endothelial Growth Factor Receptor (VEGFR) (Fig. 10).

3.4.1. Inhibition of VEGF

VEGF is a key signaling molecule involved in angiogenesis. Under normal physiological conditions, VEGF facilitates wound healing and tissue regeneration. However, in disease states such as cancer, overexpression of VEGF can drive pathological angiogenesis, accelerating the growth and metastasis of malignant tumors. Andro can regulate VEGF by influencing several molecules, including Activator Protein-1 (AP-1), Hypoxia-Inducible Factor-1α (HIF-1α), and COX-2.

3.4.1.1. AP-1. AP-1 is a heterodimer composed of c-Fos and c-Jun. Activated AP-1 can promote the expression of downstream target genes such as VEGF and MMPs, which in turn facilitate the migration of vascular endothelial cells to form new blood vessels by degrading the vascular basement membrane and extracellular matrix. Reports indicate that Andro reduces AP-1 binding to DNA by promoting the ubiquitin-dependent proteasome degradation of c-Fos, thereby inhibiting VEGF mRNA and protein expression in hepatocellular carcinoma cells Hep3B and HepG2 [78]. Additionally, the Neurogenic locus notch homolog protein 1 (Notch1)/Mitogen-Activated Protein Kinase (MAPK) signaling axis regulates tumor angiogenesis. Studies have shown that Andro downregulates CD133 expression at the transcriptional level by inhibiting the Notch1 Intracellular Domain 1 (NICD1), which reduces the phosphorylation of MEK3/6 and p38. This inhibition decreases the expression of c-Jun and c-Fos, reduces AP-1 nuclear translocation, downregulates VEGF and MMP-2/9, and ultimately inhibits $CD133^{+}$ tumor stem cell-mediated melanoma angiogenesis, self-growth, and lung metastasis [79].

3.4.1.2. HIF-1α. HIF-1α is a critical regulatory molecule in response to hypoxia, promoting cell survival and angiogenesis. HIF-1α activates transcription by binding to Hypoxia Response Elements (HRE) in the VEGF promoter. Research has shown that the stability of HIF-1α is associated with a complex formed by Recombinant Metastasis Associated Protein 1 (MTA1) and HDAC1. Andro inhibits the formation of this complex by downregulating MTA1 and HDAC1, thereby promoting the ubiquitination of HIF-1α in Hep3B and HepG2 cells and ultimately inhibiting VEGF expression [80].

3.4.1.3. COX-2. COX-2 is a significant regulator of the angiogenic environment, stimulating tumor angiogenesis by upregulating VEGF expression. COX-2 expression is regulated by the recruitment of transactivators and coactivators to its promoter regions. Andro has been shown to significantly inhibit the binding of various transactivators, including CREB2, c-Fos, and NF-κB, to the COX-2 promoter, and it blocks the recruitment of coactivator p300. Additionally, Andro effectively inhibits p300 Histone Acetyltransferase (HAT) activity, thereby reducing p300-mediated NF-κB acetylation and its binding to the COX-2 promoter region. Consequently, Andro inhibits COX-2 transcriptional activation and tumor angiogenesis in breast cancer MDA-MB-231 cells [81]. Notably, the regulatory relationship between HIF-1α and COX-2 and its role in Andro's inhibition of tumor angiogenesis remains to be elucidated.

3.4.2. Inhibition of VEGFR

Increased expression of VEGFR in tumor cells reduces their reliance on VEGF. Therefore, inhibiting VEGFR or blocking VEGF-VEGFR binding is a crucial strategy for anti-angiogenesis. Studies on Andro in colon cancer T84 and Colo205 cells have shown that Andro inhibits VEGF activation by downregulating VEGFR and upregulating the anti-angiogenic factor Thrombospondin 2 (TSP-2), thereby suppressing tumor angiogenesis [82]. Additionally, molecular docking simulations revealed that Andro has high affinity for VEGFR2 and can compete with VEGF for binding to VEGFR2 in breast cancer 4T1 cells, preventing angiogenesis signal transduction [83]. In hepatocellular carcinoma Hep3B cells, Andro inhibits the binding of VEGFA to VEGFR2, prevents the phosphorylation of downstream signaling molecules such as MAPKs, and ultimately inhibits tumor angiogenesis [84]. Andro-derived Compound 10 inhibits the phosphorylation and activation of signaling molecules related to vascular and cancer cells, including VEGFR2, MAPK1/2, ERK1/2, mTOR, AKT, and p38. Additionally, it effectively inhibits the phosphorylation of proteins associated with cell proliferation and survival (e.g., AKT, mTOR, and ERK1/2) and reduces VEGF expression in HT-29 colon cancer cells [85]. Research using the Chick Chorioallantoic Membrane (CAM) model demonstrated that Andro inhibits breast cancer angiogenesis in a concentration-dependent manner. It was found that Andro upregulates TIMP3 by downregulating miR-21–5p in human umbilical vein endothelial cells (HUVECs), blocking VEGF-VEGFR2 binding, and inhibiting MMP-9 expression [86]. In summary, Andro inhibits tumor angiogenesis through multiple pathways.

3.5. Inhibit immune escape

As tumors develop and undergo radiotherapy and chemotherapy, the body's immune system becomes compromised. However, the immune system can still monitor and eliminate tumor cells. Tumor cells evade immune surveillance by altering their antigenicity through changes in antigen expression, often retaining cells with low immunogenicity after undergoing multiple immune selections due to their high proliferation and mutability. Consequently, there is a critical need for drugs that can inhibit immune escape during tumor therapy (Fig. 11).

Normal cells induce T cell death by expressing Programmed Cell Death-Ligand 1 (PD-L1) and binding to Programmed Death 1 (PD-1) on activated T cells, thereby preventing excessive T cell activation and protecting normal tissues. Tumor cells exploit this mechanism to evade the immune response by upregulating PD-L1. Research has demonstrated that Andro inhibits the phosphorylation of Janus Kinase 2 (JAK2)

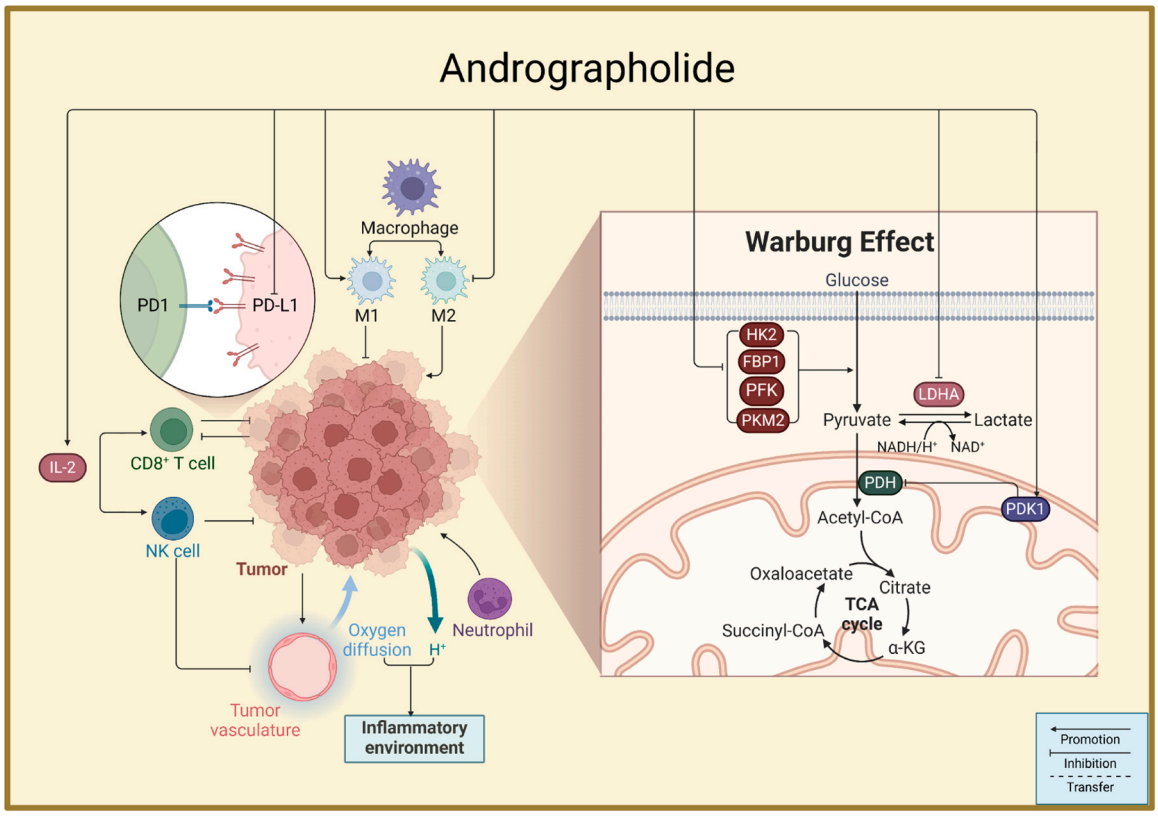

Fig. 11. The mechanism of andrographolide immunomodulatory, reprogramming energy metabolism and destroying tumor microenvironment. Andrographolide inhibits tumor immune escape by regulating JAK2/STAT3. It also reprograms the glucose metabolic pathway by downregulating glycolysis-related proteins and upregulating gluconeogenesis-related proteins. Additionally, it disrupts the tumor inflammatory microenvironment by modulating Wnt5a/β-Catenin and NF-κB.

and Signal Transducer and Activator of Transcription 3 (STAT3) by inducing ROS accumulation. This inhibition reduces PD-L1 expression and increases the expression of p62. The p62-PD-L1 complex undergoes selective autophagy and degradation, further decreasing the amount of PD-L1 on the surface of tumor cells and thereby enhancing the immune response of $CD8^+$ T cells against lung cancer [87].

3.6. Reprogramming energy metabolism of tumor cells

Normal cells primarily generate ATP through oxidative phosphorylation under aerobic conditions and rely on glycolysis under anaerobic conditions. Tumor cells, however, exhibit increased energy and macromolecule demands due to rapid proliferation and preferentially utilize glycolysis even in the presence of oxygen, a phenomenon known as the Warburg effect. Despite glycolysis producing less energy, tumor cells adapt by enhancing glycolytic efficiency to compensate for the energy deficit [88]. Andro inhibits tumor development by disrupting both oxidative phosphorylation and glycolysis (Fig. 11).

Pyruvate dehydrogenase complex (PDH) converts pyruvate into acetyl-CoA for mitochondrial oxidative phosphorylation, while Pyruvate Dehydrogenase Kinase 1 (PDK1) inhibits PDH activity through phosphorylation of its E1 subunit, leading to increased pyruvate conversion to lactic acid and reduced oxidative phosphorylation. Andro has been found to inhibit PDK1 expression, thereby alleviating PDH inhibition, increasing pyruvate conversion to acetyl-CoA, and reducing the production of proliferative raw materials, which contributes to its anti-non-small cell lung cancer activity [89]. Additionally, Andro suppressed the proliferation of thyroid cancer 8505 C and CAL 62 cells by down--regulating glycolysis-related proteins such as Hexokinase 2 (HK2), Pyruvate Kinase M2 (PKM2), Phosphofructokinase (PFK), and Lactate Dehydrogenase A (LDHA) [90]. Further studies revealed that Andro inhibited the proliferation of non-small cell lung cancer H1975 cells by up-regulating gluconeogenesis-related proteins like Phosphoenolpyruvate Carboxykinase 1 (PEPCK1), Fructose-bisphosphatase 1 (FBP1), and PFK, while down-regulating PKM2, LDHA, and GLUT1. This regulation reduced glucose uptake, lactate release, and ATP synthesis, promoted gluconeogenesis, and altered glucose metabolism pathways [91]. Moreover, Andro has been shown to target pathways such as HIF-1α, NF-κB, MAPK-Src, AP-1, JAK/STAT, Nrf2/Kelch-like ECH-associated protein 1 (Keap1), and AMPK to influence glucose metabolism [92], though its precise impact on tumor cell energy metabolism requires further investigation.

3.7. Destroying tumor inflammatory microenvironment

TME is a complex network encompassing tumor cells, immune cells, blood vessels, fibroblasts, and extracellular matrix components. These elements interact to influence tumor progression through various mechanisms such as promoting migration, angiogenesis, and inhibiting immune cell activity. Andro can impede tumor development by improving the inflammatory microenvironment (Fig. 11).

Cancer progression is often linked to chronic inflammation. Tumor-Associated Macrophages (TAMs), particularly M2 macrophages, contribute to an immunosuppressive TME by secreting cytokines that promote tumor progression. Research indicates that Andro regulates the Wnt5a/β-Catenin signaling pathway, inhibits the M2-like polarization of TAMs, enhances M1-like polarization, and reduces the secretion of immunosuppressive factors such as platelet-derived growth factor-AA (PDGF-AA) and C-C motif chemokine ligand 2 (CCL2) in M2 macrophages. This action results in decreased angiogenesis and tumor development in breast cancer [93]. Furthermore, Andro inhibits NF-κB activation in monocytes/macrophages, leading to reduced release of pro-inflammatory cytokines including CCL2, C-X-C motif chemokine 10 (CXCL10), Tumor Necrosis Factor-α (TNF-α), and Interferon-γ (IFN-γ).

Table 2
Application of andrographolide combined with other therapies in the treatment of tumors.

Disease	Animal/cell model	Types	Routes	Dose	Effects and related mechanisms	Ref
Colon	HCT116, HCT116/5-FUR cell	**In vitor**	-	Andro: 10 μM	↑ Bax, Cleaved Caspase 3, Cleaved PARP	[112]
	HCT116/5-FUR subcutaneous xenograft in Nude mice	**In vivo**	ip	5-Fu: 0–8 mM Andro: 5 mg/kg 5-Fu: 25 mg/kg		
	KRAS mutated HCT116, LoVo cell	**In vitor**	-	Andro: 4, 8 μM	↑ E-cadherin ↓ PDGFRβ, EGFR, p-EGFR, p-PI3K, p-AKT, Vimentin, C-Myc, MMP−7, β-catenin	[114]
	LoVo and HCT116 Subcutaneous xenograft and tail vein injection of lung metastases in BALB/c nude mice	**In vivo**	po ip	Cetuximab: 10, 20 μM Andro: 30 mg/kg Cetuximab: 2 mg/kg		
	HCT116 cell	**In vitor**	-	Andro: 10 μM	↑ Cleaved Caspase 3 ↓ Caspase 3, p-MET, p-AKT, p-ERK1/2	[115]
	HCT116 subcutaneous xenograft of BALB/c nude mice	**In vivo**	po ip	5-Fu: 4.28 μM Andro: 10 mg/kg 5-Fu: 10 mg/kg		
	HCT116 cell	**In vitor**	-	Andro: 5 μM CDDP: 15 μM	↑ Cleaved Caspase 3, p-EIF2α, ATF4, CHOP ↓ CDC2, Cyclin B1, MDM2, Caspase 3, p-STAT3	[120]
	LoVo cell	**In vitor**	-	Andro: 10 μM	↑ Bax, tBid, Cyto-Cyt c, FasL, Fsa, Cleaved Caspase 9, Cleaved Caspase 8, Cleaved Caspase 3 ↓ Bcl−2, Mito-Cyt c	[121]
	LoVo subcutaneous xenograft BALB/c nude mice	**In vivo**	po ip	CDDP: 10, 15 μM Andro: 10 mg/kg CDDP: 6 mg/kg		
	HCT116 cell	**In vitor**	-	Andro: 20 μM Radiate: 6 Gy	↓ PI3K/p85, PI3K/p110, AKT, p-AKT, mTOR, p-mTOR, PFK1, HK2, GLUT1	[130]
Liver cancer	HepG2 cell	**In vitor**	-	Andro: 400 nM	↑ Cleaved Caspase 3 ↓ Caspase 3, EphB4	[119]
	HepG2 subcutaneous xenograft in BALB/c nude mice	**In vivo**	ip ip	As_2O_3: 6.23 μM Andro: 20 mg/kg As_2O_3: 5 mg/kg		
	SMMC7721 cell	**In vitor**	-	Andro: 200 μM Tan II: 50 μM	↑ ROS, p53, PUMA	[123]
Kidney cancer	SK-NEP−1 cell	**In vitor**	-	Andro: 10–25 μM	↑ p-p53 ↓ p-AKT, p-ERK	[117]
	SK-NEP−1 subcutaneous xenograft in BALB/c-nude mice	**In vivo**	po ip	Vincristine: 10.8 nM ; Andro: 100 mg/kg ; Vincristine: 0.2 mg/kg		
	H-Ras transformed RK3E cells	**In vitor**	-	Andro: 10 μM ;	↓ MMP−2, p-pERK1/2, p65	[135]
	Ras transformed cells subcutaneously xenografted and tail vein injected with BALB/cAnN-Foxn1nu/CrlNarl male nude mice	**In vivo**	po	Radiate: 2, 4 Gy Andro: 10 μM ; Radiate: 2 Gy		
Lung cancer	A549/DDP−500 cell	**In vitor**	-	Andro: 7.5–30 μM	↑p62, p-AKT, p-mTOR ↓ PTEN, LC3B	[111]
	A549/DDP−500 subcutaneous xenograft NCR-nude female mice	**In vivo**	ip ip	CDDP: 33.33 μM CDDP: 0.75 mg/kg Andro: 5 mg/kg		
	A549, Lewis lung cancer cells cell	**In vitor**	-	Andro: 30 μM	↑ Cleaved PARP, p62 ↓ ATG5, LC3B-II/I	[116]
	LLC subcutaneous xenograft and in situ injection of C57BL/6 mice	**In vivo**	ip ip	CDDP: 0–10 μM Andro: 5, 20 mg/kg CDDP: 0.75 mg/kg		
Lymphoma	MCF−7 cell	**In vitor**	-	Andro: 200 μM Tan II: 50 μM	↑ ROS, p53, Bax, PUMA	[123]
	MCF−7, T47D cell	**In vitor**	-	Andro: 20 μM	↑ ROS ↓ ESR1, C-Myc, Cathepsin D, FOXM1	[125]
	MCF−7 subcutaneous xenograft in BALB/c athymic nude mice	**In vivo**	ig ip	Fulvestrant: 4 μM Andro: 150 mg/kg Fulvestrant: 5 mg/kg		
Ovaries	H22 intraperitoneal injection Male Kunming mice	**In vivo**	ig ip	Andro: 25, 50, 100 mg/kg BLM: 15 mg/kg	↑ p53, p21, Caspase 8, Caspase 3activity ↓ CyclinD1, Cyclin E1	[118]
	SKOV3 subcutaneous xenograft in BALB/C nude mice	**In vivo**	ig	Andro: 50, 100, 200, 300, 400 mg/kg Radiate: 4 Gy	↑ Caspase 3activity, Bax, LC3BII, ATG5, p-p53 ↓Bcl−2, LC3BI	[132]
Leukaemia	U937 cell	**In vitor**	-	Andro: 10 μM Topotecan: 0.05~0.3 μM	↑ Bax, Cyto-Cyt C, Cleaved Caspase 9, Cleaved Caspase 3 ↓ Bcl−2	[124]
Oral cancer	CAL−27 cell	**In vitor**	-	Andro: 16 μM	↑ p-p53, p-AKT	[136]
	CAL−27 Subcutaneous xenograft Female BALB/c-nude mice	**In vivo**	po ip	CDDP: 200 nM Andro: 50 mg/kg CDDP: 5 mg/kg		
Cervix	KBChR 8–5 cell	**In vitor**	-	Andro: 0, 2, 4 μM Dox: 0.1 μM	↑Caspase 9, Caspase 3 ↓ AKT, ABCB1	[113]
Laryngeal cancer	Hep−2 cell	**In vitor**	-	Andro: 0–30 μM Carboplatin: 0–300 μM	↑ ROS, Bax, Cleaved PARP, Cleaved Caspase 3, p-p38, p-JNK ↓ p-PI3K, p-AKT	[122]
Nasopharyngeal Carcinoma	HONE1, CNE1 cell	**In vitor**	-	Andro: 5 μM Radiate: 4 Gy	↑ RASSF1A, FoxO3a ↓ Nrf2, TXNRD1	[131]
	HONE1/HONE1-AGP subcutaneous xenograft male BALB/c nude mice	**In vivo**	-	Radiate: 4 Gy		

(*continued on next page*)

Table 2 (*continued*)

Disease	Animal/cell model	Types	Routes	Dose	Effects and related mechanisms	Ref
Esophageal cancer	ECA109 cell	In vitor	-	Andro: 342.4 μM Radiate: 6 Gy	↑ Bax, Cleaved Caspase 3 ↓ Bcl−2, NF-κB	[133]
Intestinal mucositis	NCM 460 cell 5-Fu-induced intestinal mucositis in BALB/c mice	In vitor In vivo	- ig ip	Andro: 0–20 μM 5-Fu: 10 mM Andro: 25, 50, 100 mg/kg 5-Fu: 100 mg/kg	↑ Bcl−2 ↓ p-p38, p-p53, Bax, Cleaced Caspase 8/ Caspase 8, Cleaced Caspase 3/ Caspase 3	[126]
	HCT116, HT−29, CT26 cell CT26 subcutaneous homograft BALB/c mice	In vitor In vivo	- ip ip	Andro: 3 μM irinotecan: 30 μM Andro: 12.5, 25 mg/kg Irinotecan: 22.5, 45 mg/kg	↑ RAD51 ↓ p-IRF3, P-TBK1, γH2AX, cGAS, STING, TBK1, IRF3, IFN-b, CXCL10, CCL5	[127]
Myocardial cytotoxicity	H9C2 cell	In vitor	-	Andro: 0.5–10 μM Dox: 1 μM As_2O_3: 35 μM	↑ FRAP ↓ TLR4	[128]
	H9C2 cell Doxorubicin-induced cardiotoxicity in C57BL/6 mice	In vitor In vivo	- ig ip	Andro: 0–15 μM Dox: 1 μM Andro: 25, 50 mg/kg Dox: 3 mg/kg	↑ Bcl−2 ↓ Bax, NLRP3, p20, IL−1β, TAP1, TIMP1	[129]
Lung injury	H22 intraperitoneal injection Male Kunming mice	In vivo	ig ip	Andro: 25, 50, 100 mg/kg BLM: 15 mg/kg	↑ Smad7 ↓ IL−1β, IL−6, TNF-α, TGF-β1, p-Smad2/3, α-SMA	[118]
	Bone marrow-derived macrophage 18 Gy whole chest irradiation-induced lung injury in C57BL/6 mice	In vitor In vivo	- ip	Andro: 0, 3, 30 μM Radiate: 8 Gy Andro: 5, 10, 20 mg/kg Radiate: 18 Gy	↑ Caspase 1 p20/p10, GSDMD ↓ IL−1β, IL−6, TNF-α, α-SMA, AIM2	[134]

↓indicates inhibition/reduction, while ↑indicates increase/promotion; ip, Intraperitoneal; ig, Intragastric; po, Oral administration.

Additionally, Andro down-regulates α4 integrin, impeding its adhesion to endothelial cells and decreasing monocyte/macrophage infiltration. This effect inhibits arterial dilation (a marker for abdominal aortic aneurysm progression), endothelial cell death, and elastin degradation in a mouse model of abdominal aortic aneurysm [94].

4. Improve the application potential of Andro in the treatment of cancer

Currently, the primary methods for treating tumors include surgical resection, radiotherapy, and chemotherapy. However, due to the increasing prevalence of single treatments and the genetic instability of tumors, resistance frequently develops. Additionally, the toxic and side effects of these therapies cannot be overlooked. Therefore, strategies to address these issues include reversing drug resistance or enhancing the sensitivity of radiotherapy and chemotherapy, as well as employing synergistic and attenuating effects through combined therapies. Furthermore, despite the notable anti-tumor activity of Andro, its terpene skeleton and lactone ring contribute to its low polarity, resulting in poor water solubility. This low solubility leads to a slow dissolution rate, which affects drug absorption and reduces bioavailability. Consequently, modifying the chemical structure of Andro and developing drug delivery systems have become crucial strategies to enhance its anti-tumor application potential.

4.1. Combined application

Combining Andro with chemotherapeutic agents and radiotherapy offers several advantages, including reversing drug resistance, enhancing the sensitivity to radiotherapy and chemotherapy, and achieving synergistic effects. Furthermore, Andro can mitigate the toxic and side effects associated with conventional therapies (Table 2).

4.1.1. Combined with chemotherapy drugs

4.1.1.1. Reversal of drug resistance of tumor cells. Autophagy can both inhibit tumor growth and protect tumor cells from harmful substances under various conditions. Cisplatin (CDDP) can induce autophagy in tumor cells, leading to increased drug resistance. Andro, as an autophagy inhibitor, can enhance the cytotoxicity of CDDP. Studies have shown that in drug-resistant A549/DDP-500 cells compared to non-small cell lung cancer A549 cells, the AKT/mTOR pathway is inhibited, the level of p62 is reduced, and the autophagy-related protein LC3B-I is converted to LC3B-II. When combined with CDDP, Andro can inhibit PTEN, activate the AKT/mTOR pathway, increase p62 levels, reverse LC3B-I/II transformation, and ultimately reverse drug resistance, restoring tumor cell sensitivity to CDDP [111].

In HCT116 cells resistant to Fluorouracil (5-Fu), the expression of Bax, a key molecule in the endogenous apoptotic pathway, was significantly decreased. Andro was able to upregulate Bax expression, enhance mitochondrial-mediated apoptosis, and reverse drug resistance [112].

P-glycoprotein (P-gp), which is highly expressed in cervical cancer KBChR 8–5 cells, affects chemotherapy efficacy through a drug efflux mechanism. Andro reversed the resistance of KBChR 8–5 cells to Doxorubicin (Dox) by downregulating AKT and ATP-binding cassette subfamily B member 1 (ABCB1), thereby reducing P-gp expression [113].

The EGFR signaling pathway plays a critical role in cell proliferation and differentiation, with its inhibitor Cetuximab being used for colorectal cancer treatment. However, KRAS mutations can lead to abnormal activation of AKT independent of EGFR, resulting in drug resistance. Studies have shown that Andro can reverse the abnormal activation of AKT caused by KRAS mutation by inhibiting Platelet-Derived Growth Factor Receptor Beta (PDGFRβ) and downregulating the expression of PI3K and AKT, thereby restoring the efficacy of Cetuximab [114].

4.1.1.2. Enhanced chemosensitivity of tumor cells. Andro can enhance the cytotoxic effects of chemotherapy drugs and increase the sensitivity of tumor cells to chemotherapy at doses that are generally non-toxic to these cells. C-Mesenchymal-Epithelial Transition Factor (c-MET), a hepatocyte growth factor receptor tyrosine kinase, can activate various downstream signaling pathways, including ERK 1/2 and PI3K/AKT, which mediate tumor cell proliferation, metastasis, and angiogenesis. Studies have demonstrated that Andro increased the sensitivity of

colorectal cancer cells to 5-Fu by inhibiting the phosphorylation of c-MET in 5-Fu-treated HCT116 cells and downregulating the expression of AKT, ERK1/2, and GFR [115]. Additionally, Andro improved the sensitivity of non-small cell lung cancer to CDDP by inhibiting protective autophagy [116].

Furthermore, Andro can enhance the cytotoxic effect of vincristine on nephroblastoma SK-NEP-1 cells by regulating the PI3K/AKT/p53 signaling pathway [117]. Moreover, Andro in combination with Bleomycin (BLM) was significantly more effective than BLM alone in inhibiting ascites tumor growth, arresting the cell cycle in the G0/G1 phase, and promoting the activity of Caspase 3 and Caspase 8 to induce cancer cell apoptosis. This effect may be attributed to the transcriptional regulation of the p53/p21/Cyclin pathway following combined treatment [118]. The combination of arsenic trioxide ((As_2O_3) and Andro significantly increased the apoptosis rate of HepG2 cells compared with As_2O_3 alone, potentially through the downregulation of EphB4 expression [119].

4.1.1.3. Synergistic effect with chemotherapeutic drugs. Andro can enhance the effectiveness of chemotherapeutic drugs through various mechanisms to inhibit tumors. It synergistically inhibits colon cancer by increasing intracellular ROS, enhancing CDDP-induced endoplasmic reticulum stress, and inhibiting STAT3 [120]. Additionally, Andro increases the apoptosis rate of colon cancer LoVo cells by enhancing Fas/FasL binding, activating Caspase 8, cleaving Bid, altering Bax conformation, and working with CDDP to activate the mitochondrial apoptosis pathway [121].

Beyond these pathways, Andro also collaborates with chemotherapy drugs via the mitochondrial apoptosis pathway. Studies have shown that Andro increases intracellular ROS, modulates MAPK and PI3K/AKT pathways, alters the Bcl-2/Bax ratio, activates Caspase 3, and induces PARP cleavage, thereby synergizing with carboplatin to induce apoptosis in human laryngeal cancer Hep-2 cells [122]. Furthermore, Andro interacts with the thiol group of intracellular GSH, disrupts the GSH redox cycle, elevates intracellular ROS levels, and tanshinone IIA binds to DNA and activates p53. This interaction synergistically induces tumor cell apoptosis through ROS and p53 crosstalk [123]. The synergistic effect based on the mitochondrial apoptosis pathway is also evident in Andro's enhanced anti-tumor effect when combined with topotecan against acute myeloid leukemia cells [124].

Additionally, estrogen promotes breast cancer cell proliferation by binding to estrogen receptors. Fulvestrant, a selective estrogen receptor inhibitor, is used to counteract this effect. Studies have demonstrated that Andro induces ROS accumulation in estrogen receptor-positive MCF-7 and T47D breast cancer cells, downregulates Forkhead Box Protein M1 (FOXM1) expression, thereby inhibiting Estrogen Receptor 1 (ESR1) transcription, and works synergistically with Fulvestrant to inhibit tumor cell proliferation [125].

4.1.1.4. Alleviate the side effects of chemotherapy drugs. Gastrointestinal reactions are common side effects of chemotherapy. Studies have shown that Andro can alleviate weight loss and diarrhea in H22 tumor-bearing mice. It exerts an anti-apoptotic effect by inhibiting 5-Fu-induced p38 phosphorylation, Bax expression, and Caspase 8/3 activation in human colonic mucosal epithelial cells NCM 460 [126]. Additionally, Andro significantly alleviates irinotecan-induced colitis without compromising its tumor-suppressing effects. Mechanistic studies indicate that Andro promotes homologous recombination (HR) repair, downregulates the Double-Stranded DNA (dsDNA)-Cyclic GMP-AMP Synthase (cGAS)--Stimulator of Interferon Genes (STING) signaling pathway, and helps mitigate irinotecan-induced gastrointestinal mucositis [127].

The cardiotoxicity of Dox and As_2O_3 limits their clinical application. Andro can reduce the toxicity of these chemotherapeutic drugs to rat cardiomyocytes H9C2 by decreasing hydroperoxide content, increasing Ferric Reducing Antioxidant Power (FRAP) levels, and downregulating TLR4 expression [128]. Furthermore, Andro can inhibit the activation of Nucleotide-Binding Oligomerization Domain, Leucine-Rich Repeat, and Pyrin Domain-Containing 3 (NLRP3) inflammasome and reduce IL-1β expression, further diminishing Dox-induced cardiomyocyte toxicity [129].

Some patients may develop pulmonary fibrosis following treatment with BLM. It has been reported that combining BLM with Andro can significantly reduce BLM-induced pulmonary fibrosis in tumor-bearing mice. This effect is achieved by activating Superoxide Dismutase (SOD), inhibiting the production of Malondialdehyde (MDA) and Hydroxyproline (HYP), and reducing levels of IL-1β, TNF-α, IL-6, and TGF-β1. These mechanisms may be related to the inhibition of TGF-β, α-SMA, and Smad2/3 protein expression, as well as the promotion of Smad7 expression [118]. Thus, Andro shows potential in mitigating the toxic and side effects associated with various chemotherapy drugs. In summary, the clinical application of Andro in combination with chemotherapeutic drugs to enhance efficacy and reduce toxicity holds significant promise.

4.1.2. Combined with radiotherapy

4.1.2.1. Synergistic effect of combination. Andro can act as a radiotherapy sensitizer at doses that are generally non-toxic to tumor cells. Studies have demonstrated that tumor cell radioresistance is related to glycolysis. Andro reduces glycolysis levels by inhibiting the PI3K/AKT/mTOR signaling pathway in colon cancer HCT116 cells, thereby enhancing tumor cell sensitivity to radiation [130]. Additionally, in nasopharyngeal carcinoma, the expression of Ras Association Domain Family 1 Isoform A (RASSF1A) is significantly reduced compared to typical epithelial cells. RASSF1A can inhibit the Nrf2/Thioredoxin Reductase 1 (TXNRD1) signaling pathway by activating Forkhead Box O3 (FOXO3a) expression, which increases intracellular ROS levels and enhances radiosensitivity. Andro induces RASSF1A expression, increasing the sensitivity of nasopharyngeal carcinoma cells to radiotherapy both in vitro and in vivo [131]. Furthermore, the combination of Andro and radiotherapy can trigger autophagic death and improve the sensitivity of human ovarian cancer SKOV3 cell xenograft mice to radiation [132].

Andro can also be combined with radiotherapy for enhanced antitumor effects. It has been found that Andro can activate the mitochondrial apoptosis pathway by downregulating NF-κB levels in human esophageal cancer ECA109 cells, in a manner similar to radiotherapy intervention, resulting in a synergistic effect [133]. However, it is worth noting that as the number of radiotherapy sessions increases, tumor cells may develop radiation tolerance. Whether Andro can reverse this radiation tolerance remains unknown.

4.1.2.2. Combined detoxification. Radiation-induced lung injury is a common side effect of radiotherapy. Radiation exposure to lung tissue triggers cytokine production in the early stages, leading to increased immune cell infiltration. Recruited macrophages undergo pyroptosis under radiation induction, releasing numerous inflammatory factors and initiating inflammatory cascades that contribute to lung injury. Researchers have found that Andro mitigates radiation-induced DNA damage by inhibiting the transfer of inflammasome Absent In Melanoma 2 (AIM2) into the nucleus of macrophages. This inhibition reduces Caspase 1-mediated GSDMD-dependent pyroptosis, decreases the release of inflammatory factors, and attenuates inflammatory cascades, ultimately reducing radiation-induced lung inflammation and fibrosis [134]. Additionally, radiotherapy can promote tumor cell metastasis. Studies have shown that Andro can inhibit the expression of downstream MMP-2 by preventing the nuclear translocation of NF-κB p65 and the activation of ERK1/2, thereby counteracting the enhancement of radiation on the metastatic ability of Ras-mutant RK3E cells [135]. These findings suggest that Andro holds potential as a radiotherapy

Table 3
Application of andrographolide DDS in the treatment of tumors.

DDS	Animal/cell model		Advanced effects	Ref.
Andrographolide-eluting nanofibrous membranes	**In vivo**	HIV+TC−1 subcutaneous xenograft in female C57BL/6 J mice	Larger drug loading, stable drug release. Tumour inhibiting activity.	[137]
Andrographolide-loaded poly (ethylene glycol)-poly (D.L-lactic acid)	**In vitro**	4T1 cell	Better stability and solubility. Increased encapsulation efficiency and drug loading. Enhanced in vitro cell uptake and antiproliferative activity.	[138]
Andrographolide-loaded poly (D, L-lactide-co-glycolide)-b-poly (ethylene glycol)-b-poly (D, L-lactide-co-glycolide)	**In vitro** **In vivo**	MAD-MB−231 cell Healthy Wistar rats	Better stability and solubility. Increased encapsulation efficiency and drug loading. Enhanced in vitro cell uptake.	[139]
Andrographolide-loaded Glycyrrhetinic acid and PHIS were conjugated to form poly (ethylene glycol)-poly (lactic-co-glycolic acid)	**In vitro** **In vivo**	Hep3B, MDA-MB−231 cell Hep3B subcutaneous xenograft in BALB/c nude mice	Targeting the liver cell. Specific accumulation in the liver. Prolonged in vivo retention time.	[140]
Andrographolide-loaded Polyphenylboronic acid	**In vitro** **In vivo**	MCF−7 , PC−3 cell MCF−7 subcutaneous xenograft female Balb/c- nude mice	Better solubility and stability. Increased targeting. Suppression of tumour size in vivo.	[141]
Andrographolide-loaded solid lipid nanoparticles	**In vitro** **In vivo**	HepG2 cell Healthy NIH mice	Higher encapsulation rate and loading efficiency. Significant liver targeting ability.	[142]
Andrographolide-loaded solid lipid nanoparticles	**In vitro** **In vivo**	MCF−7 cell EAC cell Intraperitoneal injection Female Balb/c mice	Increases solubility and dissolution rate. Alters cell membrane homeostasis to accelerate cell uptake. Reduced toxicity to normal cells. Stronger anti-tumour activity.	[143]
Andrographolide-loaded solid lipid nanoparticles	**In vitro**	HIOEC, Leuk1, HN6, HN30 cell	Higher proliferation inhibition and pro-apoptotic effects. Higher efficiency of cell uptake and intracellular absorption.	[144]
Andrographolide-loaded phytosomes	**In vitro**	HepG2 cell	Enhanced cell uptake and superior anti-tumour activity	[145]
Andrographolide-loaded with soya-L-α-phosphatidyl choline	**In vitro**	Neuro2a cell	Cell uptake is enhanced. Improved stability and anticancer activity.	[146]
Andrographolide-loaded solid lipid nanoparticles modified with Cell-penetrating peptide	**In vitro** **In vivo**	4T1 cell 4T1 in situ xenograft female BALB/c nude mice	Enhanced targeting. Inhibition of tumour growth in vivo. Higher ability to inhibit metastasis and invasion.	[147]
Andrographolide-loaded silver nanoparticles	**In vitro**	MDA-MB−453 cell	Increased drug loading. Reducing oxidative stress and improving anticancer effects.	[148]
Andrographolide-loaded superparamagnetic Fe_3O_4 nanoparticles	**In vitro**	A431 cell	Higher drug loading rate and good biocompatibility. Better anti-proliferative and apoptosis-inducing activity.	[149]
Novel inhalable andrographolide dry	**In vitro**	A549 cell	Good aerosol profile and storage stability. Effective anti-cancer activity.	[150]
Andrographolide Nanogel	**In vitro** **In vivo**	A431 cell Swiss albino mice	Cell uptake is enhanced. Good biocompatibility.	[151]
Andrographolide-loaded Poly (DL-lactide-Co-Glycolic acid)	**In vitro**	LM2 cell	Stable release within 48 hours. More potent cell toxicity to LM2 cells. Inhibits cell cycle block more significantly.	[152]
Andrographolide-loaded 1,2-Dimyristoyl-sn-Glycero−3-Phosphoglycerol-Sodium Lipid	**In vitro** **In vivo**	MCF−7 cell Healthy Wistar rats	pH-dependent release. Oral bioavailability increased 1.81-fold. Higher plasma concentrations. Longer termination half-life.	[153]
Andrographolide -loaded nanoemulsion	**In vitro**	A431, A375 cell	Enhanced water solubility. Good cell toxicity and selectivity.	[154]

adjuvant drug.

4.2. Drug delivery system

Recent advancements in bioengineering and materials science have made the development of Drug Delivery Systems (DDS) crucial for improving the efficacy and safety of antitumor drugs. Andro is a natural compound having anti-tumor potential, but its clinical applicability is limited by characteristics such as solubility, cell permeability and targeting. To circumvent these constraints, researchers have studied a variety of DDSs based on polymers, lipids, and inorganic nanoparticles (Table 3).

Poly (DL-lactide-Co-Glycolic acid) (PLGA) achieved a 4-week sustained release of Andro, which improved bioavailability and anti-tumor activity [137]. In addition, Poly (ethylene glycol) -poly (lactide) (mPEG-PLA) considerably increased the solubility (approximately 280 times), stability, cell absorption rate and anti-tumor proliferation

Table 4
Anticancer derivatives of andrographolide.

No	Chemical formula	Model	$IC_{50}/GI_{50}/ED_{50}/LC_{50}$			Compared with the parent compound	Ref.
				Andro	Derivative		
11	(11, Fig. 12)	HCT116, MCF−7, DU145	IC_{50}	14.87, 14.18, 44.25 μM	1.85, 1.22, 1.24 μM	Shows enhanced cytotoxic, anti-proliferative and apoptosis-inducing activity against colon, breast and prostate cancer cell lines.	[155]
12	(12, Fig. 12)	60 NCI human tumour cell	GI_{50}	16.2 μM (mean)	4.07 μM (mean)	Stronger cytotoxic activity against the majority of 60 NCI human tumour cells.	[156]
13	(13, Fig. 12)	60 NCI human tumour cell	GI_{50}	16.2 μM (mean)	1.54 μM (mean)	Stronger cytotoxic activity against the majority of 60 NCI human tumour cells.	[156]
14	(14, Fig. 12)	60 NCI human tumour cell	GI_{50}	16.2 μM (mean)	3.54 μM (mean)	Stronger cytotoxic activity against the majority of 60 NCI human tumour cells.	[156]
15	(15, Fig. 12)	60 NCI human tumour cell	GI_{50}	16.2 μM (mean)	2.18 μM (mean)	Stronger cytotoxic activity against the majority of 60 NCI human tumour cells.	[157]
16	(16, Fig. 12)	60 NCI human tumour cell	GI_{50}	16.2 μM (mean)	4.07 μM (mean)	Stronger cytotoxic activity against the majority of 60 NCI human tumour cells.	[157]
17	(17, Fig. 12)	60 NCI human tumour cell	GI_{50}	16.2 μM (mean)	1.73 μM (mean)	Stronger cytotoxic activity against the majority of 60 NCI human tumour cells.	[157]
18	(18, Fig. 12)	60 NCI human tumour cell	GI_{50}	16.2 μM (mean)	3.23 μM (mean)	Stronger cytotoxic activity against the majority of 60 NCI human tumour cells.	[157]
19	(19, Fig. 12)	60 NCI human tumour cell	GI_{50}	16.2 μM (mean)	1.54 μM (mean)	Stronger cytotoxic activity against the majority of 60 NCI human tumour cells.	[157]
20	(20, Fig. 12)	P−388, KB, HT−29, MCF−7, A549, ASK	IC_{50}	2.25, 27.37, 9.34, 15.4, 27.9, 16.18 μM	4.56, 6.49, 5.59, 4.45, 6.1, 3.33 μM	Exhibits enhanced cytotoxic activity against glioma cell lines.	[158]
21	(21, Fig. 12)	ASK	IC_{50}	16.18 μM	9.32 μM	Exhibits enhanced cytotoxic activity against glioma cell lines.	[158]
22	(22, Fig. 12)	ASK	IC_{50}	16.18 μM	6.51 μM	Exhibits enhanced cytotoxic activity against glioma cell lines.	[158]
23	(23, Fig. 12)	MCF−7	IC_{50}	-	0.7 μM	Higher cytotoxicity against breast colon cancer cell lines.	[159]
24	(24, Fig. 12)	MCF−7	IC_{50}	-	0.6 μM	Exhibits enhanced cytotoxic activity against breast cancer cell lines.	[159]
25	(25, Fig. 12)	KKU-M213, KKU−100	ED_{50}	- -	3.37, 2.93 μM	Exhibits enhanced cytotoxic activity against cholangiocarcinoma cell lines.	[160]
26	(26, Fig. 12)	KKU-M213, KKU−100	ED_{50}	- -	3.37, 2.93 μM	Exhibits enhanced cytotoxic activity against cholangiocarcinoma cell lines.	[160]
27	(27, Fig. 12)	HCT−15	IC_{50}	>25 μM	4.4 μM	Exhibits enhanced cytotoxic activity against colon cancer cell lines.	[161]
28	(28, Fig. 12)	K562	IC_{50}	>25 μM	4.6 μM	Exhibits enhanced cytotoxic activity against leukemia cell lines.	[161]
29	(29, Fig. 12)	HCT−15, Hela, K562	IC_{50}	>25, >25, >25 μM	17.2, 13.4, 16.2 μM	Exhibits enhanced cytotoxic activity against colon, cervical and leukemia cell lines.	[161]
30	(30, Fig. 12)	K562	IC_{50}	>25 μM	10.1 μM	Exhibits enhanced cytotoxic activity against leukemia cell lines.	[161]
31	(31, Fig. 12)	HCT−15, K562	IC_{50}	>25, >25 μM	11.3, 9.3 μM	Exhibits enhanced cytotoxic activity against colon and leukemia cell lines.	[161]
32	(32, Fig. 12)	HCT−15, DU145, HeLa, VERO	IC_{50}	189.1, 253.1, 213.7, 117.2 μM	81.9, 52.1, 71.7, 54.5 μM	Exhibits enhanced cytotoxic activity against colon, prostate and cervical cancer cell lines.	[162]
33	(33, Fig. 12)	HCT−15, DU145, HeLa, VERO	IC_{50}	189.1, 253.1, 213.7, 117.2 μM	62.4, 48.6, 73.1, Nt μM	Exhibited enhanced cytotoxic activity against colon, prostate and cervical cancer cell lines and was non-toxic to normal renal VERO.	[162]
34	(34, Fig. 12)	HCT−15, DU145, HeLa, VERO	IC_{50}	189.1, 253.1, 213.7, 117.2 μM	86.9, 65.4, 126.6, Nt μM	Exhibited enhanced cytotoxic activity against colon, prostate and cervical cancer cell lines and was non-toxic to normal renal VERO.	[162]
35	(35, Fig. 12)	HCT−15, DU145, HeLa, VERO	IC_{50}	189.1, 253.1, 213.7, 117.2 μM	70.9, 54.7, 76.1, Nt μM	Exhibited enhanced cytotoxic activity against colon, prostate and cervical cancer cell lines and was non-toxic to normal renal VERO.	[162]
36	(36, Fig. 13)	HCT−15, DU145, HeLa, VERO	IC_{50}	189.1, 253.1, 213.7, 117.2 μM	67.8, 42.9, 70, 49.6 μM	Exhibits enhanced cytotoxic activity against colon, prostate and cervical cancer cell lines.	[162]
37	(37, Fig. 13)	HCT−15, DU145, HeLa, VERO	IC_{50}	189.1, 253.1, 213.7, 117.2 μM	75.9, 73.1, 107.7, Nt μM	Exhibited enhanced cytotoxic activity against colon, prostate and cervical cancer cell lines and was non-toxic to normal renal VERO.	[162]
38	(38, Fig. 13)	MCF−7, KKU−055	IC_{50}	8.48, 17.73 μM	0.59, 1.36 μM	Enhanced cytotoxic activity against breast and cholangiocarcinoma cell lines.	[163]
39	(39, Fig. 13)	MCF−7	IC_{50}	8.48 μM	0.84 μM	Exhibits selective cytotoxic activity against breast cancer cell lines.	[163]
40	(40, Fig. 13)	MCF−7	IC_{50}	8.48 μM	0.68 μM	Exhibits selective cytotoxic activity against breast cancer cell lines.	[163]
41	(41, Fig. 13)	P−388, MCF−7	IC_{50}	6.91, 29.06 μM	3.14, 2.93 μM	Exhibits enhanced cytotoxic activity against breast cancer cell lines and selective activity against leukemia cell lines.	[164]
42	(42, Fig. 13)	HCT116	IC_{50}	25.34 μM	2.49 μM	Enhanced cytotoxic activity against colon cancer cell lines, high anti-proliferative and apoptosis-inducing activity.	[165]
43	(43, Fig. 13)	HCT116	IC_{50}	52.2 μM	7.32 μM	Enhanced cytotoxic activity against colon cancer cell lines, high anti-proliferative and apoptosis-inducing activity.	[166]
44	(44, Fig. 13)	HepG2, LNCaP	IC_{50}	56.6, 51.4 μM	11.1, 9.25 μM	Enhanced cytotoxic activity against hepatocellular carcinoma and prostate cancer cell lines.	[167]
45	(45, Fig. 13)	HepG2, LNCaP	IC_{50}	56.6, 51.4 μM	53.8, 35.2 μM	Enhanced cytotoxic activity against hepatocellular carcinoma and prostate cancer cell lines.	[167]
46	(46, Fig. 13)	PANC−1	IC_{50}	20.4 μM	9.56 μM	Enhanced cytotoxic activity against prostate cancer cell lines, higher antiproliferative and antimigratory activity.	[168]

(*continued on next page*)

Table 4 (*continued*)

No	Chemical formula	Model	$IC_{50}/GI_{50}/ED_{50}/LC_{50}$			Compared with the parent compound	Ref.
				Andro	Derivative		
47	(47, Fig. 13)	MDA-MB−231	IC_{50}	6 μM	3 μM	Higher apoptosis-inducing activity against breast cancer cell lines.	[169]
48	(48, Fig. 13)	MKN−45, AGS	IC_{50}	11.3, >50 μM	6.3, 1.7 μM	Higher apoptosis-inducing activity on gastric cancer cell lines.	[170]
49	(49, Fig. 13)	A549	IC_{50}	-	15 μM	Higher apoptosis-inducing activity against lung cancer cell lines.	[171]
50	(50, Fig. 13)	L5178Y TK human ABCB1-gene transfected L5178Y subline	IC_{50}	14.9, 14.52 μM	5.47, 12.31 μM	More potent cytotoxic activity against lymphoma cytotoxicity in drug-resistant human abcb1 gene-transfected L5178Y mice, which inhibits P-gp ATPase activity.	[172]
51	(51, Fig. 13)	MCF−7, HCT116	GI_{50}	6.4, 5.1 μM	4.2, 3.8 μM	Breast and colon cancer cell lines are more cytotoxic and more cell permeable to colon cancer cells.	[173]

efficacy of Andro [138]. Combining the advantages of PLGA and PEG, the developed PLGA-PEG-PLGA triblock copolymer carrier can enhance the sustained release, degradability and anti-tumor activity of Andro [139]. In order to optimize the targeting of Andro, it was encapsulated within the copolymer micelles Glycyrrhetinic acid and PHIS were coupled to generate poly (ethylene glycol) -poly (lactic-co-glycolic acid) (GA-PPP), which can increase the targeting of Hep3B liver cells, selectively accumulate in the liver, and enhance the anti-tumor action [140]. In addition, Andro was combined with Polyphenylboronic acid (pPBA) to produce nanoparticles, which improved its solubility, stability and targeted delivery ability, and enhanced the anti-cancer activity [141].

Liposomes offer considerable promise as drug delivery carriers due to their superior biocompatibility and degradability. Solid lipid nanoparticles (SLNs) [142–144] and phospholipid compounds such as Soybean-L-α-Phosphatidylcholine (SPC) have shown good results in the treatment of head and neck cancer and neuroblastoma by improving the solubility and stability of drugs and enhancing the accumulation of drugs in cells [145,146]. In addition, cell-penetrating peptide (CPP) modification of Dox and Andro-loaded liposomes can avoid the breakdown of medicines by enzymes and the influence of tumor microenvironment, accomplish tumor-targeted administration, and effectively block the migration and invasion of tumor cells [147].

Inorganic nanoparticles, such as silver nanoparticles (AgNPs) [148] and superparamagnetic Fe_3O_4 nanoparticles (Fe_3O_4/HAp) [149], with their unique physical and chemical properties, such as electrostatic adsorption, antioxidant effect, large specific surface area, mesoporous volume and magnetism, have high drug loading rate and good biocompatibility, showing potential in anti-tumor therapy. In addition, inhalation dry powder [150] or skin nanogels [151] can be prepared by adjusting the physical and chemical properties of Andro. This direct administration method improves the bioavailability and anticancer effect of the drug.

Although significant progress has been made, insufficient drug targeting, precise control of drug release kinetics, long-term biosafety and potential toxicity assessment still need to be further studied. In the future, we should focus on the development of multifunctional DDS with high targeting, intelligent response, controllable release, easy degradation and good biocompatibility, so as to promote clinical transformation and achieve more effective tumor treatment.

4.3. Structural modification of Andro

Structural modification of Andro is an effective method to improve its anticancer activity. At present, a variety of strategies have been proposed for the synthesis of Andro derivatives, including the modification of C-3, C-14 and C-19 hydroxyl groups, the modification of C-8,17 and C-11,12 double bonds, the modification of the lactone ring and the modification of other positions. These modifications have a significant impact on the pharmacodynamics, pharmacokinetics and physicochemical properties of drug molecules.

The potential of Andro derivatives in the treatment of cancer has been studied (Table 4) (Figs. 12,13). These derivatives based on different site modifications can correspondingly obtain superior biological activity in different molecular mechanisms to exhibit stronger anti-tumor effects. Compared with the parent compound, the derivatives have stronger cytotoxic activity against a variety of tumors [155–168], and are superior to the parent compound in anti-proliferation [31,33,56,155,165,166,168], induction of death [30,31,33,47,50,56,62,72,98,155,165,166,169–171], inhibition of invasion and migration [72,168], and reversal of multidrug resistance in multidrug-resistant cells [172]. In addition, by modifying different sites, the ability of derivatives to penetrate cell membranes is greatly improved compared to Andro [173], and can be used as P-gy inhibitors to reduce drug excretion [172] Increased bioavailability of the drug. It can be seen that the structural modification of Andro is an effective way to improve its anticancer activity.

5. Clinical application

The ultimate goal of theoretical research is to apply safe and effective medications to clinical practice. In recent years, investigations have discovered that Andro may induce reproductive toxicity, nephrotoxicity and certain other serious responses. It has been found that Andro may trigger apoptosis of most oocytes at a dose of 20 μM. Mechanism investigations have indicated that Andro decreases the fertilization capability of mouse oocytes and reduces the reproductive capacity of female mice by preventing cytoskeletal rearrangement and affecting meiotic maturation of oocytes [174]. In terms of nephrotoxicity, Andro disrupts the redox equilibrium of human renal tubular epithelial cells HK-2 in a dose-and time-dependent manner, prompting endoplasmic reticulum stress-mediated apoptosis, which in turn causes kidney damage [175]. In clinical trials for the treatment of multiple sclerosis, it was observed that oral administration of Andro twice a day at a dose of 140 mg would elicit rash and taste problems [176]. Through a literature analysis, it is anticipated that the toxicity of Andro is mostly related to the concentration and period of administration. Therefore, it needs to be further implemented to identify the dose and time of administration to control adverse medication reactions.

Using the keyword "Andrographolide", we searched the *ClinicalTrails.gov* website for 20 clinical research projects (as of July 05, 2024) (Table 5), of which 2 were cancer-related. One of these trials particularly evaluated the efficacy and safety of Andro coupled with capecitabine in the treatment of elderly adults with locally progressed or recurrent or metastatic inoperable colorectal cancer. However, due to the limited accuracy of the data, the experiment was halted after phase 2 trials [177]; the other is a prospective cohort study assessing the influence of Andro on palliative care in patients with advanced or metastatic esophageal cancer. The study involved 30 participants, and the trial was completed after the phase 3 trial [178]. Andro 's anti-tumor research is still in its infancy and incomplete. Therefore, we need further research to develop Andro 's chronic toxicity and drug interaction investigations, as well as more and larger clinical trials. These investigations will provide the groundwork for the clinical application of Andro as an anticancer treatment and give more solid evidence for the application of Andro in

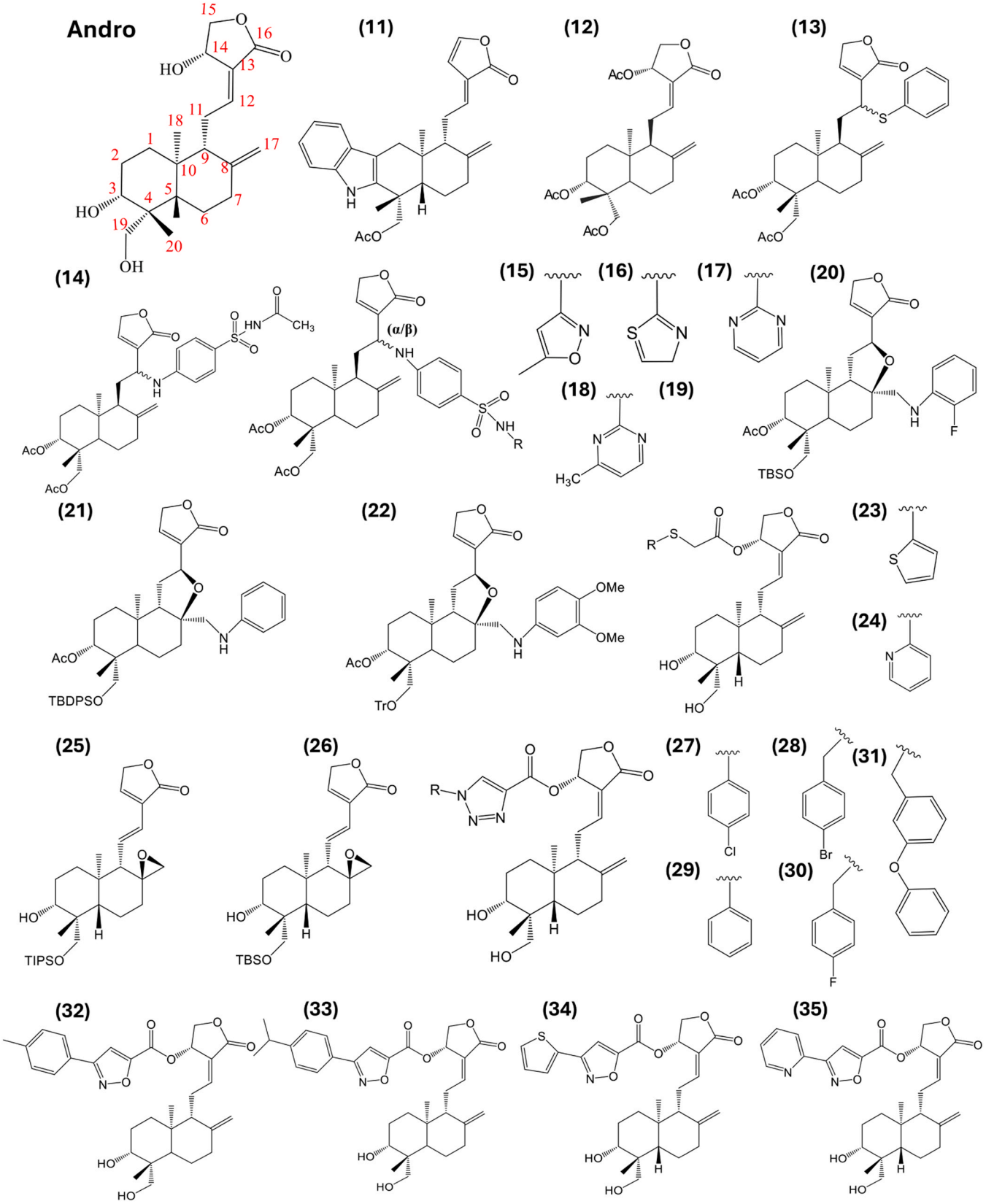

Fig. 12. Andrographolide antitumor derivatives.

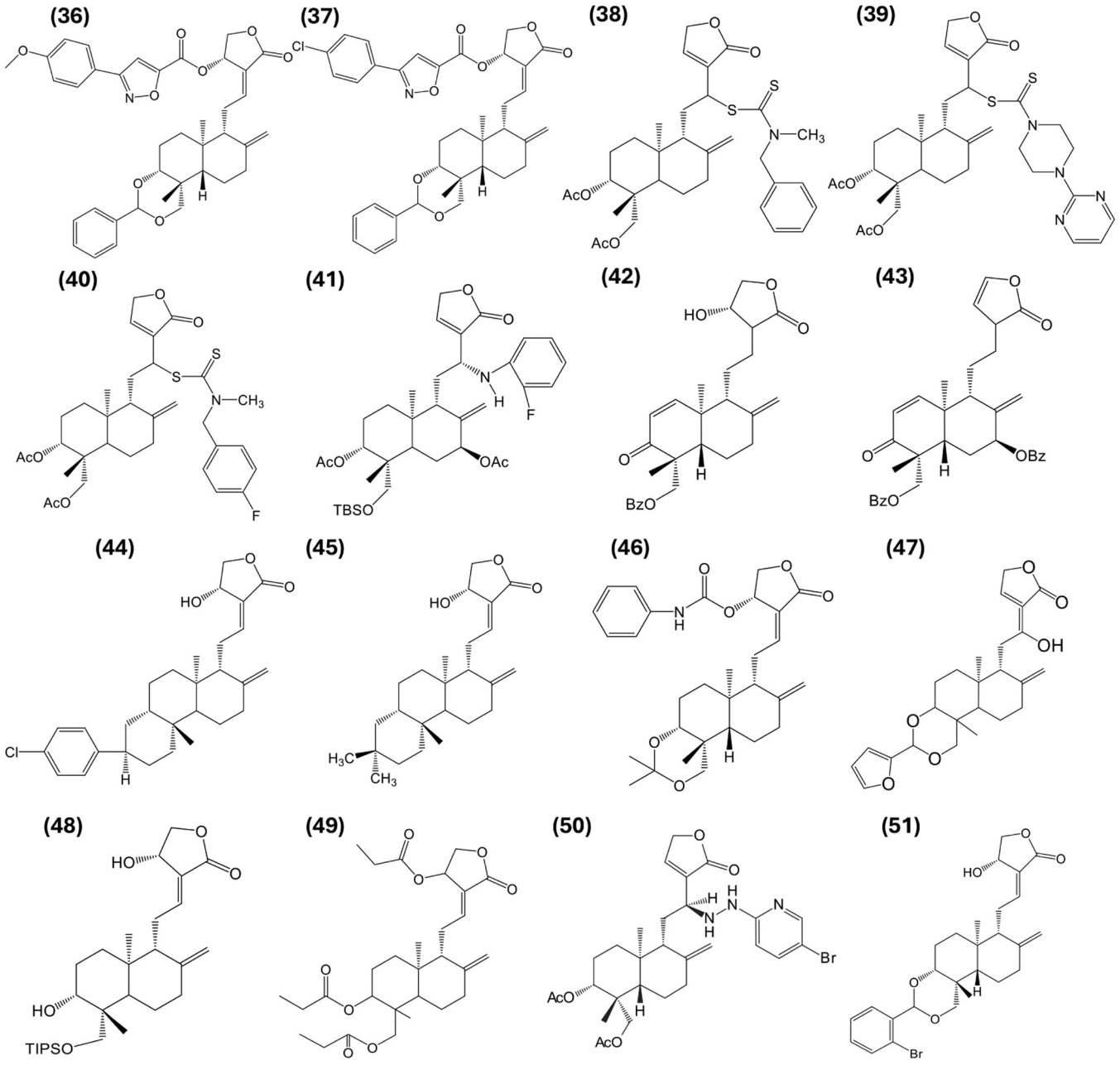

Fig. 13. Andrographolide antitumor derivatives.

clinical oncology.

6. Summary and prospect

With the increasing prevalence and mortality of global cancer, human life and health are significantly threatened. Due to the intricate pathophysiology of cancers, and the available treatment techniques have issues such as high recurrence rate, low cure rate and major adverse responses. Therefore, the hunt for a safe, efficient and minimal side effects of anti-tumor medications has become the top goal of global research.

Andro is a diterpene compound extracted from the whole grass or leaves of Andrographis paniculata, which has been widely concerned because of its extensive pharmacological activity against various diseases. Recent studies have shown that Andro is a potential antitumor drug. This article summarizes the anti-tumor pharmacological activities of Andro in vitro and in vivo, such as proliferation inhibition, death induction, inhibition of angiogenesis, inhibition of tumor metastasis and invasion, inhibition of tumor immune escape, reprogramming of uncontrolled energy metabolism of tumor cells, and destruction of tumor microenvironment. Also discussed in the paper are new approaches to Andro co-administration and improved bioavailability, highlighting the promise of Andro as an anticancer drug. When combined with chemotherapy and radiotherapy, Andro showed the characteristics of reversing the drug resistance of tumor cells, increasing the sensitivity of tumor cells to treatment, synergistic effect and reducing toxic and side effects. In addition, by carrying a drug delivery system or chemical modification, it can make up for the defects of poor water solubility and short drug half-life caused by terpene skeletons and lactone groups, and provide a highly connotative strategy for improving Andro bioavailability.

There are also some limitations in the current research. Although Andro has shown extensive anti-tumor pharmacological activity in phenotypic screening, the exact molecular targets associated with this

Table 5
Clinical Trials of Andrographolide for the Prevention and Treatment of Related Diseases Registered at ClinicalTrials.gov.

No	Study title	Conditions	Status	Identifier	Ref.
1	A Study of Andrographolide Sulfonate in Patients with Acute Exacerbation of Chronic Bronchitis	Acute Exacerbation of Chronic Bronchitis	Unknown, Phase 4	NCT03132610	[179]
2	Evaluate the Efficacy and Safety of Andrographolide Sulfonate in Patients with Acute Bronchitis	Acute Bronchitis	Unknown, Phase 4	NCT03132623	[180]
3	Evaluate the Efficacy and Safety of Andrographolide Sulfonate in Patients with Acute Tonsillitis	Acute Tonsillitis	Unknown, Phase 4	NCT03134443	[181]
4	Assessment of the Efficacy of Andrographis paniculata in Subjects with Mild to Moderate Osteoarthritis	Knee Osteoarthritis	Completed, N/A	NCT03262792	[182]
5	The Effect of Andrographis paniculata (AP) on Palliative Management of Advanced Esophageal Cancer	Squamous Cell Carcinoma of Esophagus	Completed, Phase 3	NCT04196075	[178]
6	The Effect of Andrographis paniculata to GLP−1, Fasting Insulin, Insulin 2-h Post OGTT, and HOMA-IR	Increased Insulin	Completed, N/A	NCT03455049	[183]
7	Efficacy Study of Andrographis paniculata Purified Standardized Extract (ApE) in Patients with Multiple Sclerosis (MS)	Multiple Sclerosis, Relapsing-Remitting	Completed, Phase 1/2	NCT02280876	[184]
8	Andrographis paniculata vs Boesenbergia rotunda vs Control in Asymptomatic COVID−19	Covid19	Unknown, Phase 3	NCT05019326	[185]
9	Pharmacometabolomics of Andrographis paniculata and Metformin In Healthy Volunteers Under Fasting Condition	Molecular Mechanisms of Pharmacological Action, Pharmacokinetics	Unknown, Phase 1	NCT04161404	[186]
10	Effects of an Adaptogenic Extract on Electrical Activity of the Brain in Elderly Subjects with Cognitive Impairment	Cognitive Impairment (Mild)	Completed, Phase 1	NCT03780621	[187]
11	To Assess the Effect of 336 Days Exposure of Paractin® on Pain & Disease Progression in Patients Suffering from Osteoarthritis of Knee Joint.	Knee Osteoarthritis (Knee OA)	Recruiting, N/A	NCT04833946	[188]
12	Efficacy, Safety and Tolerability of Andrographolides Versus Placebo in Patients with Progressive Forms of MS	Multiple Sclerosis, Secondary Progressive, Primary Progressive Multiple Sclerosis	Unknown, Phase 1/2	NCT02273635	[189]
13	Magnesium, Vitamin B2, Feverfew, Andrographis paniculata and Coenzyme Q10 for Episodic Migraine Prophylaxis	Migraine	Completed, Observational	NCT04463875	[190]
14	Magnesium, Partenium, Andrographis, Co-enzyme Q10 and Riboflavin (PACR) in Migraine Prophylaxis	Migraine Disorders	Unknown, Not Applicable	NCT03190044	[191]
15	Efficacy Study of FANG (30) for Active Rheumatoid Arthritis in Adult Patients	Arthritis, Rheumatoid	Completed, Phase 2	NCT00749645	[192]
16	To Compare the Efficacy and Tolerability of A. Paniculata/A. Chilensis in Individuals With URTI	Upper Respiratory Tract Infection	Completed, Phase 3	NCT04955327	[193]
17	Study of Andrographolides with or Without Capecitabine to Treat Colorectal Cancer	Colorectal Neoplasms	Terminated, Phase 2	NCT01993472	[177]
18	Assessment of Efficacy of KAN-JANG® in Mild COVID−19	Covid19	Unknown, Phase 2/3	NCT04847518	[194]
19	A Post-marketing Research on Jinyebaidu Granule in Treating Patients with Acute Upper Respiratory Infection	Acute Upper Respiratory Infection	Unknown, Phase 4	NCT02539277	[195]
20	Echinacea and Acute Respiratory Illness	Acute Respiratory Infections	Completed, Not Applicable	NCT02003651	[196]

have not yet been fully determined. Therefore, it is a fast and effective method to further screen out valuable targets for the treatment of cancer and related diseases by using Andro biological activity probe, network pharmacology, bioinformatics analysis and omics technology, and to draw the corresponding signal network diagram. At the same time, it is necessary to consider Andro's crosstalk between metabolism and other components of the tumor microenvironment, as well as Andro's potential in tumor immunotherapy. Studying the regulatory effect of Andro on tumor metabolism and immunity will help to develop more targeted drugs and improve immunotherapy strategies.

It is critical to identify specific cancer types that are sensitive to Andro, which will expand the range of benefits associated with Andro treatment and increase the potential for its clinical application. According to the current research and clinical progress of its anticancer mechanism, it is very important to comprehensively evaluate the reactivity and unique effects of Andro on different types of cancer. In addition, Andro can also be used as a preventive and adjuvant treatment for cancer. Exploring natural foods and nutritional supplements rich in Andro may have potential protective effects on certain types of cancer.

Although the drug delivery system has made some progress in solving the poor water solubility and short half-life of Andro, and has performed well in animal models, there are significant differences in oral metabolism between different species, and the performance of animal models cannot fully reflect the pathophysiological process of human body. Therefore, it is necessary to further study the model that is more in line with the physiological environment of human body and strengthen the preclinical study of Andro nano-drug delivery system. Although the development of drug delivery systems and Andro derivatives has improved the bioavailability and other pharmacokinetic properties of Andro, the supplemental materials or modified structures used in these delivery systems or derivatives may change the mechanism and results compared with the use of Andro alone. Therefore, the mechanism of the two needs to be further explored. Considering that biosynthesis or biotransformation has become an increasingly powerful tool for the total synthesis and structural modification of natural products, it will be meaningful to explore the key enzymes responsible for the synthesis of Andro key intermediates and the site-specific functionalization of Andro.

The ultimate goal of the study is the clinical application of drugs. The research on the anti-tumor effect of Andro is mostly limited to cell and animal experiments, and the successful clinical transformation may be subject to many factors, such as the difference of drug administration, the difference of drug dose, the difference between animal models and patients, and the complexity of clinical trial conditions. Therefore, it is necessary for researchers to carry out clinical trials to verify the exact efficacy and safety of Andro anti-tumor.

Overall, this review demonstrates that numerous preclinical studies and some clinical trials provide strong support for the application of andrographolide in cancer treatment. These findings also support and accelerate the clinical research of andrographolide and its derivatives in modern pharmaceutical formulations.

Ethical approval

This study did not include any studies with human participants or animals.

Author contributions

All authors contributed to data collection and manuscript writing. Jiaxuan Hu, Yi Li, and Xin Xie have contributed equally to this work.

Funding

This study was supported by National Natural Science Foundation of China (No. 82260793); The Key R &D Project of Ganzhou Science and Technology Plan Project (2022B-SF8897); Jiangxi Provincial Natural Science Foundation (No.20212BAB216002); China Postdoctoral Science Foundation funded project (No.2020M680834); Jiangxi Provincial Natural Science Foundation funded project (No.20224BAB216047).

CRediT authorship contribution statement

Jiaxuan Hu: Writing – original draft. **Yi Li:** Writing – review & editing. **Xin Xie:** Writing – review & editing. **Yunlei Song:** Investigation. **Wenjing Yan:** Formal analysis. **Yan Luo:** Validation. **Yumao Jiang:** Writing – review & editing, Supervision, Project administration, Funding acquisition.

Declaration of Competing Interest

The authors declare that there are no conflict of interests, we do not have any possible conflicts of interest.

Data availability

No data was used for the research described in the article.

Acknowledgements

Figures in the article were drawn using BioRender.com

References

[1] F. Bray, M. Laversanne, E. Weiderpass, I. Soerjomataram, The ever-increasing importance of cancer as a leading cause of premature death worldwide, Cancer 127 (16) (2021) 3029–3030.
[2] H. Sung, J. Ferlay, R.L. Siegel, M. Laversanne, I. Soerjomataram, A. Jemal, F. Bray, Global cancer statistics 2020: GLOBOCAN estimates of incidence and mortality worldwide for 36 cancers in 185 countries, CA Cancer J. Clin. 71 (3) (2021) 209–249.
[3] Y. Qin, M. Ashrafizadeh, V. Mongiardini, B. Grimaldi, F. Crea, K. Rietdorf, B. Győrffy, D.J. Klionsky, J. Ren, W. Zhang, X. Zhang, Autophagy and cancer drug resistance in dialogue: Pre-clinical and clinical evidence, Cancer Lett. 570 (2023) 216307.
[4] Y. Yang, L. Liu, Y. Tian, M. Gu, Y. Wang, M. Ashrafizadeh, A. Reza Aref, I. Cañadas, D.J. Klionsky, A. Goel, R.J. Reiter, Y. Wang, M. Tambuwala, J. Zou, Autophagy-driven regulation of cisplatin response in human cancers: exploring molecular and cell death dynamics, Cancer Lett. 587 (2024) 216659.
[5] Q. Lu, D. Kou, S. Lou, M. Ashrafizadeh, A.R. Aref, I. Canadas, Y. Tian, X. Niu, Y. Wang, P. Torabian, L. Wang, G. Sethi, V. Tergaonkar, F. Tay, Z. Yuan, P. Han, Nanoparticles in tumor microenvironment remodeling and cancer immunotherapy, J. Hematol. Oncol. 17 (1) (2024) 16.
[6] Z. Wang, S. Pang, X. Liu, Z. Dong, Y. Tian, M. Ashrafizadeh, N. Rabiee, Y.N. Ertas, Y. Mao, Chitosan- and hyaluronic acid-based nanoarchitectures in phototherapy: combination cancer chemotherapy, immunotherapy and gene therapy, Int. J. Biol. Macromol. 273 (Pt 1) () (2024) 132579.
[7] G.E.B. Wright, U. Amstutz, B.I. Drogemoller, J. Shih, S.R. Rassekh, M.R. Hayden, B.C. Carleton, C.J.D. Ross, C. Canadian pharmacogenomics network for drug safety, pharmacogenomics of vincristine-induced peripheral neuropathy implicates pharmacokinetic and inherited neuropathy genes, Clin. Pharm. Ther. 105 (2) (2019) 402–410.
[8] J.U. Seo, M.H. Kim, H.M. Kim, H.J. Jeong, Anticancer potential of magnolol for lung cancer treatment, Arch. Pharm. Res 34 (4) (2011) 625–633.
[9] D.B. Xiang, K.Q. Zhang, Y.L. Zeng, Q.Z. Yan, Z. Shi, Q.H. Tuo, L.M. Lin, B.H. Xia, P. Wu, D.F. Liao, Curcumin: from a controversial "panacea" to effective antineoplastic products, Medicine 99 (2) (2020) e18467.
[10] N. Sultana, Clinically useful anticancer, antitumor, and antiwrinkle agent, ursolic acid and related derivatives as medicinally important natural product, J. Enzym. Inhib. Med. Chem. 26 (5) (2011) 616–642.
[11] C. Liu, S. Sun, Q. Feng, G. Wu, Y. Wu, N. Kong, Z. Yu, J. Yao, X. Zhang, W. Chen, Z. Tang, Y. Xiao, X. Huang, A. Lv, C. Yao, H. Cheng, A. Wu, T. Xie, W. Tao, Arsenene nanodots with selective killing effects and their low-dose combination with SS-elemene for cancer therapy, Adv. Mater. 33 (37) (2021) e2102054.
[12] A.H. Schonthal, D.M. Peereboom, N. Wagle, R. Lai, A.J. Mathew, K.M. Hurth, V. F. Simmon, S.P. Howard, L.P. Taylor, F. Chow, C.O. da Fonseca, T.C. Chen, Phase I trial of intranasal NEO100, highly purified perillyl alcohol, in adult patients with recurrent glioblastoma, Neurooncol Adv. 3 (1) (2021) vdab005.
[13] M. Martin, nab-Paclitaxel dose and schedule in breast cancer, Breast Cancer Res 17 (2015) 81.
[14] X. Liu, J. Xu, J. Zhou, Q. Shen, Oridonin and its derivatives for cancer treatment and overcoming therapeutic resistance, Genes Dis. 8 (4) (2021) 448–462.
[15] K. Kuchta, S. Cameron, M. Lee, S.Q. Cai, Y. Shoyama, Which East Asian herbal medicines can decrease viral infections? Phytochem Rev. (2021) 1–19.
[16] B. Zeng, A. Wei, Q. Zhou, M. Yuan, K. Lei, Y. Liu, J. Song, L. Guo, Q. Ye, Andrographolide: a review of its pharmacology, pharmacokinetics, toxicity and clinical trials and pharmaceutical researches, Phytother. Res.: PTR 36 (1) (2022) 336–364.
[17] S. Kumar, B. Singh, V. Bajpai, Andrographis paniculata (Burm.f.) Nees: traditional uses, phytochemistry, pharmacological properties and quality control/quality assurance, J. Ethnopharmacol. 275 (2021) 114054.
[18] I. Khan, S. Mahfooz, M. Faisal, A.A. Alatar, I.A. Ansari, Andrographolide induces apoptosis and cell cycle arrest through inhibition of aberrant hedgehog signaling pathway in colon cancer cells, Nutr. Cancer 73 (11-12) (2021) 2428–2446.
[19] N.A. Murugan, C.J. Pandian, J. Jeyakanthan, Computational investigation on Andrographis paniculata phytochemicals to evaluate their potency against SARS-CoV-2 in comparison to known antiviral compounds in drug trials, J. Biomol. Struct. Dyn. 39 (12) (2021) 4415–4426.
[20] X. Liu, S. Zhang, X. Wang, Y. Wang, J. Song, C. Sun, G. Chen, G. Yang, Y. Tao, Y. Hu, D. Bu, Y. Huang, J. Du, H. Jin, Endothelial cell-derived SO2 controls endothelial cell inflammation, smooth muscle cell proliferation, and collagen synthesis to inhibit hypoxic pulmonary vascular remodelling, Oxid. Med. Cell Longev. 2021 (2021) 5577634.
[21] L. Gan, Y. Zheng, L. Deng, P. Sun, J. Ye, X. Wei, F. Liu, L. Yu, W. Ye, C. Fan, J. Liu, W. Zhang, Diterpenoid lactones with anti-inflammatory effects from the aerial parts of andrographis paniculata, Molecules 24 (15) (2019).
[22] L. Gu, J. Lu, Q. Li, N. Wu, L. Zhang, H. Li, W. Xing, X. Zhang, A network-based analysis of key pharmacological pathways of Andrographis paniculata acting on Alzheimer's disease and experimental validation, J. Ethnopharmacol. 251 (2020) 112488.
[23] J. Shu, R. Huang, Y. Tian, Y. Liu, R. Zhu, G. Shi, Andrographolide protects against endothelial dysfunction and inflammatory response in rats with coronary heart disease by regulating PPAR and NF-kappaB signaling pathways, Ann. Palliat. Med. 9 (4) (2020) 1965–1975.
[24] Y. Song, X. Wu, D. Yang, F. Fang, L. Meng, Y. Liu, W. Cui, Protective effect of andrographolide on alleviating chronic alcoholic liver disease in mice by inhibiting nuclear factor kappa B and tumor necrosis factor alpha activation, J. Med Food 23 (4) (2020) 409–415.
[25] R.N. Chakravarti, D. Chakravarti, Andrographolide, the active constituent of Andrographis paniculata Nees; a preliminary communication, Ind. Med Gaz. 86 (3) (1951) 96–97.
[26] D. Hanahan, R.A. Weinberg, The hallmarks of cancer, Cell 100 (1) (2000) 57–70.
[27] X. Luo, W. Luo, C. Lin, L. Zhang, Y. Li, Andrographolide inhibits proliferation of human lung cancer cells and the related mechanisms, Int. J. Clin. Exp. Med. 7 (11) (2014) 4220–4225.
[28] T. Peng, M. Hu, T.T. Wu, C. Zhang, Z. Chen, S. Huang, X.H. Zhou, Andrographolide suppresses proliferation of nasopharyngeal carcinoma cells via attenuating NF-κB pathway, BioMed. Res. Int. 2015 (2015) 735056.
[29] K.A. Schafer, The cell cycle: a review, Vet. Pathol. 35 (6) (1998) 461–478.
[30] C.C. Wong, S.H. Lim, S.R. Sagineedu, N.H. Lajis, J. Stanslas, SRJ09, a promising anticancer drug lead: Elucidation of mechanisms of antiproliferative and apoptogenic effects and assessment of in vivo antitumor efficacy, Pharmacol. Res. 107 (2016) 66–78.
[31] H.C. Wong, C.C. Wong, S.R. Sagineedu, S.C. Loke, N.H. Lajis, J. Stanslas, SRJ23, a new semisynthetic andrographolide derivative: in vitro growth inhibition and mechanisms of cell cycle arrest and apoptosis in prostate cancer cells, Cell Biol. Toxicol. 30 (5) (2014) 269–288.
[32] H. Sato, M. Hiraki, T. Namba, N. Egawa, K. Baba, T. Tanaka, H. Noshiro, Andrographolide induces degradation of mutant p53 via activation of Hsp70, Int. J. Oncol. 53(2 (2018) 761–770.
[33] J. Nateewattana, S. Dutta, S. Reabroi, R. Saeeng, S. Kasemsook, A. Chairoungdua, J. Weerachayaphorn, S. Wongkham, P. Piyachaturawat, Induction of apoptosis in cholangiocarcinoma by an andrographolide analogue is mediated through topoisomerase II alpha inhibition, Eur. J. Pharmacol. 723 (2014) 148–155.
[34] X.Y. Li, X. Cui, C.Q. Xie, Y. Wu, T. Song, J.D. He, J. Feng, Q.R. Cui, J.L. Bin, Q. Y. Li, C. Xiao, J.H. Deng, G.D. Lu, J. Zhou, Andrographolide causes p53-independent HCC cell death through p62 accumulation and impaired DNA damage repair, Phytomedicine: Int. J. Phytother. Phytopharm. 121 (2023) 155089.
[35] H.T. Zhang, J. Yang, G.H. Liang, X.J. Gao, Y. Sang, T. Gui, Z.J. Liang, M.S. Tam, Z. G. Zha, Andrographolide induces cell cycle arrest and apoptosis of chondrosarcoma by targeting TCF-1/SOX9 axis, J. Cell. Biochem. 118 (12) (2017) 4575–4586.
[36] N.S. Othman, D.K. Mohd Azman, Andrographolide Induces G2/M Cell Cycle Arrest and Apoptosis in Human Glioblastoma DBTRG-05MG Cell Line via ERK1/2 /c-Myc/p53 Signaling Pathway, Molecules 27 (19) (2022).
[37] H. Huang, Q. Lu, X. Yuan, P. Zhang, C. Ye, M. Wei, C. Yang, L. Zhang, Y. Huang, X. Luo, J. Luo, Andrographolide inhibits the growth of human osteosarcoma cells

by suppressing Wnt/β-catenin, PI3K/AKT and NF-κB signaling pathways, Chem. -Biol. Interact. 365 (2022) 110068.
[38] Z.Q. Zhou, P.J. Hurlin, The interplay between Mad and Myc in proliferation and differentiation, Trends Cell Biol. 11 (11) (2001) S10–S14.
[39] L. Wang, C. Li, P. Chen, C. Liu, Z. Cui, S. Deng, H. Yang, Identification of PDCD2 as a candidate target of andrographolide that arrests the tumor cell cycle by human proteome-scale screening, ACS Pharmacol. Transl. Sci. 5 (7) (2022) 479–490.
[40] A.S. Budiatin, I.B. Sagitaras, I.P. Nurhayati, N. Khairah, K. Nisak, I. Susilo, J. Khotib, Attenuation of hyperplasia in lung parenchymal and colonic epithelial cells in DMBA-induced cancer by administering Andrographis paniculata Nees extract using animal model, J. Basic Clin. Physiol. Pharmacol. 32 (4) (2021) 497–504.
[41] S.C. Lim, H.J. Jeon, K.H. Kee, M.J. Lee, R. Hong, S.I. Han, Andrographolide induces apoptotic and non-apoptotic death and enhances tumor necrosis factor-related apoptosis-inducing ligand-mediated apoptosis in gastric cancer cells, Oncol. Lett. 13 (5) (2017) 3837–3844.
[42] R.J. Wei, X.S. Zhang, D.L. He, Andrographolide sensitizes prostate cancer cells to TRAIL-induced apoptosis, Asian J. Androl. 20 (2) (2018) 200–204.
[43] Y. Deng, R. Bi, H. Guo, J. Yang, Y. Du, C. Wang, W. Wei, Andrographolide enhances TRAIL-induced apoptosis via p53-mediated death receptors up-regulation and suppression of the NF-κB pathway in bladder cancer cells, Int. J. Biol. Sci. 15 (3) (2019) 688–700.
[44] R. Bi, Y. Deng, C. Tang, L. Xuan, B. Xu, Y. Du, C. Wang, W. Wei, Andrographolide sensitizes human renal carcinoma cells to TRAIL-induced apoptosis through upregulation of death receptor 4, Oncol. Rep. 44(5 (2020) 1939–1948.
[45] H. Doi, T. Matsui, J.M. Dijkstra, A. Ogasawara, Y. Higashimoto, S. Imamura, T. Ohye, H. Takematsu, I. Katsuda, H. Akiyama, Andrographolide, isolated from Andrographis paniculata, induces apoptosis in monocytic leukemia and multiple myeloma cells via augmentation of reactive oxygen species production, F1000Research 10 (2021) 542.
[46] I. Khan, F. Khan, A. Farooqui, I.A. Ansari, Andrographolide exhibits anticancer potential against human colon cancer cells by inducing cell cycle arrest and programmed cell death via augmentation of intracellular reactive oxygen species level, Nutr. Cancer 70 (5) (2018) 787–803.
[47] G. Kumar, S. Thapa, J.A. Tali, D. Singh, B.K. Sharma, K.N. Panda, S.K. Singh, R. Shankar, Site-selective synthesis of C-17 Ester derivatives of natural andrographolide for evaluation as a potential anticancer agent, ACS Omega 8 (6) (2023) 6099–6123.
[48] H. Gao, H. Li, W. Liu, S.K. Mishra, C. Li, Andrographolide induces apoptosis in gastric cancer cells through reactivation of p53 and inhibition of Mdm-2, Dokl. Biochem. Biophys. 500 (1) (2021) 393–401.
[49] S.H. Yang, S.M. Wang, J.P. Syu, Y. Chen, S.D. Wang, Y.S. Peng, M.F. Kuo, H. N. Kung, Andrographolide induces apoptosis of C6 glioma cells via the ERK-p53-caspase 7-PARP pathway, BioMed. Res. Int. 2014 (2014) 312847.
[50] R. Preet, B. Chakraborty, S. Siddharth, P. Mohapatra, D. Das, S.R. Satapathy, S. Das, N.C. Maiti, P.R. Maulik, C.N. Kundu, C. Chowdhury, Synthesis and biological evaluation of andrographolide analogues as anti-cancer agents, Eur. J. Med. Chem. 85 (2014) 95–106.
[51] H. Gao, J. Wang, Andrographolide inhibits multiple myeloma cells by inhibiting the TLR4/NF-κB signaling pathway, Mol. Med. Rep. 13 (2) (2016) 1827–1832.
[52] L. Xuan, J.H. Hu, R. Bi, S.Q. Liu, C.X. Wang, Andrographolide inhibits proliferation and promotes apoptosis in bladder cancer cells by interfering with NF- κ B and PI3K/AKT signaling in vitro and in vivo, Chin. J. Integr. Med 28 (4) (2022) 349–356.
[53] B. Wu, X. Chen, Y. Zhou, P. Hu, D. Wu, G. Zheng, Y. Cai, Andrographolide inhibits proliferation and induces apoptosis of nasopharyngeal carcinoma cell line C666-1 through LKB1-AMPK-dependent signaling pathways, Die, Pharmazie 73 (10) (2018) 594–597.
[54] A. Pasha, K. Kumar, S.K. Heena, I. Arnold Emerson, S.C. Pawar, Inhibition of NF-kB and COX-2 by andrographolide regulates the progression of cervical cancer by promoting PTEN expression and suppressing PI3K/AKT signalling pathway, Sci. Rep. 14 (1) (2024) 12020.
[55] J. Zeng, Y. Zheng, S. Dong, T. Ding, S. Zhang, K. Li, H. Liu, Q. Fang, S. Yuan, Y. Wei, J. Li, T. Liu, Andrographolide inhibits Burkitt's lymphoma by binding JUN and CASP3 proteins, Cancer Chemother. Pharmacol. 93 (4) (2024) 381–391.
[56] C.C. Wong, S.R. Sagineedu, S.H. Sumon, S.M. Sidik, R. Phillips, N.H. Lajis, J. Stanslas, NCI in vitro and in silico anticancer screen, cell cycle pertubation and apoptosis-inducing potential of new acylated, benzylidene and isopropylidene derivatives of andrographolide, Environ. Toxicol. Pharmacol. 38 (2) (2014) 489–501.
[57] Y. Luo, J. Hu, Y. Jiao, L. Liu, D. Miao, Y. Song, W. Yan, Y. Li, Y. Jiang, Andrographolide anti-proliferation and metastasis of hepatocellular carcinoma through LncRNA MIR22HG regulation, J. Nat. Med. (2023).
[58] A. Banerjee, V. Banerjee, S. Czinn, T. Blanchard, Increased reactive oxygen species levels cause ER stress and cytotoxicity in andrographolide treated colon cancer cells, Oncotarget 8 (16) (2017) 26142–26153.
[59] A. Banerjee, H. Ahmed, P. Yang, S.J. Czinn, T.G. Blanchard, Endoplasmic reticulum stress and IRE-1 signaling cause apoptosis in colon cancer cells in response to andrographolide treatment, Oncotarget 7 (27) (2016) 41432–41444.
[60] C. Heawchaiyaphum, P. Malat, C. Pientong, S. Roytrakul, Y. Yingchutrakul, S. Aromseree, S. Suebsasana, P. Mahalapbutr, T. Ekalaksananan, The Dual Functions of Andrographolide in the Epstein-Barr Virus-Positive Head-and-Neck Cancer Cells: The Inhibition of Lytic Reactivation of the Epstein-Barr Virus and the Induction of Cell Death, Int J. Mol. Sci. 24 (21) (2023).
[61] Y. Liu, Y. Zhang, J. Zou, L. Yan, X. Yu, P. Lu, X. Wu, Q. Li, R. Gu, D. Zhu, Andrographolide induces autophagic cell death and inhibits invasion and metastasis of human osteosarcoma cells in an autophagy-dependent manner, Cell. Physiol. Biochem.: Int. J. Exp. Cell. Physiol., Biochem., Pharmacol. 44 (4) (2017) 1396–1410.
[62] D. Kumar, B. Das, R. Sen, P. Kundu, A. Manna, A. Sarkar, C. Chowdhury, M. Chatterjee, P. Das, Andrographolide analogue induces apoptosis and autophagy mediated cell death in U937 cells by inhibition of PI3K/Akt/mTOR pathway, PloS One 10 (10) (2015) e0139657.
[63] L. Jiaqi, H. Siqing, W. Qin, Z. di, Z. Bei, Y. Jialin, Andrographolide promoted ferroptosis to repress the development of non-small cell lung cancer through activation of the mitochondrial dysfunction, Phytomedicine: Int. J. Phytother. Phytopharm. 109 (2023) 154601.
[64] W. Li, H. Fu, L. Fang, H. Chai, B. Ding, S. Qian, Andrographolide induced ferroptosis in multiple myeloma cells by regulating the P38/Nrf2/HO-1 pathway, Arch. Biochem. Biophys. 742 (2023) 109622.
[65] Y. Wang, D. Huang, T. Song, X. Qi, M. Li, H. Zhang, Y. Liu, M. Yang, Andrographolide elevates tumor necrosis factor-related apoptosis-inducing ligand lethality through reactive oxygen species accumulation and gasdermin E cleavage in breast cancer cells, Med. Oncol. (North., Lond., Engl.) 40 (1) (2022) 11.
[66] Q. Wang, Y. Wang, J. Ding, C. Wang, X. Zhou, W. Gao, H. Huang, F. Shao, Z. Liu, A bioorthogonal system reveals antitumour immune function of pyroptosis, Nature 579 (7799) (2020) 421–426.
[67] C. Kaewpiboon, N. Boonnak, A.W. Salae, S. Pakdeepromma, N. Yawut, Y. H. Chung, Andrographolide targets EGFR to impede epithelial-mesenchymal transition in human breast cancer cells, J. Pharm. Biomed. Anal. 248 (2024) 116267.
[68] P. Friedl, K. Wolf, Tumour-cell invasion and migration: diversity and escape mechanisms, Nat. Rev. Cancer 3 (5) (2003) 362–374.
[69] L. Dai, G. Wang, W. Pan, Andrographolide Inhibits Proliferation and Metastasis of SGC7901 Gastric, Cancer Cells, BioMed. Res. Int. 2017 (2017) 6242103.
[70] Z. Zhai, X. Qu, H. Li, Z. Ouyang, W. Yan, G. Liu, X. Liu, Q. Fan, T. Tang, K. Dai, A. Qin, Inhibition of MDA-MB-231 breast cancer cell migration and invasion activity by andrographolide via suppression of nuclear factor-κB-dependent matrix metalloproteinase-9 expression, Mol. Med. Rep. 11 (2) (2015) 1139–1145.
[71] Z. Zhai, X. Qu, H. Li, Z. Ouyang, W. Yan, G. Liu, X. Liu, Q. Fan, T. Tang, K. Dai, A. Qin, Corrigendum] Inhibition of MDA-MB-231 breast cancer cell migration and invasion activity by andrographolide via suppression of nuclear factor-κB-dependent matrix metalloproteinase-9 expression, Mol. Med. Rep. 19 (3) (2019) 1979.
[72] S. Reabroi, R. Saeeng, N. Boonmuen, T. Kasemsuk, W. Saengsawang, K. Suksen, W. Zhu, P. Piyachaturawat, A. Chairoungdua, The anti-cancer activity of an andrographolide analogue functions through a GSK-3β-independent Wnt/β-catenin signaling pathway in colorectal cancer cells, Sci. Rep. 8 (1) (2018) 7924.
[73] H. Gong, X. Yang, L. An, W. Zhang, X. Liu, L. Shu, L. Yang, PCSK5 downregulation promotes the inhibitory effect of andrographolide on glioblastoma through regulating STAT3, Mol. Cell. Biochem. (2024).
[74] S.L. Yang, F.H. Kuo, P.N. Chen, Y.H. Hsieh, N.Y. Yu, W.E. Yang, M.J. Hsieh, S. F. Yang, Andrographolide suppresses the migratory ability of human glioblastoma multiforme cells by targeting ERK1/2-mediated matrix metalloproteinase-2 expression, Oncotarget 8 (62) (2017) 105860–105872.
[75] J. Li, Z. Liu, X. Wu, S.M. Lee, S.W. Seto, J. Zhang, G.C. Zhou, G.P. Leung, Anti-metastatic effects of AGS-30 on breast cancer through the inhibition of M2-like macrophage polarization, Biomed. Pharmacother. = Biomedecine Pharmacother. 172 (2024) 116269.
[76] H. Mir, N. Kapur, R. Singh, G. Sonpavde, J.W. Lillard, Jr, S. Singh, Andrographolide inhibits prostate cancer by targeting cell cycle regulators, CXCR3 and CXCR7 chemokine receptors, Cell Cycle (Georget., Tex.) 15 (6) (2016) 819–826.
[77] Q.Q. Zhang, D.L. Zhou, Y. Ding, H.Y. Liu, Y. Lei, H.Y. Fang, Q.L. Gu, X.D. He, C. L. Qi, Y. Yang, T. Lan, J.C. Li, P. Gong, X.Y. Wu, X. Yang, W.D. Li, L.J. Wang, Andrographolide inhibits melanoma tumor growth by inactivating the TLR4/NF-κB signaling pathway, Melanoma Res. 24 (6) (2014) 545–555.
[78] L. Ji, Z. Zheng, L. Shi, Y. Huang, B. Lu, Z. Wang, Andrographolide decreased VEGFD expression in hepatoma cancer cells by inducing ubiquitin/proteasome-mediated cFos protein degradation, Biochim. Et. Biophys. Acta 1850 (4) (2015) 750–758.
[79] D. Kumar, S. Kumar, M. Gorain, D. Tomar, H.S. Patil, N.N.V. Radharani, T.V. S. Kumar, T.V. Patil, H.V. Thulasiram, G.C. Kundu, Notch1-MAPK signaling axis regulates CD133(+) cancer stem cell-mediated melanoma growth and angiogenesis, J. Invest. Dermatol. 136 (12) (2016) 2462–2474.
[80] L. Shi, G. Zhang, Z. Zheng, B. Lu, L. Ji, Andrographolide reduced VEGFA expression in hepatoma cancer cells by inactivating HIF-1α: The involvement of JNK and MTA1/HDCA, Chem. -Biol. Interact. 273 (2017) 228–236.
[81] Y. Peng, Y. Wang, N. Tang, D. Sun, Y. Lan, Z. Yu, X. Zhao, L. Feng, B. Zhang, L. Jin, F. Yu, X. Ma, C. Lv, Andrographolide inhibits breast cancer through suppressing COX-2 expression and angiogenesis via inactivation of p300 signaling and VEGF pathway, J. Exp. Clin. Cancer Res.: CR 37 (1) (2018) 248.
[82] T.G. Blanchard, R. Lapidus, V. Banerjee, A.C. Bafford, S.J. Czinn, H. Ahmed, A. Banerjee, Upregulation of RASSF1A in colon cancer by suppression of angiogenesis signaling and akt activation, Cell. Physiol. Biochem.: Int. J. Exp. Cell. Physiol., Biochem., Pharmacol. 48 (3) (2018) 1259–1273.
[83] K. Kajal, A.K. Panda, J. Bhat, D. Chakraborty, S. Bose, P. Bhattacharjee, T. Sarkar, S. Chatterjee, S.K. Kar, G. Sa, Andrographolide binds to ATP-binding pocket of

VEGFR2 to impede VEGFA-mediated tumor-angiogenesis, Sci. Rep. 9 (1) (2019) 4073.
[84] K. Shen, L. Ji, B. Lu, C. Xu, C. Gong, G. Morahan, Z. Wang, Andrographolide inhibits tumor angiogenesis via blocking VEGFA/VEGFR2-MAPKs signaling cascade, Chem. -Biol. Interact. 218 (2014) 99–106.
[85] J. Li, F. Li, F. Tang, J. Zhang, R. Li, D. Sheng, S.M. Lee, G.C. Zhou, G.P. Leung, AGS-30, an andrographolide derivative, suppresses tumor angiogenesis and growth in vitro and in vivo, Biochem. Pharmacol. 171 (2020) 113694.
[86] J. Dai, Y. Lin, Y. Duan, Z. Li, D. Zhou, W. Chen, L. Wang, Q.Q. Zhang, Andrographolide inhibits angiogenesis by inhibiting the Mir-21-5p/TIMP3 signaling pathway, Int. J. Biol. Sci. 13 (5) (2017) 660–668.
[87] X.R. Wang, Z.B. Jiang, C. Xu, W.Y. Meng, P. Liu, Y.Z. Zhang, C. Xie, J.Y. Xu, Y. J. Xie, T.L. Liang, H.X. Yan, X.X. Fan, X.J. Yao, Q.B. Wu, E.L. Leung, Andrographolide suppresses non-small-cell lung cancer progression through induction of autophagy and antitumor immune response, Pharmacol. Res. 179 (2022) 106198.
[88] S. Ganapathy-Kanniappan, J.F. Geschwind, Tumor glycolysis as a target for cancer therapy: progress and prospects, Mol. Cancer 12 (2013) 152.
[89] E.S. Yang, Y. Do, S.Y. Cheon, B. Kim, J. Ling, M.K. Cho, T. Kim, S.J. Bae, K.T. Ha, Andrographolide suppresses aerobic glycolysis and induces apoptotic cell death by inhibiting pyruvate dehydrogenase kinase 1 expression, Oncol. Rep. 49 (4) (2023).
[90] K. Yang, K. Wu, J. Feng, L. Yutian, X. Zhu, D. Xu, Study on the Antitumor Effect and Glycolysis of Andrographolide in Anaplastic Thyroid Carcinoma, Evid. Based Complement Altern. Med 2021 (2021) 5526581.
[91] Z. Chen, W.J. Tang, Y.H. Zhou, Z.M. Chen, K. Liu, Andrographolide inhibits non-small cell lung cancer cell proliferation through the activation of the mitochondrial apoptosis pathway and by reprogramming host glucose metabolism, Ann. Transl. Med. 9 (22) (2021) 1701.
[92] R.A. Burgos, P. Alarcón, J. Quiroga, C. Manosalva, J. Hancke, Andrographolide, an Anti-Inflammatory Multitarget Drug: All Roads Lead to Cellular Metabolism, Molecules 26 (1) (2020).
[93] L. Li, L.L. Yang, S.L. Yang, R.Q. Wang, H. Gao, Z.Y. Lin, Y.Y. Zhao, W.W. Tang, R. Han, W.J. Wang, P. Liu, Z.L. Hou, M.Y. Meng, L.W. Liao, Andrographolide suppresses breast cancer progression by modulating tumor-associated macrophage polarization through the Wnt/β-catenin pathway, Phytother. Res.: PTR 36 (12) (2022) 4587–4603.
[94] J. Ren, Z. Liu, Q. Wang, J. Giles, J. Greenberg, N. Sheibani, K.C. Kent, B. Liu, Andrographolide ameliorates abdominal aortic aneurysm progression by inhibiting inflammatory cell infiltration through downregulation of cytokine and integrin expression, J. Pharmacol. Exp. Ther. 356 (1) (2016) 137–147.
[95] M. Yuan, W. Meng, W. Liao, S. Lian, Andrographolide Antagonizes TNF-α-Induced IL-8 via Inhibition of NADPH Oxidase/ROS/NF-κB and Src/MAPKs/AP-1 Axis in Human Colorectal Cancer HCT116 Cells, J. Agric. Food Chem. 66 (20) (2018) 5139–5148.
[96] I. Khan, S. Mahfooz, M. Saeed, I. Ahmad, I.A. Ansari, Andrographolide inhibits proliferation of colon cancer SW-480 cells via downregulating notch signaling pathway, Anti-Cancer Agents Med. Chem. 21 (4) (2021) 487–497.
[97] I. Khan, S. Mahfooz, I.A. Ansari, Antiproliferative and apoptotic properties of andrographolide against human colon cancer DLD1 cell line, Endocr., Metab. Immune Disord. Drug Targets 20 (6) (2020) 930–942.
[98] Z. Liu, X. Wu, K. Dai, R. Li, J. Zhang, D. Sheng, S.M. Lee, G.P. Leung, G.C. Zhou, J. Li, The new andrographolide derivative AGS-30 induces apoptosis in human colon cancer cells by activating a ROS-dependent JNK signalling pathway, Phytomedicine: Int. J. Phytother. Phytopharm. 94 (2022) 153824.
[99] B. Lu, Y. Sheng, J. Zhang, Z. Zheng, L. Ji, The altered microRNA profile in andrographolide-induced inhibition of hepatoma tumor growth, Gene 588 (2) (2016) 124–133.
[100] J. Zhang, C. Li, L. Zhang, Y. Heng, T. Xu, Y. Zhang, X. Chen, R.M. Hoffman, L. Jia, Andrographolide induces noxa-dependent apoptosis by transactivating ATF4 in human lung adenocarcinoma, Cells, Front. Pharmacol. 12 (2021) 680589.
[101] J. Zhang, C. Li, L. Zhang, Y. Heng, S. Wang, Y. Pan, L. Cai, Y. Zhang, T. Xu, X. Chen, R.M. Hoffman, L. Jia, Andrographolide, a diterpene lactone from the Traditional Chinese Medicine Andrographis paniculate, induces senescence in human lung adenocarcinoma via p53/p21 and Skp2/p27, Phytomedicine: Int. J. Phytother. Phytopharm. 98 (2022) 153933.
[102] J. Li, L. Huang, Z. He, M. Chen, Y. Ding, Y. Yao, Y. Duan, L. Zixuan, C. Qi, L. Zheng, J. Li, R. Zhang, X. Li, J. Dai, L. Wang, Q.Q. Zhang, Andrographolide Suppresses the Growth and Metastasis of Luminal-Like Breast Cancer by Inhibiting the NF-κB/miR-21-5p/PDCD4 Signaling Pathway, Front. Cell Dev. Biol. 9 (2021) 643525.
[103] J. Li, C. Zhang, H. Jiang, J. Cheng, Andrographolide inhibits hypoxia-inducible factor-1 through phosphatidylinositol 3-kinase/AKT pathway and suppresses breast cancer growth, OncoTargets Ther. 8 (2015) 427–435.
[104] I.S. Forestier-Román, A. López-Rivas, M.M. Sánchez-Vázquez, K. Rohena-Rivera, G. Nieves-Burgos, H. Ortiz-Zuazaga, C.A. Torres-Ramos, M. Martínez-Ferrer, Andrographolide induces DNA damage in prostate cancer cells, Oncotarget 10 (10) (2019) 1085–1101.
[105] R. Ma, T. Shimura, C. Yin, Y. Okugawa, T. Kitajima, Y. Koike, Y. Okita, M. Ohi, K. Uchida, A. Goel, L. Yao, X. Zhang, Y. Toiyama, Antitumor effects of Andrographis via ferroptosis-associated genes in gastric cancer, Oncol. Lett. 22 (1) (2021) 523.
[106] S. Wang, H. Li, S. Chen, Z. Wang, Y. Yao, T. Chen, Z. Ye, P. Lin, Andrographolide induces apoptosis in human osteosarcoma cells via the ROS/JNK pathway, Int. J. Oncol. 56(6 (2020) 1417–1428.
[107] T. Yang, S. Yao, X. Zhang, Y. Guo, Andrographolide inhibits growth of human T-cell acute lymphoblastic leukemia Jurkat cells by downregulation of PI3K/AKT and upregulation of p38 MAPK pathways, Drug Des., Dev. Ther. 10 (2016) 1389–1397.
[108] P. Pearngam, S. Kumkate, S. Okada, T. Janvilisri, Andrographolide Inhibits Cholangiocarcinoma Cell Migration by Down-Regulation of Claudin-1 via the p-38 Signaling Pathway, Front. Pharmacol. 10 (2019) 827.
[109] P. Udomwan, C. Pientong, P. Tongchai, A. Burassakarn, N. Sunthamala, S. Roytrakul, S. Suebsasana, T. Ekalaksananan, Proteomics Analysis of Andrographolide-Induced Apoptosis via the Regulation of Tumor Suppressor p53 Proteolysis in Cervical Cancer-Derived Human Papillomavirus 16-Positive Cell Lines, Int. J. Mol. Sci. 22 (13) (2021).
[110] S.L. Beesetti, M. Jayadev, G.V. Subhashini, L. Mansour, S. Alwasel, A.H. Harrath, Andrographolide as a Therapeutic Agent Against Breast and Ovarian Cancers, Open life Sci. 14 (2019) 462–469.
[111] S. Mi, G. Xiang, D. Yuwen, J. Gao, W. Guo, X. Wu, X. Wu, Y. Sun, Y. Su, Y. Shen, Q. Xu, Inhibition of autophagy by andrographolide resensitizes cisplatin-resistant non-small cell lung carcinoma cells via activation of the Akt/mTOR pathway, Toxicol. Appl. Pharmacol. 310 (2016) 78–86.
[112] W. Wang, W. Guo, L. Li, Z. Fu, W. Liu, J. Gao, Y. Shu, Q. Xu, Y. Sun, Y. Gu, Andrographolide reversed 5-FU resistance in human colorectal cancer by elevating BAX expression, Biochem. Pharmacol. 121 (2016) 8–17.
[113] D.S. Lakra, P. Bharathiraja, T. Dhanalakshmi, N.R. Prasad, Andrographolide reverts multidrug resistance in KBCh(R) 8-5 cells through AKT signaling pathway, Cell Biochem. Funct. 42 (2) (2024) e3948.
[114] Y.F. Liu, Z.Q. Feng, T.H. Chu, B. Yi, J. Liu, H. Yu, J. Xue, Y.J. Wang, C.Z. Zhang, Andrographolide sensitizes KRAS-mutant colorectal cancer cells to cetuximab by inhibiting the EGFR/AKT and PDGFRβ/AKT signaling pathways, Phytomedicine: Int. J. Phytother. Phytopharm. 126 (2024) 155462.
[115] M. Su, B. Qin, F. Liu, Y. Chen, R. Zhang, Andrographolide enhanced 5-fluoro-uracil-induced antitumor effect in colorectal cancer via inhibition of c-MET pathway, Drug Des., Dev. Ther. 11 (2017) 3333–3341.
[116] D. Yuwen, S. Mi, Y. Ma, W. Guo, Q. Xu, Y. Shen, Y. Shu, Andrographolide enhances cisplatin-mediated anticancer effects in lung cancer cells through blockade of autophagy, Anti-Cancer Drugs 28 (9) (2017) 967–976.
[117] M. Zhang, E. Xue, W. Shao, Andrographolide promotes vincristine-induced SK-NEP-1 tumor cell death via PI3K-AKT-p53 signaling pathway, Drug Des., Dev. Ther. 10 (2016) 3143–3152.
[118] H. Guo, Z. Zhang, Z. Su, C. Sun, X. Zhang, X. Zhao, X. Lai, Z. Su, Y. Li, J.Y. Zhan, Enhanced anti-tumor activity and reduced toxicity by combination andrographolide and bleomycin in ascitic tumor-bearing mice, Eur. J. Pharmacol. 776 (2016) 52–63.
[119] X. Duan, T. Li, X. Han, J. Ren, P. Chen, H. Li, S. Gong, The antitumor effect of arsenic trioxide on hepatocellular carcinoma is enhanced by andrographolide, Oncotarget 8 (53) (2017) 90905–90915.
[120] H. Hong, W. Cao, Q. Wang, C. Liu, C. Huang, Synergistic antitumor effect of Andrographolide and cisplatin through ROS-mediated ER stress and STAT3 inhibition in colon cancer, Med. Oncol. (North., Lond., Engl.) 39 (5) (2022) 101.
[121] H.H. Lin, M.D. Shi, H.C. Tseng, J.H. Chen, Andrographolide sensitizes the cytotoxicity of human colorectal carcinoma cells toward cisplatin via enhancing apoptosis pathways in vitro and in vivo, Toxicol. Sci.: Off. J. Soc. Toxicol. 139 (1) (2014) 108–120.
[122] W. Mao, P. He, W. Wang, X. Wu, C. Wei, Andrographolide sensitizes Hep-2 human laryngeal cancer cells to carboplatin-induced apoptosis by increasing reactive oxygen species levels, Anti-Cancer Drugs 30 (7) (2019) e0774.
[123] Y. Li, B. Jiang, R. Wang, J. Wang, Y. Li, Y. Bao, Synergistic effects of tanshinone IIA and andrographolide on the apoptosis of cancer cells via crosstalk between p53 and reactive oxygen species pathways, Pharmacol. Rep.: PR 72 (2) (2020) 400–417.
[124] M.H. Hodroj, A. Jardaly, S. Abi Raad, A. Zouein, S. Rizk, Andrographolide potentiates the antitumor effect of topotecan in acute myeloid leukemia cells through an intrinsic apoptotic pathway, Cancer Manag. Res. 10 (2018) 1079–1088.
[125] T. Xu, Y. Jiang, S. Yuan, L. Zhang, X. Chen, W. Zhao, L. Cai, B. Xiao, L. Jia, Andrographolide Inhibits ER-Positive Breast Cancer Growth and Enhances Fulvestrant Efficacy via ROS-FOXM1-ER-α Axis, Front. Oncol. 12 (2022) 899402.
[126] D.C. Xiang, J.Y. Yang, Y.J. Xu, S. Zhang, M. Li, C. Zhu, C.L. Zhang, D. Liu, Protective effect of Andrographolide on 5-Fu induced intestinal mucositis by regulating p38 MAPK signaling pathway, Life Sci. 252 (2020) 117612.
[127] Y. Wang, B. Wei, D. Wang, J. Wu, J. Gao, H. Zhong, Y. Sun, Q. Xu, W. Liu, Y. Gu, W. Guo, DNA damage repair promotion in colonic epithelial cells by andrographolide downregulated cGAS-STING pathway activation and contributed to the relief of CPT-11-induced intestinal mucositis, Acta Pharm. Sin. B 12 (1) (2022) 262–273.
[128] L. Safaeian, F. Shafiee, S. Haghighatnazar, Andrographolide protects against doxorubicin-and arsenic trioxide-induced toxicity in cardiomyocytes, Mol. Biol. Rep. 50 (1) (2023) 389–397.
[129] S. Liu, J. Liu, N. Su, S. Wei, N. Xie, X. Li, S. Xie, J. Liu, B. Zhang, W. Li, S. Tan, An Integrated Network Pharmacology and RNA-seq Approach for Exploring the Protective Effect of Andrographolide in Doxorubicin-Induced Cardiotoxicity, Cardiovasc. Drugs Ther. (2024).
[130] X. Li, R. Tian, L. Liu, L. Wang, D. He, K. Cao, J.K. Ma, C. Huang, Andrographolide enhanced radiosensitivity by downregulating glycolysis via the inhibition of the PI3K-Akt-mTOR signaling pathway in HCT116 colorectal cancer cells, J. Int. Med. Res. 48 (8) (2020), 300060520946169.

[131] Y. Si, L. Meng, B. Zhang, Y. Wu, Q. Du, J. Xu, J. Qi, RASSF1A promotes radiosensitivity in nasopharyngeal carcinoma by promoting FoxO3a and inhibiting the Nrf2/TXNRD1 signaling pathway, Neoplasma 70 (5) (2023) 633–644.
[132] C. Zhang, X. Qiu, Andrographolide radiosensitizes human ovarian cancer SKOV3 xenografts due to an enhanced apoptosis and autophagy, Tumour Biol.: J. Int. Soc. Oncodev. Biol. Med. 36 (11) (2015) 8359–8365.
[133] Z.M. Wang, Y.H. Kang, X. Yang, J.F. Wang, Q. Zhang, B.X. Yang, K.L. Zhao, L. P. Xu, L.P. Yang, J.X. Ma, G.H. Huang, J. Cai, X.C. Sun, Andrographolide radiosensitizes human esophageal cancer cell line ECA109 to radiation in vitro, Diseases of the esophagus: official journal of the International Society for, Dis. Esophagus 29 (1) (2016) 54–61.
[134] J. Gao, S. Peng, X. Shan, G. Deng, L. Shen, J. Sun, C. Jiang, X. Yang, Z. Chang, X. Sun, F. Feng, L. Kong, Y. Gu, W. Guo, Q. Xu, Y. Sun, Inhibition of AIM2 inflammasome-mediated pyroptosis by Andrographolide contributes to amelioration of radiation-induced lung inflammation and fibrosis, Cell death Dis. 10 (12) (2019) 957.
[135] C.C. Yu, C.A. Chen, S.L. Fu, H.Y. Lin, M.S. Lee, W.Y. Chiou, Y.C. Su, S.K. Hung, Andrographolide enhances the anti-metastatic effect of radiation in Ras-transformed cells via suppression of ERK-mediated MMP-2 activity, PloS One 13 (10) (2018) e0205666.
[136] S. Chen, H. Hu, S. Miao, J. Zheng, Z. Xie, H. Zhao, Anti-tumor effect of cisplatin in human oral squamous cell carcinoma was enhanced by andrographolide via upregulation of phospho-p53 in vitro and in vivo, Tumour Biol.: J. Int. Soc. Oncodev. Biol. Med. 39 (5) (2017), 1010428317705330.
[137] Y.P. Chen, Y.W. Liu, D. Lee, J.T. Qiu, T.Y. Lee, S.J. Liu, Biodegradable andrographolide-eluting nanofibrous membranes for the treatment of cervical cancer, Int. J. Nanomed. 14 (2019) 421–429.
[138] H. Yao, S. Song, X. Miao, X. Liu, J. Zhao, Z. Wang, X. Shao, Y. Zhang, G. Han, mPEG-PLA Micelle for Delivery of Effective Parts of Andrographis paniculata, Curr. Drug Deliv. 15 (4) (2018) 532–540.
[139] J. Zhang, Y. Li, W. Gao, M.A. Repka, Y. Wang, M. Chen, Andrographolide-loaded PLGA-PEG-PLGA micelles to improve its bioavailability and anticancer efficacy, Expert Opin. Drug Deliv. 11 (9) (2014) 1367–1380.
[140] J. Zhang, M. Zhang, J. Ji, X. Fang, X. Pan, Y. Wang, C. Wu, M. Chen, Glycyrrhetinic Acid-Mediated Polymeric Drug Delivery Targeting the Acidic Microenvironment of Hepatocellular Carcinoma, Pharm. Res. 32 (10) (2015) 3376–3390.
[141] J. Kim, J. Lee, Y.M. Lee, S. Pramanick, S. Im, W.J. Kim, Andrographolide-loaded polymerized phenylboronic acid nanoconstruct for stimuli-responsive chemotherapy, J. Control. Release: Off. J. Control. Release Soc. 259 (2017) 203–211.
[142] Y.S. Tu, D.M. Sun, J.J. Zhang, Z.Q. Jiang, Y.X. Chen, X.H. Zeng, D.E. Huang, N. Yao, Preparation and characterisation of andrographolide niosomes and its anti-hepatocellular carcinoma activity, J. Microencapsul. 31 (4) (2014) 307–316.
[143] R. Parveen, F.J. Ahmad, Z. Iqbal, M. Samim, S. Ahmad, Solid lipid nanoparticles of anticancer drug andrographolide: formulation, in vitro and in vivo studies, Drug Dev. Ind. Pharm. 40 (9) (2014) 1206–1212.
[144] H. Li, X. Qu, W. Qian, Y. Song, C. Wang, W. Liu, Andrographolide-loaded solid lipid nanoparticles enhance anti-cancer activity against head and neck cancer and precancerous cells, Oral. Dis. 28 (1) (2022) 142–149.
[145] T. Neamatallah, A.M. Malebari, A.J. Alamoudi, S. Nazreen, M.M. Alam, H.H. Bin-Melaih, O.A. Abuzinadah, S.M. Badr-Eldin, G. Alhassani, L. Makki, M. Z. Nasrullah, Andrographolide nanophytosomes exhibit enhanced cellular delivery and pro-apoptotic activities in HepG2 liver cancer cells, Drug Deliv. 30 (1) (2023) 2174209.
[146] A. Mourya, P. Pingle, C.K. Babu, H. Veerabomma, V.G.S. Sainaga Jyothi, J. Novak, P. Pathak, M. Grishina, A. Verma, R. Kumar, P.K. Singh, D.K. Khatri, S. B. Singh, J. Madan, Computational and experimental therapeutic efficacy analysis of andrographolide phospholipid complex self-assembled nanoparticles against Neuro2a cells, Biochim. Et. Biophys. Acta Gen. Subj. 1867 (2) (2023) 130283.
[147] X. Kang, Z. Zheng, Z. Liu, H. Wang, Y. Zhao, W. Zhang, M. Shi, Y. He, Y. Cao, Q. Xu, C. Peng, Y. Huang, Liposomal codelivery of doxorubicin and andrographolide inhibits breast cancer growth and metastasis, Mol. Pharm. 15 (4) (2018) 1618–1626.
[148] A. Karuppiah, R. Rajan, M. Ramanathan, A. Nagarajan, Cytotoxicity and synergistic effect of biogenically synthesized ternary therapeutic nano conjugates comprising plant active principle, silver and anticancer drug on MDA-MB-453 breast cancer cell line, Asian Pac. J. Cancer Prev.: APJCP 21 (1) (2020) 195–204.
[149] B. Govindan, B. Swarna Latha, P. Nagamony, F. Ahmed, M.A. Saifi, A.H. Harrath, S. Alwasel, L. Mansour, E.H. Alsharaeh, Designed synthesis of nanostructured magnetic hydroxyapatite based drug nanocarrier for anti-cancer drug delivery toward the treatment of human epidermoid carcinoma, Nanomaterials 7 (6) (2017).
[150] S. Jothi, N. Mohtar, M.J. Masarudin, T. Parumasivam, Novel inhaled andrographolide for treatment of lung cancer: In vitro assessment, Heliyon 10 (9) (2024) e30761.
[151] V.L.S.M.N., S. Kumar, M. Dhara, G. Dheeraj Rajesh, P. Kumar, Statistical modeling, optimization and characterization of andrographolide loaded emulgel for its therapeutic application on skin cancer through enhancing its skin permeability, Saudi Pharm. J.: SPJ: Off. Publ. Saudi Pharm. Soc. 32 (6) (2024) 102068.
[152] B.A. Oseni, C.P. Azubuike, O.O. Okubanjo, C.I. Igwilo, J. Panyam, Encapsulation of andrographolide in poly(lactide-co-glycolide) nanoparticles: formulation optimization and in vitro efficacy studies, Front. Bioeng. Biotechnol. 9 (2021) 639409.
[153] R.J. Ahiwale, B. Chellampillai, A.P. Pawar, Investigation of 1,2-Dimyristoyl-sn-Glycero-3-Phosphoglycerol-Sodium (DMPG-Na) Lipid with Various Metal Cations in Nanocochleate Preformulation: Application for Andrographolide Oral Delivery in Cancer Therapy, AAPS PharmSciTech 21 (7) (2020) 279.
[154] R. Asasutjarit, N. Sooksai, A. Fristiohady, K. Lairungruang, S.F. Ng, A. Fuongfuchat, Optimization of production parameters for andrographolide-loaded nanoemulsion preparation by microfluidization and evaluations of its bioactivities in skin cancer cells and UVB radiation-exposed skin, Pharmaceutics 13 (8) (2021).
[155] Y. Song, Z. Xin, Y. Wan, J. Li, B. Ye, X. Xue, Synthesis and anticancer activity of some novel indolo[3,2-b]andrographolide derivatives as apoptosis-inducing agents, Eur. J. Med. Chem. 90 (2015) 695–706.
[156] S.G. Kandanur, N.R. Golakoti, S. Nanduri, Synthesis and in vitro cytotoxicity of novel C-12 substituted-14-deoxy-andrographolide derivatives as potent anti-cancer agents, Bioorg. Med. Chem. Lett. 25 (24) (2015) 5781–5786.
[157] S.G.S. Kandanur, S. Nanduri, N.R. Golakoti, Synthesis and biological evaluation of new C-12(α/β)-(N-) sulfamoyl-phenylamino-14-deoxy-andrographolide derivatives as potent anti-cancer agents, Bioorg. Med. Chem. Lett. 27 (13) (2017) 2854–2862.
[158] T. Kasemsuk, P. Piyachaturawat, R. Bunthawong, U. Sirion, K. Suksen, A. Suksamrarn, R. Saeeng, One-pot three steps cascade synthesis of novel isoandrographolide analogues and their cytotoxic activity, Eur. J. Med. Chem. 138 (2017) 952–963.
[159] Y. Liu, R.M. Liang, Q.P. Ma, K. Xu, X.Y. Liang, W. Huang, R. Sutton, J. Ding, P.M. O.'Neil, C.R. Cheng, Synthesis of thioether andrographolide derivatives and their inhibitory effect against cancer cells, MedChemComm 8 (6) (2017) 1268–1274.
[160] S. Sombut, R. Bunthawong, U. Sirion, T. Kasemsuk, P. Piyachaturawat, K. Suksen, A. Suksamrarn, R. Saeeng, Synthesis of 14-deoxy-11,12-didehydroandrographolide analogues as potential cytotoxic agents for cholangiocarcinoma, Bioorg. Med Chem. Lett. 27 (23) (2017) 5139–5143.
[161] S. Mokenapelli, M. Gutam, N. Vadiyaala, J.R. Yerrabelli, S. Banerjee, P. Roy, R. K. Kancha, B.R. Kunduru, S.R. Sagurthi, P.R. Chitneni, Synthesis and cytotoxicity of novel 14α-O-(1,4-disubstituted-1,2,3-triazolyl) ester derivatives of andrographolide, Nat. Prod. Res. 35 (2) (2021) 289–297.
[162] S. Mokenapelli, J.R. Yerrabelli, N. Das, P. Roy, P.R. Chitneni, Synthesis and cytotoxicity of novel 14α-O-(andrographolide-3-subsitutedisoxazole-5-carboxylate) derivatives, Nat. Prod. Res. 35 (21) (2021) 3738–3744.
[163] P. Arsakhant, U. Sirion, A. Chairoungdua, K. Suksen, P. Piyachaturawat, A. Suksamrarn, R. Saeeng, Design and synthesis of C-12 dithiocarbamate andrographolide analogues as an anticancer agent, Bioorg. Med Chem. Lett. 30 (14) (2020) 127263.
[164] R. Bunthawong, U. Sirion, A. Chairoungdua, K. Suksen, P. Piyachaturawat, A. Suksamrarn, R. Saeeng, Synthesis and cytotoxic activity of new 7-acetoxy-12-amino-14-deoxy andrographolide analogues, Bioorg. Med. Chem. Lett. 33 (2021) 127741.
[165] W. Cai, J. Li, C. Chen, J. Wu, J. Li, X. Xue, Design, synthesis, and anticancer evaluation of novel andrographolide derivatives bearing an α,β-unsaturated ketone moiety, Bioorg. Chem. 112 (2021) 104941.
[166] W. Han, J. Li, Q. Li, Y. Yang, J. Li, X. Xue, Synthesis and anticancer activity evaluation of 7-oxygen-substituted and 8,17-epoxydized 1,2-didehydro-3-ox-14-deoxyandrographolide derivatives, Fitoterapia 163 (2022) 105347.
[167] T. Van Chien, T. Van Loc, N. The Anh, T. Van Sung, T.T. Phuong Thao, Cytotoxic and Anti-Inflammatory Activity of 3,19-Isopropylidene-/Arylidene-Andrographolide Analogs, Chem. Biodivers. 20 (8) (2023) e202300420.
[168] T.C. Yang, Y.J. Chiang, P.Y. Chiang, H.Y. Chen, K.R. Zhuang, Y.C. Wang, C.H. Lin, L.C. Lo, S.L. Fu, Design, synthesis, and anti-cancer evaluation of C-14 arylcarbamate derivatives of andrographolide, Bioorg. Med. Chem. 98 (2024) 117582.
[169] N. Tamang, C. Andrews, S.K. Mavileti, S. Nanduri, N.R. Golakoti, B. Karanam, Anti-cancer activity of heteroaromatic acetals of andrographolide and its isomers, N. J. Chem. = Nouv. J. De. Chim. 46 (20) (2022) 9745–9754.
[170] A. Monger, N. Boonmuen, K. Suksen, R. Saeeng, T. Kasemsuk, P. Piyachaturawat, W. Saengsawang, A. Chairoungdua, Inhibition of Topoisomerase IIα and Induction of Apoptosis in Gastric Cancer Cells by 19-Triisopropyl Andrographolide, Asian Pac. J. Cancer Prev.: APJCP 18 (10) (2017) 2845–2851.
[171] J.C. Lim, E.J. Jeyaraj, S.R. Sagineedu, W.S. Wong, J. Stanslas, SRS06, a new semisynthetic andrographolide derivative with improved anticancer potency and selectivity, inhibits nuclear factor-κB nuclear binding in the A549 non-small cell lung cancer cell line, Pharmacology 95 (1-2) (2015) 70–77.
[172] J.R.L. Ribeiro, N. Szemerédi, B.M.F. Gonçalves, G. Spengler, C.A.M. Afonso, M. U. Ferreira, Nitrogen-containing andrographolide derivatives with multidrug resistance reversal effects in cancer cells, RSC Med. Chem. 15 (4) (2024) 1348–1361.
[173] C.C. Wong, N. Periasamy, S.R. Sagineedu, S. Sidik, S.H. Sumon, P. Loadman, R. Phillips, N.H. Lajis, J. Stanslas, In vitro 3D colon tumor penetrability of SRJ09, a new anti-cancer andrographolide analog, Investig. N. Drugs 32 (5) (2014) 806–814.
[174] H.X. Liang, S.S. Lu, Z. Yan, Y.P. Kuang, X.X. Zhu, Z.G. Yan, T. Du, W.R. Chai, H. Long, Q.F. Lyu, Andrographolide disrupts meiotic maturation by blocking cytoskeletal reorganisation and decreases the fertilisation potential of mouse oocytes, Reprod., Fertil., Dev. 29 (12) (2017) 2336–2344.
[175] L.L. Gu, X.Y. Zhang, W.M. Xing, J.D. Xu, H. Lu, Andrographolide-induced apoptosis in human renal tubular epithelial cells: roles of endoplasmic reticulum stress and inflammatory response, Environ. Toxicol. Pharmacol. 45 (2016) 257–264.

[176] E. Ciampi, R. Uribe-San-Martin, C. Cárcamo, J.P. Cruz, A. Reyes, D. Reyes, C. Pinto, M. Vásquez, R.A. Burgos, J. Hancke, Efficacy of andrographolide in not active progressive multiple sclerosis: a prospective exploratory double-blind, parallel-group, randomized, placebo-controlled trial, BMC Neurol. 20 (1) (2020) 173.
[177] G. Yanhong, T.F.A.H.w.N.M. University, Study of Andrographolides With or Without Capecitabine to Treat Colorectal Cancer, ⟨https://classic.clinicaltrials.gov/show/NCT01993472⟩, 2013.
[178] C.Uo.H. Kong, The Effect of Andrographis paniculata (AP) on Palliative Management of Advanced Esophageal Cancer, ⟨https://classic.clinicaltrials.gov/show/NCT04196075⟩, 2018.
[179] J.Q.P.C. Ltd., A Study of Andrographolide Sulfonate in Patients With Acute Exacerbation of Chronic Bronchitis, ⟨https://classic.clinicaltrials.gov/show/NCT03132610⟩, 2016.
[180] J.Q.P.C. Ltd, Evaluate the Efficacy and Safety of Andrographolide Sulfonate in Patients With Acute Bronchitis, ⟨https://classic.clinicaltrials.gov/show/NCT03132623⟩, 2016.
[181] J.Q.P.C. Ltd, Evaluate the Efficacy and Safety of Andrographolide Sulfonate in Patients With Acute Tonsillitis, ⟨https://classic.clinicaltrials.gov/show/NCT03134443⟩, 2016.
[182] V.L.P. Ltd, Assessment of the Efficacy of Andrographis paniculata in Subjects With Mild to Moderate Osteoarthritis, ⟨https://classic.clinicaltrials.gov/show/NCT03262792⟩, 2017.
[183] I. University, The Effect of Andrographis paniculata to GLP-1, Fasting Insulin, Insulin 2-h Post OGTT, and HOMA-IR, ⟨https://classic.clinicaltrials.gov/show/NCT03455049⟩, 2017.
[184] U.Ad Chile, C.Nd.I.Cy Tecnológica, Uo Chile, Efficacy Study of Andrographis paniculata Purified Standardized Extract (ApE) in Patients With Multiple Sclerosis (MS), ⟨https://classic.clinicaltrials.gov/show/NCT02280876⟩, 2012.
[185] M. University, T. Ministry of Health, Andrographis paniculata vs Boesenbergia rotunda vs Control in Asymptomatic COVID-19, ⟨https://classic.clinicaltrials.gov/show/NCT05019326⟩, 2021.
[186] U.o. Malaya, M. Ministry of Health, Pharmacometabolomics of Andrographis paniculata And Metformin In Healthy Volunteers Under Fasting Condition, ⟨https://classic.clinicaltrials.gov/show/NCT04161404⟩, 2019.
[187] I. EuroPharma, Effects of an Adaptogenic Extract on Electrical Activity of the Brain in Elderly Subjects With Cognitive Impairment, ⟨https://classic.clinicaltrials.gov/show/NCT03780621⟩, 2019.
[188] V.L.P. Ltd, To Assess the Effect of 336 Days Exposure of Paractin® on Pain & Disease Progression in Patients Suffering From Osteoarthritis of Knee Joint, ⟨https://classic.clinicaltrials.gov/show/NCT04833946⟩, 2021.
[189] I. SpA, P.U.Cd Chile, Uo Chile, U.Ad Chile, Efficacy, Safety and Tolerability of Andrographolides Versus Placebo in Patients With Progressive Forms of MS, ⟨https://classic.clinicaltrials.gov/show/NCT02273635⟩, 2014.
[190] C.H. Clinic, Magnesium, Vitamin B2, Feverfew, Andrographis paniculata and Coenzyme Q10 for Episodic Migraine Prophylaxis, ⟨https://classic.clinicaltrials.gov/show/NCT04463875⟩, 2018.
[191] Uo.R.L. Sapienza, G. Coppola, F. Pierelli, Magnesium, Partenium, Andrographis, Co-enzyme Q10 and Riboflavin (PACR) in Migraine Prophylaxis, ⟨https://classic.clinicaltrials.gov/show/NCT03190044⟩, 2017.
[192] M. Juan C. Bertoglio, C. Fondo Nacional de Desarrollo Científico y Tecnológico, U.Ad Chile, Efficacy Study of FANG(30) for Active Rheumatoid Arthritis in Adult Patients, ⟨https://classic.clinicaltrials.gov/show/NCT00749645⟩, 2006.
[193] V.L.P. Ltd, To Compare the Efficacy and Tolerability of A. Paniculata/A. Chilensis in Individuals With URTI, ⟨https://classic.clinicaltrials.gov/show/NCT04955327⟩, 2021.
[194] S.H.I. AB, T.S.M. University, P. AB, Assessment of Efficacy of KAN-JANG® in Mild COVID-19, ⟨https://classic.clinicaltrials.gov/show/NCT04847518⟩, 2021.
[195] C.A.o.C.M. Sciences, F.A.H.o.H.C.M. University, G.a.H.o.C.A.o.C.M. Sciences, B. H.o.T.C. Medicine, C.U.o.C. Medicine, L.U.o.T.C. Medicine, S.U.o.T.C. Medicine, G.P.H.o.T.C. Medicine, A Post-marketing Research on Jinyebaidu Granule in Treating Patients With Acute Upper Respiratory Infection, ⟨https://classic.clinicaltrials.gov/show/NCT02539277⟩, 2014.
[196] A.S. University, G.H. Inc., Echinacea and Acute Respiratory Illness, ⟨https://classic.clinicaltrials.gov/show/NCT02003651⟩, 2013.